Microbial Alteration of Carbonate Archives

Dissertation

Zur Erlangung des Doktorgrades

der Naturwissenschaften

Dr. rer. nat.

an der Mathematisch-Naturwissenschaftlichen Fakultät

der Christian-Albrechts-Universität zu Kiel

vorgelegt von

Skadi Lange

Kiel, 2017

Hiermit erkläre ich, dass ich die vorliegende Doktorarbeit selbständig und ohne unerlaubte Hilfe erstellt habe. Weder diese noch eine ähnliche Arbeit wurde an einer anderen Abteilung oder Hochschule im Rahmen eines Prüfungsverfahrens vorgelegt, veröffentlicht oder zur Veröffentlichung vorgelegt. Ferner versichere ich, dass die Arbeit unter Einhaltung der Regeln guter wissenschaftlicher Praxis der Deutschen Forschungsgemeinschaft entstanden ist.

Kiel, den

Skadi Lange

54° 29.6' N   10° 15.1' E

Table of contents

Abstract

Marine biogenic carbonates are comprehensive archives of paleoenvironmental conditions. The main environmental variables that can be deduced from carbonate elemental- and isotopic composition are past sea-surface temperature, salinity and related ocean-circulation patterns, and -trace element concentration. These parameters are crucial to understand climate-linked paleo-ocean and atmospheric conditions, and to furthermore allow for interpolation to future environmental scenarios. However, the respective signals in carbonates can be biased by diagenetic alteration, and the abiotic processes involved in the diagenetic processes are being thoroughly investigated. A less considered, but potentially profound (co-) factor in early diagenesis are benthic microbial communities. Microbe-mineral interactions are known to shape the earth´s lithosphere through carbonate formation, dissolution, and geochemical alteration over geological timescales. However, the benthic microbial impact on marine carbonate archives after post mortem deposition in sediments has rarely been included in diagenetic concepts so far. The present study investigates the carbonate-alteration potential of benthic microbe-mineral interaction during early diagenesis, thereby elucidating the underlying mechanisms, and the potential consequences for carbonate-archive interpretation.

The investigations led to the following insights:

1) Incubation of aragonitic shell samples from the bivalve *Arctica islandica* in (i) anoxic seawater medium containing the anaerobic benthic bacterial strain *Shewanella sediminis* HAW-EB3 and (ii) anoxic sediment slurries containing the respective natural microbial communities, led to microbially-induced shell structural and geochemical alteration within a time span of only three months. Media carbonate chemistry reflected the observed shell-sample alterations, through an increase in total alkalinity, dissolved inorganic carbon, and the saturation state of aragonite. Furthermore, the concentrations of dissolved calcium (Ca) and strontium (Sr) ions in both the bacterial culture- and the anoxic sediment medium increased, relative to the controls, over time. Subsequently decreasing Ca^{2+} and Sr^{2+} concentrations in the bacterial culture medium hinted at cation adsorption by cell-wall and extracellular polymeric substances (EPS) functional groups that furthermore prevented secondary precipitation of calcium carbonate ($CaCO_3$) in the supersaturated medium. This assumption was furthermore supported by a moderate increase in Sr concentrations in exposed areas of an aragonitic shell sample presumably reflecting attachment of microbial bacterial cells and/or EPS to the carbonate. The

suggested underlying processes are (i) hydrolysis of the chitinous constituents of periostracal, and inter- and intracrystalline organic-matrix through a *S. sediminis* chitinase and (ii) anaerobic metabolic usage of organic (i.e. foremost periostracal) shell constituents by benthic microbial communities in organic-poor winter sediments. Both processes apparently increased the shells´ reactive surface area, thereby subsequently inducing shell dissolution through mineral-porewater exchange. Shell isotopic composition displayed no clear pattern, relative to pristine samples and controls.

2) Coral-aragonitic skeleton hard parts from the hermatypic coral *Porites* sp. were incubated in (i) oxic seawater media at two temperatures (10°C and 20°C) containing the aerobic benthic bacterial strain *Alcanivorax borkumenis* SK2[T], (ii) anoxic seawater medium containing the benthic anaerobic strain *S. sediminis* HAW-EB3, and (iii) anoxic sediment slurries with the respective natural microbial communities. In all incubations, medium-carbonate chemistry underwent an increase in pH, total alkalinity, and the saturation state of aragonite, relative to the controls, over time. In the oxic *A. borkumensis* incubations, concomitant withdrawal of Sr^{2+} (10°C incubation), and Ca^{2+} and Sr^{2+} (20°C incubation) from the media, and the resulting increase in the magnesium to calcium (Mg/Ca) and and magnesium to strontium (Mg/Sr) ratios indicated secondary carbonate precipitation, with the 20°C incubation undergoing the stronger changes in all parameters. In the anoxic *S. sediminis*-incubation and anoxic-sediment media, an increase in Ca^{2+} and Sr^{2+} concentrations and the related decrease in Mg/Ca and Mg/Sr ratios indicated carbonate dissolution. No characteristics of either precipitation or dissolution were detected on the coral surface or in the coral geochemical composition, and the coral isotopic composition was not significantly changed ($p > 0.5$). The changes in the incubation media apparently were induced through (i) *A. borkumensis* carbonic anhydrase activity, and (ii), (iii) anaerobic microbial activity. Measured organic carbon (C_{org}) content in the coral samples of only 0.04% was primarily held responsible for missing microbial carbonate alteration of the samples.

3) Foraminferal tests were incubated in (i) oxic seawater medium containing the aerobic benthic bacterial strain *A. borkumenis* SK2[T], (ii) anoxic seawater medium containing the anaerobic benthic bacterial strain *S. sediminis* HAW-EB3, and (iii) anoxic sediment slurries with the respective natural microbial communities. Tests incubated in the oxic *A. borkumensis* culture medium were intensively covered with precipitates at the end of the experiment. The medium reflected the observed precipitation with an increase in pH,

total alkalinity, and the saturation state of calcite, and a decrease in Mg^{2+}, Ca^{2+}, and Sr^{2+} concentrations over time. Secondary carbonate precipitation supposedly was induced through *A. borkumensis* carbonic-anhydrase activity. In the anoxic incubations, no microbially-induced changes in medium chemistry, test structure, or test geochemistry were detected. This was apparently owed to low microbial activity that was reflected in the media chemistry.

In summary, the present studies demonstrated that benthic microbial activity has the potential to alter biogenic carbonate archives with respect to carbonate surficial structure and geochemistry over very short time frames (i.e. 25 days to three months), when compared to geological timescales. Consequently, benthic microbial communities contribute to early biogenic carbonate diagenesis. While the magnitude of microbial carbonate alteration is a function of time, (growth-) temperature, and the C_{org} share in the respective carbonate, microbially-induced changes in carbonate properties should be considered when interpreting these archives.

Zusammenfassung

Marine biogene Karbonate sind umfassende Archive von Paläo-Umweltbedingungen. Die Haupt-Umweltvariablen, die aus elementarer Zusammensetzung und Isotopenkomposition von Karbonaten hergeleitet werden können, sind Meeresoberflächentemperatur, Salinität und Ozeanzirkulation, sowie Spurenelementkonzentrationen. Diese Parameter sind entscheidend für das Verständnis klimatisch gekoppelter Paläo-Ozean und Atmosphärenbedingungen und erlauben darüber hinaus Aussagen über gegenwärtige und zukünftige Umweltvariablen. Die entsprechenden Signale in den Karbonat-Archiven können allerdings durch diagenetische Alteration verzerrt werden. Die dem zugrunde liegenden, abiotischen diagenetischen Prozesse werden intensiv erforscht. Ein entscheidender (Ko-) Faktor in der Frühdiagenese von Karbonaten sind benthische, mikrobielle Gemeinschaften. Die Wechselwirkungen zwischen Mikroorganismen und Mineralen prägten über geologische Zeiträume hinweg die Erd-Lithosphäre durch Karbonatbildung, -Auflösung, und Veränderung der Karbonat-Geochemie. Dennoch wurde der Einfluss benthischer Mikroorganismen auf Karbonat-Archive nach deren post-mortem Ablagerung in Sedimenten bisher selten in diagenetische Konzepte mit einbezogen. In der vorliegenden Studie wurden das Karbonat-Alterationspotenzial benthischer Mikroorganismen während der Frühdiagenese und die zugrunde liegenden Mechanismen unter Einbeziehung möglicher Konsequenzen für die Interpretation von Karbonat-Archiven untersucht.

Die Untersuchungen ergaben folgende Ergebnisse:

1) Die Inkubation aragonitischer *Arctica islandica* Schalenproben in (i) anoxischem Seewasser-Medium mit dem anaeroben, benthischen Bakterienstamm *Shewanella sediminis* HAW-EB3, und (ii) einem anoxischem Sediment-slurry, der die natürlichen mikrobiellen Gemeinschaften enthielt, führte zu mikrobiell-induzierter struktureller und geochemischer Veränderung der Schalen in einem Zeitraum von nur drei Monaten. Die Karbonatchemie der Medien spiegelte die beobachteten Schalenalterationen wider: Im Verhältnis zu den Kontrollen wurden ein deutlicher Anstieg in Alkalinität, gelösten, organischen Kohlenstoffkonzentrationen und dem Sättigungszustand von Aragonit festgestellt. Ferner stiegen die Konzentrationen der gelösten Calcium (Ca) und Strontium (Sr) Ionen in beiden Medien über die Zeit an. Anschließend abnehmende Ca^{2+} und Sr^{2+} Konzentrationen in dem mikrobiellen Kultur-Medium ließen auf Kationen Adsorption durch funktionelle Gruppen in mikrobiellen Zellwänden und extrazellulären polymeren Substanzen (EPS) schließen. Die Konzentrationsabnahme verhinderte darüber hinaus möglicherweise Karbonat-Präzipitierung im übersättigten Medium. Diese Annahme wurde von einer leichten Zunahme von Sr-Konzentrationen in exponierten Schalenbereichen gestützt, die

offenbar die Anlagerung mikrobieller Zellen und/oder EPS an das Karbonat widerspiegeln. Als die zugrunde liegenden Prozesse werden (i) die Hydrolyse der Chitinbestandteile in der Organik des Periostracums und der inter- und intrakristallinen organischen Matrix durch *S. sediminis* Chitinase, und (ii) die anaerobe Metabolisierung organischer Schalenbestandteile (vor allem des Periostracums) durch benthische mikrobielle Gemeinschaften in Winter-Sedimenten, die arm an organischem Kohlenstoff waren, vermutet. Beide Prozesse haben offensichtlich die Oberflächenstruktur der Schalen für Reaktionen mit dem umgenden Porenwasser erweitert, und somit die Auflösung der Schalen induziert. Die Isotopenzusammensetzung der Schalen zeigte kein deutliches mikrobiell-induziertes Alterationsmuster.

2) Aragonitische Skelettproben der hermatypischen Koralle *Porites sp*. wurden in (i) oxischen Seewassermedien in zwei Temperaturen (10°C und 20°C), die jeweils den aeroben benthischen Bakterienstamm *Alcanivorax borkumensis* SK2[T] beinhalteten, (ii) anoxischem Seewassermedium mit dem anaeroben Bakterienstamm *S. sediminis* HAW-EB3, und (ii) einem anoxischem Sediment-slurry mit den entsprechenden mikrobiellen Gemeinschaften inkubiert. In allen Inkubationen unterlief die Medium-Karbonatchemie im Verhältnis zu den Kontrollen einen Anstieg in pH, Alkalinität, und dem Sättigungszustand von Aragonit. In den oxischen *A. borkumensis*-Inkubationen wurde eine gleichzeitige Abnahme der Konzentrationen von Sr^{2+} (10°C Inkubation), sowie Ca^{2+} und Sr^{2+} (20°C Inkubation) beobachtet. Die daraus resultierende Zunahme der Verhältnisse von Magnesium zu Calcium (Mg/Ca) und Magnesium zu Strontium (Mg/Sr) deutete auf sekundäre Karbonat-Präzipitation hin. Die Veränderung der Parameter war in der 20°C Inkubation stärker, als in der 10°C Inkubation. Der Anstieg von Ca^{2+} und Sr^{2+} Konzentrationen in den anoxischen Inkubationen, und die respektive Abnahme der Mg/Ca und Mg/Sr Verhältnisse ließen auf Karbonat-Auflösung schließen. Die Oberflächen der Korallenproben zeigten keinerlei Anzeichen von Karbonat-Präzipitierung oder -Auflösung, und die Isotopenchemie der Proben hatte sich nach den Inkubationen nicht signifikant verändert ($p > 0.5$). Die Veränderungen in den Inkubationsmedien wurden offenbar durch (i) Carboanhydrase-Aktivität von *A. borkumensis*, und (ii), (iii) anaerobe mikrobielle Aktivität hervorgerufen. Für die fehlenden Anzeichen mikrobieller Alteration der Korallenproben war offenbar vor allem deren geringer Anteil organischen Kohlenstoffs (0.04%) verantwortlich.

3) Foraminiferenschalen wurden in (i) oxischem Seewassermedium mit einer Kultur des aeroben, benthischen Bakterienstammes *A. borkumensis* SK2[Z], (ii) anoxischem Seewassermedium mit dem anaeroben benthischen Bakterienstamm *S. sediminis* HAW-EB3, und (iii) einem anoxischen

Sediment-slurry und dessen natürlichen, mikrobiellen Gemeinschaften inkubiert. Schalen die in dem *A. borkumensis*-Medium inkubiert wurden, waren intensiv mit (vermutlich Karbonat-) Präzipitaten bedeckt. Das Medium spiegelte die beobachtete Präzipitierung durch ansteigenden pH, Alkalinität, dem Sättigungszustand von Calcit, und durch eine Abnahme der Mg^{2+}, Ca^{2+}, und Sr^{2+} Konzentrationen wider. Die sekundäre Karbonat-Präzipitierung wurde vermutlich durch Carboanhydrase-Aktivität von *A. borkumensis* induziert. In den anoxischen Inkubationen wurden keine mikrobiell-induzierten Änderungen der Medium-Chemie, der Schalenstruktur, oder der Schalengeochemie festgestellt. Dies war offenbar der geringen mikrobiellen Aktivität geschuldet, die in der Medienchemie reflektiert wurde.

Zusammengefasst demonstrieren die vorgelegten Studien, dass benthische, mikrobielle Aktivität das Potenzial hat, biogene Karbonatarchive in Bezug auf deren Oberflächenstruktur und Geochemie zu alterieren. Die mikrobielle Alteration fand darüber hinaus über sehr kurze Zeiträume (d.h., 25 Tage bis drei Monate), verglichen mit geologischen Zeiträumen, statt. Insofern tragen mikrobielle Gemeinschaften zur Frühdiagenese von biogenen Karbonaten bei. Auch, wenn das Ausmaß der mikrobiellen Karbonat-Alteration eine Funktion von Zeit, (Wachstums-)Temperatur und dem organischen Kohlenstoffanteil des jeweiligen Karbonates ist, sollten mikrobiell induzierte Veränderungen von Karbonat-Charakteristika bei der Interpretation dieser Archive in Betracht gezogen werden.

Chapter 1

General Introduction

1   Introduction

The origin of microbes can be traced back about 3.5 billion years (Schopf and Packer, 1987), and microbial influence on global biogeochemical cycling has been widely recognized (e.g. Jørgensen, 1982; Thamdrup et al., 1994; Gruber and Sarmiento, 1997; Arrigo, 2005). Recent estimates of microbial cell abundance on earth range between 9.2×10^{29} and 31.7×10^{29} cells (Kallmeyer et al., 2012) and microbes are literally present in all environments of the atmosphere, hydrosphere, and lithosphere. Considering furthermore, that microbial diversity is based on their versatile metabolic redox reactions that take place in direct exchange with the surrounding environment, the role of microorganisms in shaping their respective habitat and its constituents becomes evident. To date, microbe-mineral interaction has become the focus of numerous studies (Vasconcelos et al., 1995; Ehrlich, 1999; Benzera et al., 2011). However, despite the reports on microbial potential to alter biogenic carbonates, the role of benthic microbial communities in the alteration of these archives during early diagenesis has yet to be investigated.

1.1   Microorganisms

The domains of life to date are categorized through 16S ribosomal ribonucleic acid (rRNA) sequences of prokaryotes (bacteria and archaea) and the respective 18S rRNA sequences of eukaryotes. While the denotation "microbial" refers to unicellular organisms that can be found in all three domains and cover the whole phylogenetic tree of life, within this work the terms "microorganism", "microbe", and "microbial" will exclusively refer to the group of bacteria and, where appropriate, archaea.

Microbial cells have an average size of only 500 nm - 2 µm in diameter and contain neither a nucleus nor further cellular organelles facilitating metabolic reactions. Consequently, microbial metabolism is cell-wall facilitated, and direct exchange of metabolic educts and products takes place with their respective environment. To optimize this exchange, microorganisms have established a high cell surface area to volume ratio. In addition, microbial cell walls contain amphoteric functional groups that allow for pH-dependent cation complexation through deprotonation of the respective moieties (Beveridge and Murray, 1976; Beveridge and Koval, 1981; Fein et al., 1997; Small et al., 2009). Both characteristics lead to high microbial cell-surface reactivity.
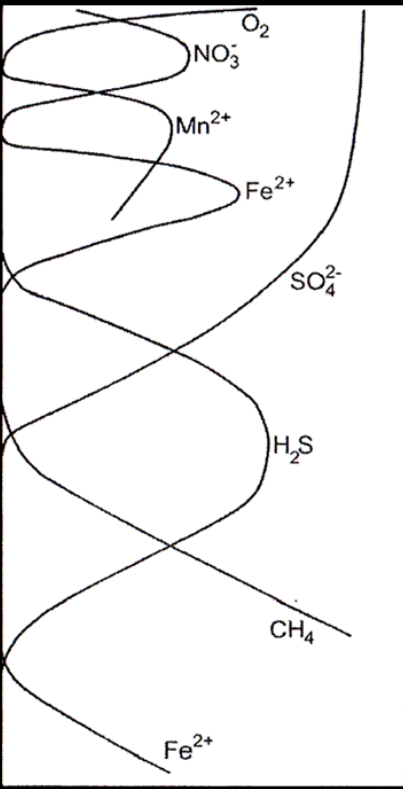
1.1.1 Microbial biofilms and extracellular polymeric substances

Biofilms consist of microbially secreted extracellular polymeric substances (EPS) that provide a habitat for microbial microcolonies (Costerton, 1987). The EPS gel-like substance provides mechanical stability for microbial cells in a diffusion-driven system, and allows for cell attachment to

solid substrate by generation of a hydrophobic environment (Donlan, 2002). Within the EPS, the continuous exchange of genetic material, nutrients and metabolites generates microenvironments of strong chemical heterogeneity (Hunter and Beveridge, 2005). The main EPS constituents include polysaccharides, proteins, nucleic acids, lipids, and humic substances that act as chelating agents (Sutherland, 2001) futhermore, analogous to the microbial cell wall, EPS contain functional groups that facilitate cation complexation (Guibaud et al., 2005).

### 1.1.2 Microbial life in marine sediments

Marine sediments provide a habitat for highly diverse microbial communities. Microbial distribution in the sediment is governed by the availability of electron acceptors for metabolic breakdown of labile organic carbon. The main available electron acceptors are oxygen (O_2), nitrate (NO_3^-), manganese (Mn(IV)), iron (Fe(III)), sulfate (SO_4^{2-}), and organic matter, that are distributed vertically in the sediments. The resulting vertical microbial zonation is based on the energy yield of the respective electron acceptors per mole organic carbon until it is exhausted (Jørgensen, 2006; Orcutt et al., 2011) (Fig. 1): Oxygen reduction in the upper parts of the sediment is vertically followed by anaerobic reduction of NO_3^-. In exhaust of NO_3^- the next energetically favorable electron acceptors are Mn(IV) that is reduced to Mn(II) and Fe(III) being reduced to Fe(II) as the oxidant. Further down the sediment, sulfate reduction, anaerobic oxidation of methane (AOM), and methanogenesis are the predominant microbial metabolic pathways. These metabolic redox processes by no means are hermetic, but intertwined: metabolic products of one microbial group can be used to fuel the metabolism of another, and microbial competition for electron donors can lead to usage of non-competitive substrates by microbial communities (Maltby et al., 2015). Consequently, marine sediments are intensely imprinted by benthic microbial activity.

Figure 1. Scheme of the biogeochemical zonation in marine sediments (modified after Jørgensen and Kasten, 2006). The main zones have been proposed by Froelich et al. (1979), associated Standard Gibbs free energies were added after Orcutt et al. (2011).

1.2   The marine carbonate system

Carbonate formation and dissolution in the marine realm are governed by the marine carbonate system that regulates the carbon dioxide (CO_2) exchange with the atmosphere: Atmospheric CO_2 dissolves in the oceans to form carbonic acid (H_2CO_3, or $CO_{2\ (aq)}$), that dissociates to bicarbonate (HCO_3^-) and carbonate (CO_3^{2-}) ions (Fig. 2). In equilibrium conditions, the respective thermodynamic constants are expressed in terms of ion activities:

$$K_0 \qquad K_1 \qquad K_2$$
$$CO_2(f) + H_2O \iff H_2CO_3 \iff HCO_3^- + H^+ \iff CO_3^{2-} + 2H^+ \qquad (1)$$
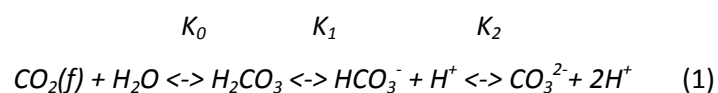
With $CO_2(f)$ representing the unhydrated CO_2 molecules in solution, and the equilibrium constants being formulated as:

$$K_0 = \frac{[H_2CO_3]}{[H_2O][CO_2(f)]} \qquad (1.1)$$

$$K_1 = \frac{[HCO_3^{2-}][H^+]}{[H_2CO_3]} \qquad (1.2)$$

$$K_2 = \frac{[CO_3^{2-}][H^+]}{[HCO_3^-]} \qquad (1.3)$$

The dissolved carbon dioxide forms are resumed as the total dissolved organic carbon (DIC):

$$DIC = [CO_2] + [HCO_3^-] + [CO_3^{2-}] \qquad (2)$$

At equilibrium conditions, seawater has a pH ranging between 7.9 and 8.4 (Pilson, 1998) and the rate and direction of reaction (1) is mainly determined by the total alkalinity (TA) of seawater:

$$[TA] = 2 [CO_3^{2-}] + [HCO_3^-] + [B(OH)_4^-] + [OH^-] - [H^+] \qquad (3)$$

The respective carbon species contributing to TA are defined as the carbonate alkalinity (CA):

$$[CA] = 2 [CO_3^{2-}] + [HCO_3^-] \qquad (3.1)$$

Formation and dissolution of carbonate ($CaCO_3$) structures in seawater is determined by the thermodynamic equilibrium constants K_1 (1.2) and K_2 (1.3), and follows the general principle of carbonate formation in aqueous solutions:

$$Ca^{2+} + 2 HCO_3^- <-> CaCO_3 + H_2O + CO_2 \qquad (4)$$

Calcium carbonate precipitates in two major mineralogical forms: rhombohedral calcite and orthorhombic aragonite. The differences in crystal structure lead to differing solubility of the two $CaCO_3$ polymorphs, with calcite being more stable than aragonite. The mineral-specific solubility product constant (K_{sp}^*) for $CaCO_3$ is expressed as follows:

$$K_{sp} = [Ca^{2+}] [CO_3^{2-}] \qquad (5)$$

The degree of saturation of any substance is determined by the ratio of the ion product to the solubility product constant. For calcium carbonate this is denoted as the $CaCO_3$ saturation state (Ω):

$$\Omega = \frac{[Ca^{2+}]_{SW}[CO_3^{2-}]_{SW}}{K_{sp}^{*}} \qquad (5.1)$$

where $[Ca^{2+}]_{sw}$ and $[CO_3^{2-}]_{sw}$ represent the concentrations of dissolved Ca^{2+} and CO_3^{2-} at a given temperature, salinity and pressure.

Consequently, seawater undersaturation with respect to $CaCO_3$ ($\Omega < 1$) induces mineral dissolution, while supersaturation ($\Omega > 1$) induces mineral precipitation.
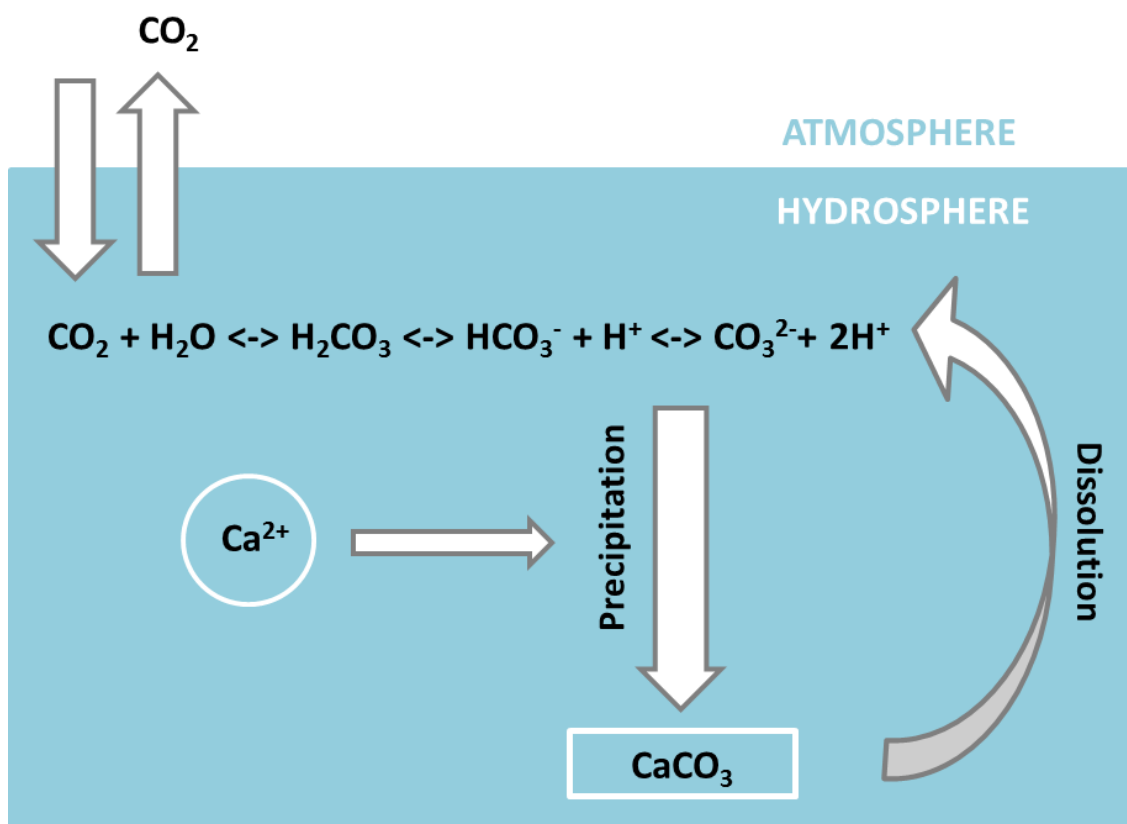
Figure 2. The marine carbonate system and related $CaCO_3$ precipitation and dissolution (modified after Kanwisher, 1960).

1.3 Marine biogenic carbonates

The diversity of biogenic carbonates in the marine realm encompasses structures ranging from microbially-induced stromatolite formations to metazoan exo- and endoskeletons. The underlying two main biomineralization pathways will therefore briefly be described in the following.

1.3.1 Biologically induced mineralization

Biologically induced mineralization is governed by the interaction of biological activity with the environment (Lowenstam, 1981) and is predominantly mediated by microbial communities (Frankel and Bazylinski, 2003, Dupraz, 2009). The influence of metabolic redox reactions on environmental pH and CO_2 concentrations fosters carbonate precipitation, often directly on cell walls (Weiner and Dove, 2003). Induced mineralization is furthermore facilitated through biofilms and associated EPS, and prominent examples for this biofilm-driven process are fossil and recent stromatolites (Braissant et al., 2009). The mineral structures deriving from induced-mineralization processes are unordered and vary in morphism, polymorphism and geochemical composition, thereby resembling inorganically precipitated minerals (Franke and Bazylinski, 2003).

1.3.2 Biologically-controlled mineralization

Biologically-controlled mineralization is almost exclusively conducted by metazoan organisms, and earliest calcifying metazoans can be traced back until the Proterozoic-Cambrian transition (Knoll et al., 2003). The process involves the active ion uptake from the surrounding environment, related transport to mineralization sites, and elaboration of an organic matrix from which nucleation subsequently takes place. Mineral nucleation, polymorphism, and morphology are under delicate physiological and genetic control and result in highly ordered minerals (Lowenstam and Weiner, 1989; Falini et al., 1996; Levi-Kalisman et al., 2001; Addadi, 2006), with the organic matrix being incorporated in the intra- and intercrystalline carbonate structure (Marin et al., 1996).

Biogenic carbonates focused on within this thesis originate from controlled biomineralization of bivalves, corals and foraminifera. While both the bivalve shell and the coral skeleton purely consisted of aragonite, the foraminiferal tests were calcitic and allowed for potential polymorph-dependent susceptibility of the samples to microbial alteration.

1.4 Paleoenvironmental application of biogenic carbonates

Understanding the variations in past oceanic and atmospheric conditions is a prerequisite for the evaluation of present - and potential future environmental variables. Fossil and recent metazoan carbonate exo- and endoskeletons are valuable archives for the reconstruction of paleoenvironmental conditions. This is owed to the fact that, during the biomineralization process trace elements of the surrounding environment are incorporated in the resulting calcium carbonate structure. Conservative elements in seawater like Mg^{2+}, Ca^{2+}, and Sr^{2+} with a comparably long residence time are well suited as proxies for paleo-ocean temperature reconstruction which is linked to most other climate variables (Beck et al., 1992). The inverse correlation between sea-surface

temperature (SST) and trace-element uptake allows for paleo-thermometry application of Sr/Ca ratios, foremost in aragonitic coral skeletons (e.g. Weber et al., 1973; Swart et al., 2002) and bivalve shells (e.g. Vander Putten et al.; 2000; Schöne et al., 2013), and of Mg/Ca ratios in calcitic foraminiferal tests (e.g. Nürnberg, 1995; Elderfield and Ganssen, 2000).

Moreover, stable carbon and oxygen isotopes (δ^{13}C and δ^{18}O) are frequently applied tools in paleoenvironmental research: Urey (1947) stated that variations in calcium carbonate δ^{18}O are directly related to temperature variations in the seawater in which $CaCO_3$ precipitation took place, therefore allowing for deduction of past-ocean temperature regimes. Furthermore the δ^{18}O composition in biogenic carbonate is reflecting the oxygen isotopic composition of the ambient seawater during calcification, from which, in combination with trace-elemental records, ocean thermohaline circulation patterns and ice-sheet dynamics can be deduced (Lea et al, 2000). Additionally, the δ^{13}C signature provides information on ocean circulation patterns, and the variability of atmospheric CO_2 concentrations (Duplecy et al., 1988).

To allow for accurate interpretation of these proxies the respective organisms must have precipitated the carbonate structures in equilibrium with their environment. However, genetic and physiological control on the biomineralization process, as well as metabolic and kinetic isotope fractionation, can compromise proxy-signature robustness (McConnaughey, 1989).

1.5 Alteration of biogenic carbonates

1.5.1 Diagenesis

Diagenesis is, per definition, the sum of physical, chemical, or biological processes that are altering sediments or sedimentary rocks after their deposition in water. Early diagenetic processes include organic matter degradation, and carbonate dissolution and compaction (Berner, 1980). The diagenetic impact on marine skeletal- and non-skeletal carbonates include the neomorphism of metastable carbonate polymorphs, and the dissolution and re-crystallization of sediment-deposited $CaCO_3$ structures leading to subsequent alteration of their isotopic composition through pore water-crystal lattice exchange (Bathurst, 1971, Brand and Morrison, 1987, Tucker and Bathurst, 1990). On the biological side, boring organisms that weather carbonate structures, thereby enhancing reactive surface areas have been included in diagenetic concepts (Golubic et al., 1975). The share of microbial influence in the early diagenetic alteration of carbonate structures, and specifically the role of benthic microbial communities after deposition in marine sediments has been acknowledged (Hillgärtner et al., 2001), but scarcely been investigated to date.

1.5.2 Microbe-carbonate mineral interaction

A wide range of microbial metabolic redox processes has the potential to alter carbonate structures through their influence on the marine carbonate system. While several metabolic activities induce carbonate precipitation through generation of carbonate alkalinity (e.g. photosynthesis, sulfate reduction, and methanogenesis) (Knoll, 1985; Talbot and Kelts, 1986; Braissant et al., 2007), others foster carbonate dissolution through generation of DIC (e.g. oxygen respiration; Walter and Burton, 1990). Benthic metabolic activity extends over the redox zonation in the sediments: Aerobic oxygen respiration in the upper, oxic sediment zone (Fig. 1) generates CO_2 that is shifting the carbonate system to the right (Eqn. 1), thereby inducing acidic conditions in the adjacent environment that foster carbonate dissolution. Anaerobic metabolic processes in the suboxic and anoxic zone of the sediment lead to the formation of HCO_3^- contributing to total- and carbonate alkalinity in the respective environment (Eqns. 3 and 3.1, respectively). The additional removal of CO_2 through methanogenesis leads to an increase in pH that could further induce carbonate precipitation through generation of CO_3^{2-} and a related increase in the carbonate saturation state (Ω) (Eqn. 5.1). Additionally, the EPS in microbial biofilms is a key player in carbonate precipitation, or inhabitation of this process, respectively (Dupraz et al., 2009; Decho, 2010). EPS monomers contain attached functional groups that complex cations involved in the precipitation process (i.e. Mg^{2+}, Ca^{2+}, and Sr^{2+}). The degradation or modification of EPS through the respective microbial community results in the release of metabolic HCO_3^- and the cations into the environment, and to subsequent carbonate precipitation through an increase in carbonate alkalinity and the Ω in the system (Decho, 2000). On the other hand, the affinity of EPS functional groups for Mg^{2+} and Ca^{2+} can inhibit carbonate precipitation by withdrawal of the cations from the environment (Flemming, 1995). Furthermore, the pure attachment of bacterial cells to minerals through EPS can lead to weathering (Uroz, et al., 2009; Krause et al., 2014), or etch pit formation (Davis et al., 2007). Eventually, even single bacterial cells can bind cations through cell-wall functional groups, thereby fostering carbonate precipitation or inhibition with the binding capacity being a function of pH (Beveridge and Murray, 1976).

2   Objectives

The main objective of this study was to constrain the role of benthic microbial activity in the alteration of biogenic carbonate archives during early diagenesis, and to identify the processes involved.

Three in-vitro laboratory experiments were conducted with biogenic carbonate hard parts incubated in natural seawater culture media including heterotrophic, benthic microbial strains and natural anoxic sediments to answer the related research questions:

- Is microbial alteration of biogenic carbonates at the seafloor and in the upper sediment column a significant component of the early diagenetic system in carbonate research?

- Are potential microbial alteration processes reflected in crystal structure, geochemistry, and isotopic composition of biogenic carbonates?

- Does microbial activity affect the stability of carbonate archives?

3 Publication outline

Chapters 2 - 4 present the results obtained during the PhD thesis "Microbial Alteration of Carbonate Archives". Each chapter is written in the form of a scientific manuscript, of which chapter 2 is in review for Sedimentology, chapter 3 is in preparation for submission to Sedimentology, and chapter 4 is an advanced draft. My contributions to each manuscript are described hereafter.

Chapter 2: Anaerobic microbial activity affects earliest diagenetic pathways of bivalve shells

Skadi M. Lange, Stefan Krause, Ann-Christine Ritter, Vanessa Fichtner, Adrian Immenhauser, Harald Strauss, and Tina Treude

In revision for publication in Sedimentology

This study was initiated by Tina Treude. Skadi Lange designed the experiments with input from Tina Treude and Stefan Krause. Sediment sampling was carried out by Skadi Lange with assistance from Johanna Maltby. Microbial cultivation was carried out by Skadi Lange with assistance from Stefan Krause. Medium sampling and measurements of carbonate-system parameters were carried out by Skadi Lange. Sample preparation, stereomicroscopy, fluorescence microscopy and scanning electron microscopy (SEM) were carried out by Skadi Lange, the latter with assistance from technical personnel. Electron microprobe (EMP) sample preparation and -mapping was carried out by Skadi Lange, the latter with assistance from technical personnel. Analyses for isotopic sample composition were carried out by Ann-Christine Ritter with assistance from technical personnel. Micro X-ray flourescence (μ-XRF) mapping was carried out by Vanessa Fichtner with assistance from technical personnel. The manuscript was written by Skadi Lange with input from all co-authors.

Chapter 3: Effects of heterotrophic bacterial activity on coral aragonite

Skadi M. Lange, Stefan Krause, Ann-Christine Ritter, Vanessa Fichtner, Thomas Huthwelker, Sebastian Büsse, Adrian Immenhauser, Harald Strauss, Stanislav N. Gorb, and Tina Treude

In preparation for submission to Sedimentology

This study was initiated by Tina Treude. Skadi Lange designed the experiments with input from Tina Treude and Stefan Krause. Sediment sampling was carried out by Skadi Lange with assistance from Stefan Krause. Microbial cultivation, medium sampling and measurements of carbonate-system parameters were carried out by Skadi Lange. Sample preparation, fluorescence microscopy and SEM were carried out by Skadi Lange. EMP sample preparation and -mapping was carried out by Skadi Lange, the latter with assistance from technical personnel. X-ray microtomography (μ-CT) scanning was carried out by Skadi Lange with assistance from Sebastian Büsse. Sample preparation and analyses for isotopic sample composition were carried out by Ann-Christine Ritter and Skadi Lange with assistance from technical personnel. μ-XRF mapping was carried out by Skadi Lange, Vanessa Fichtner, and Stefan Krause with assistance from Thomas Huthwelker. The manuscript was written by Skadi Lange with input from all co-authors.

Chapter 4: Effects of heterotrophic bacterial activity on calcitic foraminifera

Skadi M. Lange, Stefan Krause, Nicolaas Glock, and Tina Treude

Advanced draft

This study was initiated by Tina Treude. Skadi Lange designed the experiments with input from Tina Treude and Stefan Krause. Microbial cultivation, medium sampling and measurements of carbonate-system parameters were carried out by Skadi Lange. Sampling of foraminiferal tests was conducted by Nicolaas Glock. Sample preparation and SEM were carried out by Skadi Lange. EMP sample preparation was carried out by Skadi Lange with assistance of Nicolaas Glock. EMP mapping was carried out by Skadi Lange with assistance from technical personnel. The manuscript (in its current form) was written by Skadi Lange with input from Tina Treude.

4   References

Arrigo, K.R. (2005) Marine microorganisms and global nutrient cycles. *Nature*, **437**, 349-355

Bathurst, R.G.C (1975) Carbonate Sediments and Their Diagenesis**.** *Developments in Sedimentology*, Elsevier Science, Oxford, 640 pp.

Beck, J.W., Edwards, R.L., Ito, E., Taylor, F. W., Reciy, J., Rougerie, F., Joannot, P. Henin, C. (1992) Sea-Surface Temperature from Coral Skeletal Strontium/Calcium Ratios. *Science*, **257**, 644-647.

Benzera, K., Miot, J., Morin, G., Ona-Nguema, G., Skouri-Panet, F., Férard, C. (2011) Significance, mechanisms and environmental implications of microbial biomineralization. *Comptes Rendus Geoscience*, **343**, 2-3, 160-167.

Berner, R.A. (1980) EARLY DIAGENESIS A Theoretical Approach. Princeton Series in Geochemistry, (Ed Holland, H.D.), 241 pp.

Beveridge, T.J. and Murray, R.G.E. (1976) Uptake and Retention of Metals by Cell Walls of *Bacillus subtilis*. *Journal of Bacteriology*, **127**, 3, 1502-1518.

Beveridge, T.J. and Koval, S. F. (1981) Binding of metals to cell envelopes of Escherichia coli K-12. *Applied Environmental Microbiology*, **42**, 2, 325-335.

Braissant, O., Decho, A.W., Dupraz, C., Glunkk, C., Przekop, K.M., and Visscher, P.T. (2007) Exopolymeric substances of sulfate-reducing bacteria: Interactions with calcium at alkaline pH and implication for formation of carbonate minerals. *Geobiology*, **5**, 4, 401-411.

Brand, U., and Morrison, J.O. (1987) Biogeochemistry of Fossil Marine Invertebrates. *Paleoscene*, **6**.

Costerton, J.W. (1987) Bacterial Biofilms in Nature and Disease. *Annual Reviews in Microbiology*, **41**, 435-464.

Davis, K.J., Nealson, K.H., and Lüttge, A. (2007) Calcite and dolomite dissolution rates in the context of microbe-mineral surface interactions. *Geobiology*, **5**, 191-205.

Decho, A.W. (2010) Overview of biopolymer-induced mineralization: What goes on in biofilms? *Ecological Engineering*, **36**, 137-144.

Donlan, R.M. (2002) Biofilms: Microbial Life on Surfaces. *Emerging Infectious Diseases*, **8**, 881-890

Dupraz, C., Reid, P.R., Braissant, O., Decho, A.W., Normann, R.S., and Visscher, P.T. (2009) Processes of carbonate precipitation in modern microbial mats. *Earth-Science Reviews*, **96**, 141-162.

Ehrlich, H. L. (1999) Microbes as Geologic Agents: Their Role in Mineral Formation. *Geomicrobiology Journal*, **16**, 2, 135-153.

Elderfield, H., and Ganssen, G. (2000) Past temperature and δ^{18}O of surface ocean waters inferred from foraminiferal Mg/Ca ratios. *Nature*, **405**, 442-445.

Erez, J. (2003) The Source of Ions for Biomineralization in Foraminifera and Their Implications for Paleoceanographic Proxies. *Reviews in Mineralogy and Geochemistry*, **54**, 1, 115-149.

Falini, G., Fermani, S., and Goffredo, S. (2015) Coral biomineralization: A focus on intra-skeletal organic matrix and calcification. *Seminars in Cell & Developmental Biology*, **46**, 17-26.

Fein, J., Daughney, C.J., Yee, N., and Davis, T.A. (1997) A chemical equilibrium model for metal adsorption onto bacterial surfaces. *Geochimica et Cosmochimica Acta*, **61**, 3319-3328.

Field, C.B., Behrenfeld, M.J., Randerson, J.T., and Falkowski, P (1998) Primary production of the biosphere: integrating terrestrial and oceanic components. *Sience*, **281**, 237-240.

Flemming, H.C. and Wingender, J. (2010) The biofilm matrix. *Nature Reviews Microbiology*, **8**, 623-633.

Frankel, R.B., and Bazylinski, D.A. (2003) Biologically Induced Mineralization by Bacteria. *Reviews in Mineralogy and Geochemistry*, **54**, 1.

Freiwald, A. (1995) Bacteria-Induced Carbonate Degradation: A Taphonomic Case Study of *Cibicides lobatulus* from a High-Boreal Carbonate Setting. *PALAIOS*, **10**, 4, 337-346.

Froelich, P.N., Klinkhammer, G.P., Bender, M.L., Luedtke, N.A., Heath, G.R., Cullen, D., Dauphin, P., Hammond, D. and Hartman, B. (1979) Early oxidation of organic matter in pelagic sediments of the eastern equatorial Atlantic : suboxic diagenesis. *Geochimica et Cosmochimica Acta* **43**, 1057-1090

Golubic, S., Perkins, R.D., and Lukas, K. (1975) Boring Microorganisms and Microborings in Carbonate Substrates. In: *The Study of Trace Fossils III, A Synthesis of Principles, Problems, and Procedures in Ichnology*. Springer, Berlin, Heidelberg, Frey, R.W. (Ed.), 229-259.

Gruber, N., and Sarmiento, J.L. (1997) Global patterns of marine nitrogen fixation and denitrification. *Global Biogeochemical Cycles*, **11**, 2, 235-266.

Guibaud, G., Comte, S., Bordas, F., Dupuy, S., and Baudu, M. (2005) Comparison of the complexation potential of extracellular polymeric substances (EPS), extracted from activated sludges and produced by bacteria strains, for cadmium, lead and nickel. *Chemosphere*, **59**, 5, 629-638.

Hillgärtner, H., Dupraz, C. and Hug, W. (2001) Microbially induced cementation of carbonate sands: are micritic meniscus cements good indicators of vadose diagenesis? *Sedimentology*, **48**, 117 - 131.

Hunter, C.R. and Beveridge, T.J. (2005) Application of a pH-Sensitive Fluoroprobe (C-SNARF-4) for pH Microenvironment Analysis in Pseudomonas aeruginosa Biofilms. *Appied and Environmental Microbiology*, 2501-2510

Jørgensen, B.B. (1982) Mineralization of organic matter in the sea bed - the role of sulphate reduction. *Nature*, **296**, 643-645.

Jørgensen, B.B. (2006) Bacteria and Marine Biogeochemistry. In: *Marine Geochemistry* (Eds H.D. Schulz and M. Zabel), 173-207. Springer, Berlin, Heidelberg.

Jörgensen, B.B., and Kasten, S. (2006) Sulfur Cycling and Methane Oxidation. In: *Marine Geochemistry*, (Eds H.D. Schulz and M. Zabel), 271-309. Springer, Berlin, Heidelberg.

Kallmeyer J., Pockalny, R., Dhikari, R.R., Smith, D.C., and D´Hondt, S. (2012) Global distribution of microbial abundance and biomass in subseafloor sediment. *Proceedings of the National Academy of Sciences of the United States of America*, **109**, 40, 16212-16216.

Kanwisher, J. (1960) pCO_2 in Sea Water and its Effect on the Movement of CO_2 in Nature. *Tellus*, **12**, 2, 209-215.

Knoll, A.H. (1985) Exceptional Preservation of Photosynthetic Organisms in Silicified Carbonates and Silicified Peats. *Philosophical Transactions of the Royal Society B – Biological Sciences*, **311**, 1148.

Knoll, A.H. (2003) Biomineralization and evolutionary history. *Biomineralization*, **54**, 329-350.

Krause, S., Aloisi, G., Engel, A., Liebetrau, V. and Treude, T. (2014) Enhanced Calcite Dissolution in the Presence of the Aerobic Methanotroph *Methylosinus trichosporium*. *Geomicrobiology Journal*, **31**, 325-337.

Lea, D.W., Pak, D.K., and Spero, H.J. (2000) Climate Impact of Late Quaternary Equatorial Pacific Sea Surface Temperature Variations. *Science*, **289**, 1719-1742.

Levi-Kalisman, Y. Falini, G., Addadi, L., and Weiner, S. (2001) Structure of the nacreous organic matrix of a bivalve mollusc shell examined in the hydrated state using cryo-TEM. *Journal of Structural Biology*, **135**, 8-17.

Lowenstam, H.A. (1981) Minerals formed by organisms. *Science*, **211**, 1126-1131.

Lowenstam, H.A., and Weiner, S (1989) On biomineralization. Oxford University Press.

Maltby J., Sommer, S., Dale, A.W., and Treude, T. (2015) Microbial methanogenesis in the sulfate-reducing zone of surface sediments traversing the Peruvian margin. *Biogeosciences*, **13**, 1, 283-299

Marin, F., Smith, M., Isa, Y., Muyzer, G., Westbroek, P. (1996) Skeletal matrices, muci, and the origin of invertebrate calcification. *Proceedings of the National Academy of Sciences of the United States of America*, **93**, 1554-1559.

McConnaughey, T. (1989) ^{13}C and ^{18}O isotopic disequilibrium in biological carbonates: I Patterns. *Geochimica et Cosmochimica Acta*, **53**, 151-162.

Nürnberg, D., Bijma, J., and Hemleben, C. (1995) Assessing the reliability of magnesium in foraminiferal calcite as a proxy for water mass temperatures. *Geochimica et Cosmochimica Acta*, **60**, 5, 803-814.

Orcutt, B.N., Sylvan, J.B., Knab, N.J. and Edwards, K.J. (2011) Microbial Ecology of the Dark Ocean above, at, and below the Seafloor. *Microbiology and Molecular Biology Reviews*, **75**, 361-422.

Pilson, M.E.Q. (1988) An Introduction to the Chemistry of the Sea. Cambridge University Press.

Schöne, B.R. (2013) *Arctica islandica* (Bivalvia): A unique paleoenvironmental archive of the northern North Atlantic Ocean. *Global and Planetary Chan*ge, **111**, 199-225.

Schopf, J.W. and Packer, B.M. (1987) Early Archean (3.3-Billion to 3.5-Billion-Year-Old) Microfossils from Warrawoona Group, Austraila. *Science*, **237**, 4810, 70-73.

Small, T.S., Warren, L.A., and Roden, E.E. (2009) Sorption of Strontium by Bacteria, Fe(III) Oxide, and Bacteria-Fe(III) Oxide Composites. *Environmental Science and Technology*, **33**, 4465-4470.

Sutherland, I.W. (2001) Biofilm exopolysaccharides: a strong and sticky framework. *Microbiology*, **147**, 3-9.

Swart, P.K. (2002) A high-resolution calibration of Sr/Ca thermometry using the Caribbean coral *Montastraea annularis*. *Geochemistry, Geophysics, Geosystems*, **3**, 11.

Talbot, M.R. and Kelts, K. (1986) Primary and diagenetic carbonates in the anoxic sediments of Lake Bosumtwi, Ghana. *Geology*, **1**4, 912-916.

Thamdrup, B., Fossing, H., and Jørgensen, B.B. (1994) Manganese, iron and sulfur cycling in a coastal marine sediment, Aarhus bay, Denmark. *Geochimica et Cosmochimica Acta*, **58**, 23, 5115-5129.

Tucker, M.E. and Bathurst, R.G.C. (1990) Carbonate Diagenesis. Blackwell Scientific Publications, 320 pp.

Urey, H.C. (1947)The thermodynamic properties of isotopic substances. *Journal of the Chemical Society* (Resumed), 562-581.

Uroz, S., Calvaruso, C., Turpault, M.P. and Frey-Klett, P. (2009) Mineral weathering by bacteria: ecology, actors and mechanisms. *Trends in Microbiology*, **17**, 378-387.

Vander Putten, E., Dehairs, F., Keppen, E. (2000) High resolution distribution of trace elements in the calcite shell layer of modern Mytilus edulis: Environmental and biological controls. *Geochimica et Cosmochimica Acta*, **64**, 6, 997-1011.

Vasconcelos, C., McKenzie, J.A., Bernasconi, S., Grujic, D., and Tien, A.J. (1995) Microbial mediation as a possible mechanism for natural dolomite formation at low temperatures. *Nature*, **377**, 220-222.

Walter, L.M. and Burton, E.A. (1990) Dissolution of recent platform carbonate sediments in marine pore fluids. *American Journal of Science*, **290**, 6, 601-643.

Weber, J.N. (1973) Incorporation of strontium into reef coral skeletal carbonate. *Geochimica et Cosmochimica Acta*, **37**, 2173-2190.

Weiner, S. and Dove, P.M. (2003) An Overview of Biomineralization Processes and the Problem of the Vital Effect. *Reviews in Mineralogy and Geochemistry*, **54**, 1.

Chapter 2

Anaerobic microbial activity affects earliest diagenetic pathways of bivalve shells

Skadi M. Lange[1],*, Stefan Krause[1], Ann-Christine Ritter[2], Vanessa Fichtner[3], Adrian Immenhauser[2], Harald Strauss[3], and Tina Treude[4,5]

[1] *GEOMAR Helmholtz Centre for Ocean Research Kiel, Department of Biogeochemistry, Wischhofstr. 1-3, 24148 Kiel, Germany*

[2] *Ruhr-University Bochum, Department of Geology, Mineralogy, and Geophysics, Universitätsstr. 150, 44801 Bochum, Germany*

[3] *University of Münster, Department of Geology and Paleontology, Corrensstr. 24, 48149 Münster, Germany*

[4] *Department of Earth, Planetary, and Space Sciences, University of California, Los Angeles, 595 Charles E. Young Drive, Los Angeles, California 90095-1567, USA*

[5] *Department of Atmospheric and Oceanic Sciences, University of California, Los Angeles, 595 Charles E. Young Drive, Los Angeles, California 90095-1567, USA*

Abstract

The earliest diagenetic *post mortem* exposure of biogenic carbonates at the seafloor and in the uppermost sediment column results in the colonization of hard-part surfaces by bacterial communities. Some of the metabolic redox processes related to these communities have the potential to alter carbonate shell properties and hence affect earliest diagenetic pathways with significant consequences for archive data. During a three-month *in vitro* study, shell subsamples of the ocean quahog *Arctica islandica* (Linnaeus, 1767) were incubated in natural anoxic sediment slurries and bacterial culture medium of the heterotrophic *Shewanella sediminis* HAW-EB3. Bulk-media analyses revealed an over ten-fold increase in TA, DIC, and $\Omega_{Aragonite}$ and changes in Mg/Ca, Mg/Sr, and Sr/Ca ratios relative to the controls in both incubations. The latter were most effected in the anoxic-sediment incubation with a 25% decrease in Mg/Ca, relative to the control. Incubated shell-sample surfaces displayed weak but detectable surface dissolution features, and a minor loss in calcium concentrations. No such alteration features were detected in control media and shell samples. This study depicts the potential influence of benthic bacterial metabolism on biogenic carbonate archives during the initial stages of diagenetic alteration within a, compared to diagenetic time scales, relatively short experimental duration of only three months. Our results suggest that foremost the biological effect of bacterial cation adsorption on divalent-cation ratios has the potential to complicate proxy interpretation. Results shown here highlight the necessity to include bacterial metabolic activities in marine sediments in the study of diagenetic pathways and in paleo-environmental proxy application to these archives

Introduction

Marine biogenic carbonates represent one of the most important archives in paleoenvironmental reconstruction (Dodd, 1963; Williams *et al.*, 1982; Wilson and Opdyke, 1996;; Schöne, 2013; Immenhauser *et al.*, 2016). However, following deposition as part of the marine sediment record, biogenic carbonates are subject to diagenesis. Processes involved include degradation of organic matter, diagenetic neomorphism of metastable carbonate phases by thermodynamically more stable polymorphs, and related exchange of isotopes and elemental concentrations between marine pore water and carbonate crystal lattice. Traditionally, research on early carbonate diagenesis in the marine realm has primarily focused on abiotic factors (Bathurst, 1975; Berner, 1980; Swart, 2015). Clearly, this approach has limitations as carbonates in marine sediments are exposed to a manifold of microbial influences that were acknowledged (Walker, 1984; Nealson, 1997; Vasconcelos and McKenzie, 1997; Riding, 2000) but often not considered in detail. Microbial micritization of skeletal and non-skeletal carbonates is known to contribute to carbonate alteration (Tucker and Bathurst, 1990). Moreover, microbial micritization was found to considerably influence stabilization and cementation of shallow carbonate arenites (Hillgärtner *et al.*, 2001).

These processes, however, most likely do not capture all relevant microbially-induced changes in the early stages of seafloor and shallow burial diagenetic pathways. Given its great diversity in marine sediments, microbial metabolic activity has the potential to alter primary morphology, mineralogy, chemistry, and isotopic and elemental properties of biogenic carbonate archives, thereby affecting paleoenvironmental proxy application. Alteration can be induced in two manners: (i) either by microbial "mining" for intrashell organic matter (both intercrystalline and intracrystalline) with all related dissolution, reprecipitation, and neomorphic processes and (ii) by increasing the shell reactive surface of carbonate archives. The latter process takes place via the disintegration of intercrystalline organic matter, thus creating pathways and enhancing fluid-carbonate reactions rates.

The vertical distribution of electron acceptors in marine sediments induces a subsequent succession of heterotrophic bacteria of distinct redox-metabolic demands, with the bacterial preference of electron acceptors depending on the energy yield per mole organic carbon of the respective oxidant until it is exhausted (Foelich *et al.*, 1979; Jörgensen, 2006; Orcutt *et al.*, 2011). The resulting metabolic products potentially shift the (micro-) environmental chemistry to acidic or alkaline conditions that could support carbonate ($CaCO_3$) dissolution or secondary carbonate nucleation, respectively (Sotaert *et al.*, 2007). Corrosion of shell carbonate as a result of microbial aerobic oxidation was detected at the oxic-anoxic boundary layers of hydrocarbon seeps (Cai *et al.*, 2006; Himmler *et al.*, 2011). In addition, numerous studies report the direct attachment of bacterial cells to

minerals through extracellular polymeric substances (EPS), which are predominantly consisting of polysaccharides (Sutherland, 2001). The attachment subsequently leads to either mineral weathering (Paine, 1933; Decho *et al.*, 2005; Uroz *et al.*, 2009; Krause *et al.*, 2014), excavation and etch pit formation (Davis *et al.*, 2007), or inhibition of etch pit formation and mineral dissolution through detection of $CaCO_3$ high energy sites (Lüttge *et al.*, 2005).

A wide range of microbial metabolic activity facilitates carbonate precipitation (Greenfield, 1963; Chafetz and Buczynski, 1992; Dupraz *et al.*, 2004; Wright and Wacey, 2005; Sánchez-Román *et al.*, 2007), and biofilm EPS either functions as a precipitation-facilitating microenvironment (Aloisi *et al*, 2006) or, in contrast, as an inhibitor of precipitation (Decho, 2010). Kawaguchi and Decho (2002) experimentally tested the influence of EPS on $CaCO_3$ polymorphism, where partly lithified layers of EPS from a microbial stromatolite induced calcite crystal formation, while unlithified EPS layers induced the formation of aragonite. Many bacteria are capable of divalent-cation complexation (Beveridge and Murray, 1980; Konhauser *et al.*, 1993), and the EPS of sulfate-reducing bacteria (SRB) was reported to specifically bind calcium ions (Braissant *et al.*, 2007). The latter group is known to induce carbon-isotope fractionation (Londry and Des Marais, 2003), and evidence for a two-step fractionation process in Ca isotopes by non-stoichiometric dolomite precipitating SRB has recently been provided by Krause *et al*. (2014). Furthermore, cation complexation by functional groups of gram negative bacterial cell-wall lipopolysaccharides (LPS) was confirmed in previous studies (Schindler and Osborn, 1979; Coughlin *et al.*, 1983; Selvarengan *et al.*, 2010). These findings demonstrate the necessity for an improved understanding of microbially-induced carbonate alteration in marine sediments during earliest diagenetic stages.

A three-month *in vitro* experiment was conducted, during which shell subsamples of the bivalve *Arctica islandica* were incubated in either anoxic seawater medium that contained the marine benthic bacterial strain *Shewanella sediminis* HAW-EB3 or anoxic slurries of natural marine sediment. *Arctica islandica* is a widely used archive for reconstructing the more recent climate dynamics with a focus on the North Atlantic domain. It is the longest living non-colonial animal with a potential lifespan of over 500 years (Abele *et al.*, 2008; Butler *et al.*, 2013). Furthermore, passive diffusion and uptake of seawater and carbonate ions as well as the active transport of Ca^{2+} and Sr^{2+} into *A. islandica* hemolymph result in shell-$CaCO_3$ precipitation in near isotopic equilibrium with its environment (Schöne, 2013; Shirai *et al.*, 2014). The endobenthic, burrowing lifestyle of *A. islandica* accounts for immediate post-mortem exposure to pore fluids and related earliest diagenetic processes.

Out of the many bacterial species with metabolic carbonate-alteration potential *Shewanella sediminis* HAW-EB3 (Zhao *et al.*, 2005)*,* a facultative anaerobic, gram-negative, heterotrophic bacterium, was chosen for the bacterial-culture incubation. As a psychrophilic organism, first isolated

from marine sediments off the coast of Halifax, *S. sediminis* is a representative of cold-adapted bacteria. This organism is capable of oxidizing and fermenting *N*-acetylglucosamine (Zhao *et al.*, 2005), an integral constituent of the bivalve shell inter- and intracrystalline organic matrix (Watabe, 1965; Weiner and Addadi, 1991; Marin, 2012). While the bacterial culture allowed for distinct experimental effects that could be assigned to a single bacterial species with fermentative metabolic activity, the *in vitro* sediment incubation represented an anoxic sediment system with a natural anaerobic benthic microbial community that expectedly could foster carbonate precipitation processes through metabolic generation of alkalinity.

In the context of this study the following research questions were addressed: (i) Do microbial metabolic processes in marine sediments alter biogenic carbonates during seafloor and shallow burial processes? (ii) If so, are alteration processes recorded in crystal ultrastructure and mineralogy, chemistry, and isotopic composition of biogenic carbonates? (iii) If so, does microbial activity affect the diagenetic stability of carbonate (here specifically aragonite) archives?

Work presented here is of significance for those concerned with the interpretation of proxy data from marine carbonate archives in general and sheds light on microbe-carbonate interaction in the earliest marine pore-water diagenetic realm.

Methods

Seawater-medium and bacterial culturing

All incubations were carried out in media using modified natural seawater. North Sea water was sampled south-east of Heligoland (54° 06´ N, 008° 00´ E) during R/V Heincke cruise HE-411. The seawater was stored in a bulk container (IBC) at 10°C and circulated with an EHEIM compact 600 aquarium pump (EHEIM, Deizisau, Germany) to allow for steady oxygenation. Seawater aliquots for the experiment were sterilized with a UV water sterilizer (Wiegandt GmbH, Krefeld, Germany), followed by filtration through a 0.2 µm Whatman Polycap™ 75 AS Filter (GE Healthcare Life Sciences, Buckinghamshire, UK).

Shewanella sediminis HAW-EB3 was obtained from the Leibniz Institute DSMZ - German Collection of Microorganisms and Cell Cultures (Braunschweig, Germany). The culture was grown at 10°C in DSMZ medium 514 with the following composition (g l^{-1}): peptone, 5; yeast extract for bacterial media (Carl Roth, Karlsruhe, Germany), 1; Fe(III) citrate, 0.1; NaCl, 19.45; $MgCl_2 \bullet 6H_2O$, 12.6; Na_2SO_4, 3.24; $CaCl_2 \bullet 2H_2O$, 2.39; KCl 0.55; $NaHCO_3$, 0.16; KBr, 0.08; $SrCl_2$, 0.034; H_3BO_3, 0.022; NaF, 0.0024; $(NH_4)NO_3$, 0.0016; $Na_2HPO_4 \bullet 2H_2O$, 0.01; and 2.9 µl Na-silicate (Table 1). Medium pH was adjusted to 7.6 with 1M NaOH. Prior to inoculation, sterile culturing vials and -medium were purged with N_2/CO_2 gas

(80%/20%). From the third generation on, the *S. sediminis* culture was inoculated to sterile seawater-medium containing 100 mg l^{-1} additional Fe (III) citrate, 1000 mg l^{-1} yeast, and 200 μl Resazurin as redox/oxygen indicator. Seawater medium was purged with N_2 and 900 ml were transferred to a sterile 2 l gas-tight flat flange beaker with a final 1100 ml N_2 headspace of 0.2 bar above atmospheric pressure. At the experimental start, 10 ml of the *S. sediminis* culture were inoculated into the medium. Controls included the bacteria-free sterile seawater medium containing 100 mg l^{-1} additional Fe (III) and 1000 mg l^{-1} yeast with 200 μl sterile Resazurin. Both incubations were kept at 10°C during the whole experiment.

Table 1. Composition of the bacterial culture medium.

| Component	g L^{-1}
Peptone	5.00
Yeast extract	1.00
Fe(III) citrate	0.10
NaCl	19.45
$MgCl_2 \cdot 6H_2O$	12.60
Na_2SO_4	3.24
$CaCl_2 \cdot 2H_2O$	2.39
KCl	0.55
$NaHCO_3$	0.16
KBr	0.08
$SrCl_2$	0.034
H_3BO_3	0.022
Na-silicate	0.004
NaF	0.0024
$(NH_4)NO_3$	0.0016
$Na_2HPO_4 \cdot 2H_2O$	0.01

Anoxic sediment slurries

Anoxic sediment samples were obtained with R/V Suedfall from Piep, Büsum (German Bight, 54° 50´ N, 8° 89´ E), at 17 m water depth with a Van-Veen grab sampler. Samples were extricated from organic debris and subsequently stored at 0.9°C in sterile 1 l Duran flasks that were closed with sterilized butyl rubbers. Slurries were prepared from sediment and sterile seawater (1:2) in sterile 2 l gas-tight flat flange beakers with a 1100 ml N_2 headspace of 1 bar above atmospheric pressure. Controls contained sediment and sterile seawater (1:2) without shell samples. To each incubation 200 μl sterile Resazurin was added.

Bivalve shells

Arctica islandica bivalves were dredged alive in 2010 from the seafloor off NE Iceland at water depths between 40 and 120 meters for commercial purposes. Valves were disposed on shell mittens where they were collected briefly after disposal. Shells of adult specimens (~ 70 yrs) with approximately the same shell heights (distance umbo - ventral margin of ca. 10 cm) and valve thickness (2 - 5 mm) were selected for the alteration experiments. The maximum valve length of *A. islandica* is reported to reach approximately 13 cm. Note that growth rates of bivalves differ between specimen and bivalves with near-identical dimensions are not *a priori* of the same ontogenic age. Based on sclerochronological data, the age differences between specimens used in this study were estimated to be 10 years or less. Each of the selected valves was cleaned and divided into two halves using a thin diamond saw. Subsequently, a ca. 2.5 cm wide longitudinal shell section including portions of the central axis of the bivalve and the hinge was cut from one of the half valves. This longitudinal section was then cut into approximately 8 to 10 subsamples of similar dimensions, depending on the respective valve size. The subsamples were further sawn to approximately 1 x 1 x 0.5 cm sized pieces for the alteration experiments (Fig. 1) and all available shell parts except for the umbo regions were used for the incubations.
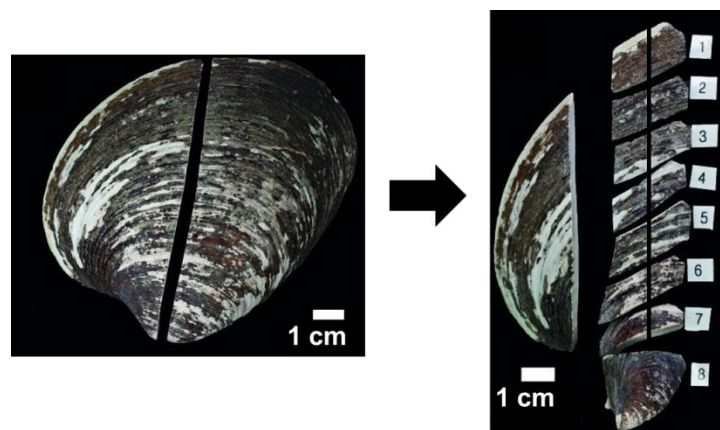

Figure 1. Scheme of shell-sample division. Valves were first cut in half and subsequently subdivided for the incubations (modified after Ritter *et al.*, 2017).

Incubation procedure and post-incubation treatment

Shell sample edges were fixed with sterile plastic cable ties. Inert Teflon-skimming ladles, disposed of handles, were used to attach sewing threads of differing lengths that were knotted to the cable ties and allowed for free distribution of samples in sterile 2 l flat flange beakers (Fig 2). Samples were

hanging in the *S. sediminis* culture medium, respectively, or deposited on the sediment surface. Flat flange beakers were smoothly pivoted every other day to mimic natural seawater movement. Seawater or medium sampling was conducted with N_2 flushed syringes and the withdrawn volumes (12 ml per sample point) were replaced with N_2 gas. The samples were transferred to sterile N_2 purged 50ml Duran flasks, from which the aliquots for subsequent analyses of medium carbonate chemistry were taken. After an incubation period of 101 days at 10°C in the dark, samples were carefully rinsed with sterile seawater, followed by ultra-purified water with a pH adjusted to ca. 8 with NH_4^+-solution. Samples were dried in parafilm-sealed Petri dishes at a temperature of 40°C and then stored at room temperature for upcoming analyses. Liquids from the shell-cleaning procedure (approx. 2 ml each) were preserved in formalin (final concentration 2%) at 4°C. For cell staining and analysis 100 µl of each liquid sample was transferred to 5 ml 1x sterile PBS and filtered on a 0.2 µm Whatman™ nucleopore™ polycarbonate membrane filter (GE Healthcare, 37586 Dassel). The filters were dried at room temperature, embedded in 1% low-melt agarose and dried at 37°C. Staining of the filters was conducted with 4,6 diamidino-2-phenylindole (DAPI) solution ($1\mu l \ ml^{-1}$) for 15 minutes in the dark, and filters were transferred to microscope slides. A drop of anti-fading agent (CitiFluor AF-1 solution) was placed on the filter before sealing with a cover slip. The slides were examined and photographed with a Zeiss Axio Imager.M2 stereomicroscope, using a DAPI filter-set, imaging was carried out with the ZEN pro 2012 software (Carl Zeiss Microscopy GmbH, Jena, Germany).
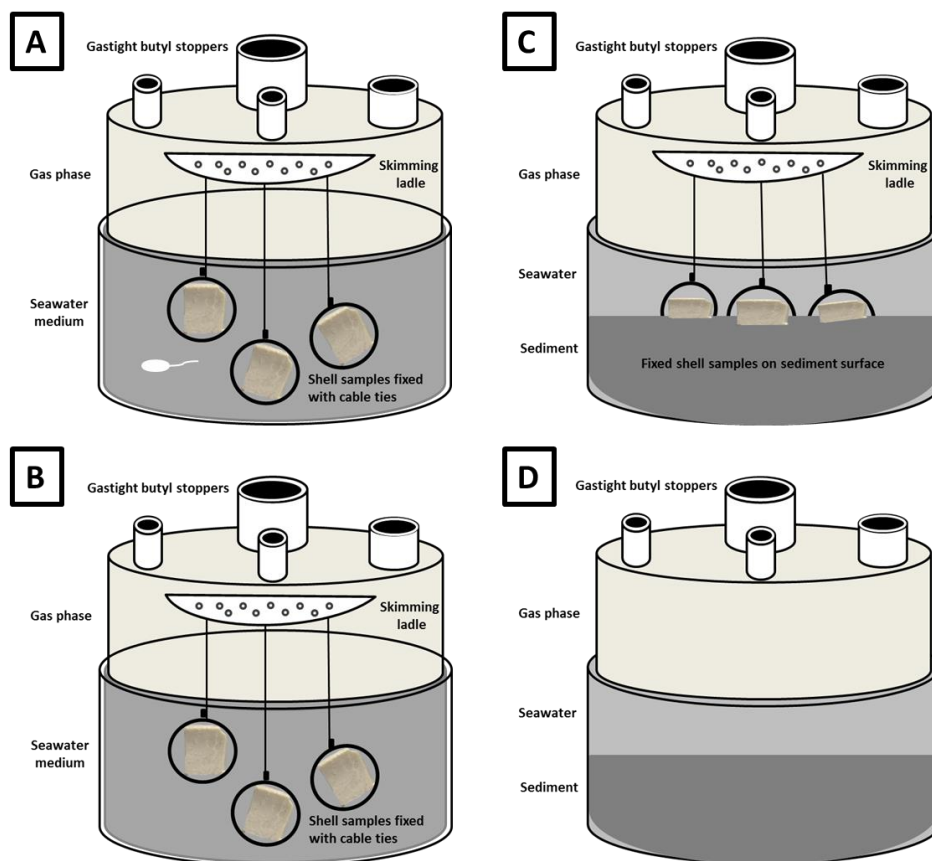
Figure 2. Sketch of the incubation set-ups: (A) The *S. sediminis* culture, (B) the cell-free control, (C) the anoxic sediment, and (D) the sediment control. In the upper top of a gas-tight flat flange beaker, an inert skimming ladle, disposed of the handle, served as mounting for shell samples that were fixed with cable ties and hung into the medium/deposited on the sediment via threads.

Media carbonate system and seawater geochemistry

Measured carbonate-system parameters were pH, Total Alkalinity (TA) and dissolved inorganic carbon (DIC). Measurements of pH and TA were done on the 12 ml aliquots. The pCO_2 and the saturation state of aragonite ($\Omega_{Aragonite}$) were calculated on the basis of measured pH and DIC concentrations after Zeebe and Wolf-Gladrow (2001) with MATLAB. Sampling for all parameters was conducted on a regular basis (daily to weekly). The pH was measured with a Schott Instruments Lab 850 pH sensor (SI analytics GmbH, Mainz, Germany). The pH sensor was calibrated with reference solution buffers (L4794, L 4796, L 4799, SI analytics GmbH, Mainz, Germany) according to the Physikalisch-Technische Bundesanstalt (PTB) and the National Institute of Standards and Technology (NIST). Measuring was conducted directly after sampling on the whole 12 ml aliquot with the pH electrode fixed to a stand. As the Duran flasks had to be opened during the measurements, the measuring time was restricted to 20 seconds each, to keep the equilibration of anoxic samples with

the ambience uniform. Total alkalinity was determined via open-cell titration of 0.5 ml samples with 0.01 M HCl in a titration vessel after Pavlova (Pavlova *et al.*, 2008), using a Metrohm 876 Dosimat plus (Ω Metrohm, Florida, USA). During titration, the vessel was continuously purged with N_2 to strip CO_2 released by acid addition. All TA measurements were calibrated with IAPSO seawater standard. For DIC measurements 1.8 ml samples were treated with 10 µl $HgCl_2$ saturated solution in a 2ml glass vial, crimp sealed and stored at 4°C for further processing. DIC concentration was determined as CO_2 with a multi N/C 2100 analyzer (Analytik Jena, Jena, Germany). The detection limit was 0.1 ppm with a precision of 2%. For minor- and trace-element concentrations 1 ml medium samples were acidified with 0.1 ml HNO_3 Suprapur$^{©}$ (1/100 v/v) in a 2 ml cryo vial and stored at 4°C for further processing. Divalent-cation concentrations were measured by inductively coupled plasma atomic emission spectroscopy (ICP-AES - JY 170 ULTRATRACE, HORIBA, Kyoto, Japan). The detection limit was 2 mg l^{-1} for Ca^{2+}, 6 mg l^{-1} for Mg^{2+} and 25 µg l^{-1} for Sr^{2+}, with a precision of 2%.

Shell structure and elemental composition

All incubated shell samples were examined with a Leica M 165 FC binocular stereomicroscope (Leica AG, Wetzlar, Germany) prior to and after incubation and pictures were generated using Leica AS software. Raman spectroscopy was conducted on one sample per incubation type prior to and after incubation with a LabRAM HR800 spectrometer (Horiba Jobin Yvon GmbH, Bensheim, Germany). Samples were analyzed at room temperature and studied without pre-treatment. Along a transect of 1 cm, the carbonate was excited with the 473 nm line of a Nd-YAG laser. Scattered radiation from the samples was measured in a 90° scattering geometry. The Raman spectra were obtained at an interval of 0.65 cm^{-1} (0 – 4000 cm^{-1}) and a slid width of 100 mm. Scanning electron microscopy (SEM) and electron-microprobe (EMP) mapping were applied post-incubation to one sample of each incubation type, the respective controls, and a non-incubated shell sample each, with a JEOL JXA 8200 Electron Probe Microanalyzer (JEOL Ltd., Tokyo, Japan). For SEM analyses, sample surfaces were air-dried and sputter-coated using a platinum/gold target. SEM images were acquired at 15 kV and a 19 µA filament current.

Prior to the EMP mapping, shell samples were sawn in quarters, and the sawn surface of one quarter each was ground using Hermes water grinding papers (P1200, P2400 and P4000) at a pressure of 25N. Each grinding step was followed by drying and cleaning of the sample with pressurized air. Samples were subsequently embedded in epoxy resin (Araldite® 2020, Huntsman, Texas, USA) and dried over night at 50°C. Electron microprobe mapping was applied to determine element distribution in relation to the surface structures observed by SEM. The maps were obtained by wavelength dispersive spectrometry (WDS) mode, and repeated to gather 8 accumulations of the selected area. Standards (Calcite, KAN1, VG-2, Strontianite A2_modernCoral) were measured prior

and after mapping to calculate trace element concentrations. For quantitative wavelength dispersive analyses the element concentrations were subsequently measured along a mapping area of 600 µm parallel to the exposed rim of the sample x 300 µm in the direction of non-exposed, inner sample parts, simultaneously measuring Mg (TAP, Ka), Sr (TAP, Strontianite), Ca (PETJ), P (PETH) and S (PETH). The measurements were conducted at a beam current of 50 nA with a beam spot size of 3 µm. Accelerating voltage was set to 15 kV.

Micro X-ray Fluorescence (µ-XRF) mapping of Sr^{2+} was conducted at the PHOENIX-beamline (Paul Scherrer Institute, Switzerland). Prior to the analyses, the samples were cut parallel to the growth direction and mounted on a glass holder in order to perform element mapping along a transect from the inner to the outer shell rim. The thin sections were polished to a thickness of 200 µm. During measurements a fixed Si (111)-monochromator (Bruker ACCEL, Germany) with an energy resolution higher than 0.5 eV was used. Fluorescence signals were collected with a detector equipped with four elements of silicon drift diodes (VORTEX, USA). With a beam-energy of 2800 eV the strontium *L*-edge electrons were excited to display the strontium distribution in the shell samples. Contemporary detection of phosphorus *K*-edge electrons allowed for discrimination between phosphorus-rich resin (Körapox 439, Kömmerling, Pirmasens, Germany) and phosphorus-poor *A. islandica* shell. The element maps were generated with a spatial resolution of 5 µm.

Carbon and oxygen isotope analyses

Following incubation, *A. islandica* shell material was sampled for its carbon- (δ^{13}C) and oxygen-(δ^{18}O) isotopic values. Samples were retrieved from one incubated shell block per incubation type. Sample material was scratched off with a scalpel directly beneath the outer organomineralic (periostracal), the inner biomineralic (aragonitic) parts of the shell (see Ritter *et al.*, 2017, for a detailed description of the sampling procedure), as well as from all surfaces of subsamples exposed to the ambient medium. A total of 0.4 ± 0.04 mg of the sub-sample were transferred into glass vials and dried at 105°C for 48 hours. The glass vials were then closed gastight and transferred into an autosampling device at 70°C. The atmosphere within the vials was removed by flushing with helium gas, and a few drops of phosphoric acid were added to the sample. Carbon- and oxygen isotope values were subsequently measured from the liberated CO_2 gas using a Thermo Finnigan MAT253 mass spectrometer (Thermo Fisher Scientific Inc., Waltham, USA) interfaced to a GasBench. Carbon and oxygen isotope results are given in ‰ relative to the VPDB standard. For correction of the measured data, international standards CO1, CO8 and NBS-19 as well as an in-house standard have been measured additionally to the samples.

Results

Seawater-medium

During all incubations, no color change in the added resazurin/resorufin indicator from colorless (anoxic conditions) to pink (partially or fully oxic conditions) was observed, confirming continuous anoxic conditions. Clear trends were observed in pH, TA and $\Omega_{Aragonite}$, and divalent-cation ratios in the medium chemistry of both the *S. sediminis* incubation and the anoxic-sediment. The cell-free control medium had fluctuating values in all measured parameters that hint at spurious mistakes, but showed no trend in the development of any of the parameters over time. The increasing pH, TA and $\Omega_{Aragonite}$ in the sediment control reflected natural anoxic sediment conditions with live bacterial communities, and no trend in medium divalent-cation concentration and/or -ratios was observed.

Total alkalinity (TA), DIC and $\Omega_{Aragonite}$ in both incubation media increased markedly during the incubation period (Figs.3, 4). The initial pH of 7.3 in the *S. sediminis* culture medium decreased to 7.1 on day 4 and increased to 7.6 on day 31. After a decrease to pH 7.5, the pH increased to values between pH 8 and 7.7 at the end of the experiment (Table 2). Total alkalinity increased from 1.8 to 22.8 mmol kg^{-1} over the entire incubation period. Undersaturation with respect to Aragonite at the experimental start was followed by an increase in $\Omega_{Aragonite}$ from 1.1 to 10.2 (Fig. 3A). The dissolved inorganic carbon (DIC) increased from 1.4 to 22.5 mmol l^{-1} (Fig. 3B), and pCO_2 increased from 1463 to 9467 µatm (Table 2). In the anoxic-sediment incubation, pH values were fluctuating between 7.7 and 7.9 throughout the experimental duration. Total alkalinity increased from an initial 2.9 to 6.3 mmol kg^{-1}, $\Omega_{Aragonite}$ from 1.9 to 4.9 (Fig. 4A), and DIC concentrations went from 2.8 to 6.2 mmol l^{-1} (Fig. 4B). The pCO_2 values were not tightly correlated to pH: The initial pCO_2 of 764 µatm increased to 2080 µatm on day 1 and varied between 1458 and 2094 µatm until the end of the experiment (Table 2).

Ca^{2+} concentration in the *S. sediminis* culture medium increased from an initial 10.3 mmol l^{-1} to 11.3 mmol l^{-1} on day 31, stayed at values between 10.9 and 10.7 mmol l^{-1} and finally decreased to 10.5 mmol l^{-1} at the very end of the experiment (Fig. 3D). Mg^{2+} and Sr^{2+} concentrations decreased from an initial 52.9 to 49.5 mmol l^{-1} and from 86.7 to 79.4 µmol l^{-1}, respectively (Fig.3C, 3E). Consequently, the Mg/Ca ratio decreased from an initial 5.1 to a constant value of 4.7 at the end of the experiment, and the Sr/Ca ratio decreased from 8.4 to 7.6, while the Mg/Sr ratio slightly increased from 0.61 to 0.62 (Fig. 3F, 3G, 3H). In the anoxic-sediment incubation a strong increase in Ca^{2+} from initial 10.3 to 13.8 mmol l^{-1}, in Mg^{2+} from 52.5 to 53.4 mmol l^{-1}, and in Sr^{2+} from 86.4 to 96.8 µmol l^{-1} during the experiment (Fig. 4C, 4D, 4E) led to a decrase in the Mg/Ca ratio from an initial 5.1 to 3.9, in the Mg/Sr ratio of 0.06 units, and in the Sr/Ca ratio from 8.4 to 7.0 (Fig. 4F, 4G, 4H, Table 2).

None of the trends in the *S. sediminis* incubation were observed in the carbonate chemistry of the cell-free control medium, where pH and TA remained stable with values around pH 8 and a TA of 2.3 mmol kg^{-1}, while $\Omega_{Aragonite}$ values fluctuated between 2.7 and 1.7 at the end of the experiment, with a drop to 1.4 on day 51 (Fig. 3A). DIC increased from an initial 2.4 to 2.7 mmol l^{-1} on day 70 and commuted in ranges of 1.9 and 2.2 mmol l^{-1} towards the end of the experiment (Fig. 3B). The pCO$_2$ values ranged between 428 and 540 µatm with two peaks on day 20 (616 µatm) and day 37 (717 µatm), and no trend was recognizable in the values throughout the experiment (Table 2). Ca^{2+}, Mg^{2+} and Sr^{2+} concentrations ranged between 10.4 and 10.1 mmol l^{-1}, 53.1 and 51.2 mmol l^{-1}, and 87.5 and 82.5 µmol l^{-1}, respectively (Fig. 3C, 3D, 3E). Consequently, the Mg/Ca ratio was at a constant 5.1 and the Mg/Sr ratio remained stable at 0.6 during the whole experiment, while the Sr/Ca ratio moderately decreased, compared to the sample bearing sediment, from 8.4 to 8.2 (Fig. 3F, 3G, 3H).

The pH in the sediment control slightly decreased with values fluctuating between 7.7 and 7.9 (Table 2). Total alkalinity increased from 6.7 to 12.0 mmol kg^{-1}, and $\Omega_{Aragonite}$ increased from an initial value of 3.6 to 6.6 during the experiment (Fig. 4A). DIC concentration increased from an initial 6.5 mmol l^{-1} to 10.8 mmol l^{-1} at day 70, and decreased to 10.7 mmol l^{-1} , dropped to 7.2 at day 51, and increased to values between 10.1 and 9.0 towards the end of the experiment (Fig. 4B). The pCO$_2$ values predominatly ranged between 2100 and 3600 µatm, dropped to 1738 and 1675 µatm on days 2 and 3, respectively, and increased to 5957 µatm on day 37 (Table 2). Ca^{2+} concentrations fluctuated between 10.2, 10.6 and 10.1 mmol l^{-1}, while Mg^{2+} concentrations increased from an initial 51.3 to 52.5 mmol l^{-1} at day 48 and further decreased to a value of 50.1 mmol l^{-1} towards the end of the experiment. Sr^{2+} concentrations decreased from 87.7 to 86.1 µmol l^{-1} (Fig. 4C, 4D, 4E). The Mg/Ca ratio decreased from 5.1 to 4.9, the Mg/Sr ratio varied around 0.6, and the Sr/Ca ratio decreased from initial 8.6 to 8.4 (Fig. 4F, 4G, 4H; Table 2).

Table 2. Overview of relevant hydrochemical parameters measured in the frame of this study.

|	Ca (mmol l^{-1})	Mg (mmol l^{-1})	Sr (µmol l^{-1})	pH	TA (meq l^{-1})	Ω_{Arag}	DIC (mmol l^{-1})	pCO_2 (µatm)	Ca (mmol l^{-1})	Mg (mmol l^{-1})	Sr (µmol l^{-1})	pH	TA (meq l^{-1})	Ω_{Arag}	DIC (mmol l^{-1})	pCO_2 (µatm)
Bulk seawater									**Bulk seawater**							
t0 (day 1)	10.08	51.60	85.00	8.06	2.34	2.38	2.44	438.46	10.08	51.60	85.00	8.06	2.34	2.38	2.44	438.46
S. sediminis									**Cell-free control**							
t0 (day 1)	10.33	53.13	87.51	7.31	1.92	0.3	1.43	1462.96	10.39	53.13	87.51	8.05	2.34	2.4	2.44	449.22
t1 (day 2)	10.28	52.35	85.69	7.54	1.72	0.8	2.64	1608.89	10.22	52.35	85.69	8.26	2.30	(3.9)	2.59	284.38
t2 (day 3)	10.22	52.69	85.79	7.21	2.15	0.1	1.03	1313.69	10.33	52.69	85.79	8.09	2.30	2.7	2.56	427.69
t3 (day 4)	10.21	50.97	83.37	7.18	3.07	0.1	0.86	1171.12	10.07	50.97	83.37	8.06	2.30	2.5	2.54	456.43
t4 (day 5)	10.21	51.69	84.52	7.14	3.14	0.2	1.32	1960.60	10.12	51.69	84.52	8.04	2.30	2.4	2.55	480.96
t5 (day 9)	10.10	51.81	84.71	7.25	4.75	1.1	1.49	1740.62	10.10	51.81	84.71	8.07	2.30	2.5	2.49	436.73
t6 (day 13)	10.41	51.41	84.41	7.38	7.74	1.5	5.08	4445.76	10.10	51.41	84.41	8.04	2.26	2.3	2.48	467.76
t7 (day 16)	10.55	52.41	85.83	7.41	8.55	1.6	6.42	5252.56	10.23	52.41	85.83	8.05	2.30	2.4	2.47	454.74
t8 (day 20)	10.98	53.83	87.27	7.32	9.27	2.0	8.04	8044.55	10.58	53.83	87.27	7.92	2.34	1.9	2.45	616.16
t9 (day 23)	10.67	53.84	87.90	7.46	9.50	4.4	7.71	5635.28	10.58	53.84	87.90	8.08	2.34	2.7	2.53	433.09
t10 (day 31)	11.34	52.50	85.00	7.60	13.34	4.0	11.30	6002.67	10.34	52.50	85.00	8.05	2.26	2.6	2.61	480.51
t11 (day37)	10.95	N/A	N/A	7.50	15.33	4.5	13.31	8884.99	10.10	N/A	N/A	7.90	2.38	1.9	2.72	717.36
t12 (day 44)	10.96	53.11	86.62	7.48	17.59	5.2	15.86	11078.87	10.48	53.11	86.62	8.02	2.34	2.6	2.74	542.36
t13 (day 51)	10.68	51.85	83.91	7.49	19.93	6.1	18.31	12503.44	10.22	51.85	83.91	7.91	2.34	1.4	1.95	502.21
t14 (day 58)	10.90	51.36	83.66	7.55	20.12	(20.9)	18.13	10799.50	10.12	51.36	83.66	7.93	2.30	N/A	N/A	N/A
t15 (day 65)	10.95	51.57	83.07	8.02	22.99	(19.6)	21.47	N/A	10.16	51.57	83.07	7.96	2.38	N/A	N/A	N/A
t16 (day 72)	10.79	51.24	82.72	7.97	22.80	10.5	22.45	N/A	10.10	51.24	82.72	7.95	2.38	1.7	2.18	510.42
t17 (day 101)	10.49	51.22	82.46	7.70	23.38	10.2	22.45	9466.92	10.11	51.22	82.46	7.97	2.41	1.8	2.18	486.58
Anoxic sediment									**Anoxic sediment control**							
t0 (day 1)	10.26	52.49	86.37	7.89	2.45	1.9	2.83	764.29	10.16	51.28	87.67	7.83	5.98	5.9	N/A	3111.90
t1 (day 2)	10.07	51.10	84.66	7.85	3.07	2.1	3.41	1012.3	10.34	51.98	86.14	7.90	6.21	4.6	6.59	1738.01
t2 (day 3)	10.31	52.18	86.40	N/A	3.45	N/A	4.20	N/A	10.09	50.67	85.42	7.92	6.55	4.8	6.66	1674.95
t3 (day 4)	10.26	51.68	86.06	7.70	3.64	1.9	4.30	1813.26	10.15	50.41	87.20	7.80	6.63	3.9	7.05	2354.16
t4 (day 5)	10.43	52.58	87.31	7.73	3.76	1.9	3.82	1502.33	10.19	51.02	88.07	7.85	6.82	4.6	7.33	2176.00
t5 (day 9)	10.36	51.92	87.17	7.73	4.06	N/A	4.84	N/A	10.27	51.30	88.44	7.89	7.66	4.9	7.09	1914.76
t6 (day 13)	10.50	52.58	88.01	7.68	4.29	2.1	4.71	2080.43	10.37	51.51	86.99	7.77	N/A	4.0	7.49	2683.17
t7 (day 16)	10.53	52.44	87.92	7.81	4.41	2.6	4.47	1458.00	10.16	50.53	88.02	7.83	7.66	4.5	7.67	2386.83
t8 (day 20)	10.50	52.15	87.29	7.80	4.14	N/A	N/A	N/A	10.42	51.25	90.82	7.91	8.81	5.9	8.17	2104.14
t9 (day 23)	10.73	52.90	88.99	7.82	4.29	3.0	4.83	1538.83	10.56	52.52	90.16	7.81	8.81	5.7	9.82	3203.04
t10 (day 31)	10.77	52.39	88.49	7.72	4.33	2.3	4.72	1899.99	10.58	51.93	86.99	7.80	N/A	5.6	9.71	3242.39
t11 (day37)	10.77	N/A	87.63	7.82	4.60	3.0	4.84	1542.02	10.28	N/A	89.30	7.65	9.93	4.2	10.47	4956.87
t12 (day 44)	11.31	52.41	90.12	7.87	5.10	3.8	5.29	1497.93	10.52	51.74	87.18	7.85	10.73	6.9	10.69	3173.45
t13 (day 51)	11.91	54.45	94.72	7.79	5.06	2.3	3.62	1237.48	10.28	50.49	85.17	7.69	10.54	3.2	7.25	3129.00
t14 (day 58)	11.85	52.97	92.22	7.80	5.21	N/A	N/A	N/A	10.06	50.52	87.60	7.77	11.11	4.8	9.38	3360.23
t15 (day 65)	11.95	52.07	91.30	7.76	5.44	3.4	5.71	2093.88	10.36	50.62	87.35	7.78	11.11	5.0	9.20	3219.52
t16 (day 72)	12.12	51.32	91.09	7.78	5.75	3.5	5.57	1949.21	10.37	50.25	86.07	7.77	11.69	5.3	10.13	3628.90
t17 (day 101)	13.79	53.42	96.81	7.82	5.90	4.9	6.24	1988.06	10.23	50.13	86.07	7.78	12.26	5.0	9.44	3303.51
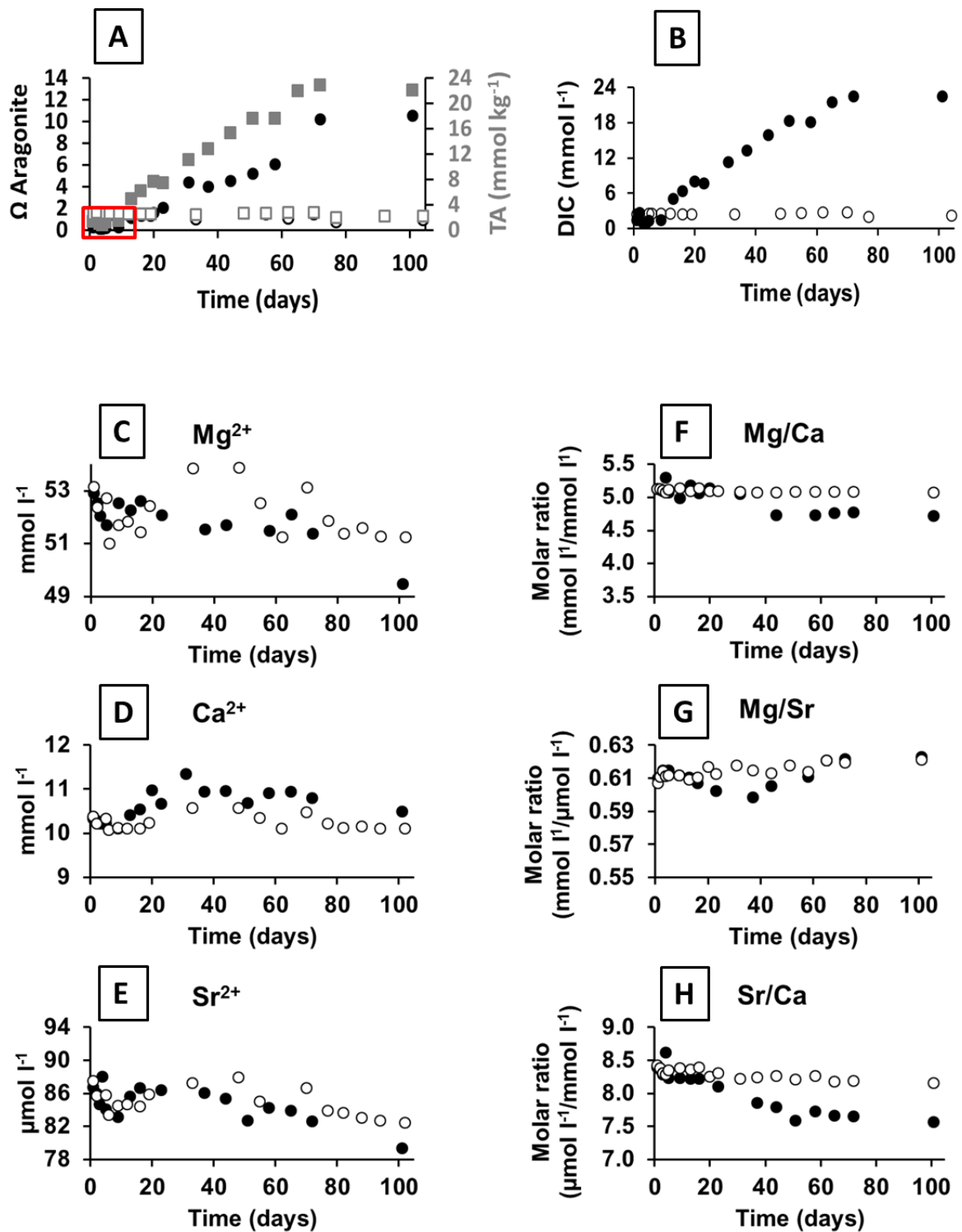
Figure 3. Medium chemistry of the *S. sediminis* incubation: Temporal development of (A) $\Omega_{Aragonite}$ (circles) and total alkalinity (TA) (squares), (B) DIC, (C-E) divalent-cation concentrations, and (F-H) divalent-cation ratios. Solid symbols show bulk-medium values, open symbols show control values. Note the $\Omega_{Aragonite}$ undersaturation at the experiment start, as well as the continuous variation in the cation-control concentration apparently caused by spurious errors.
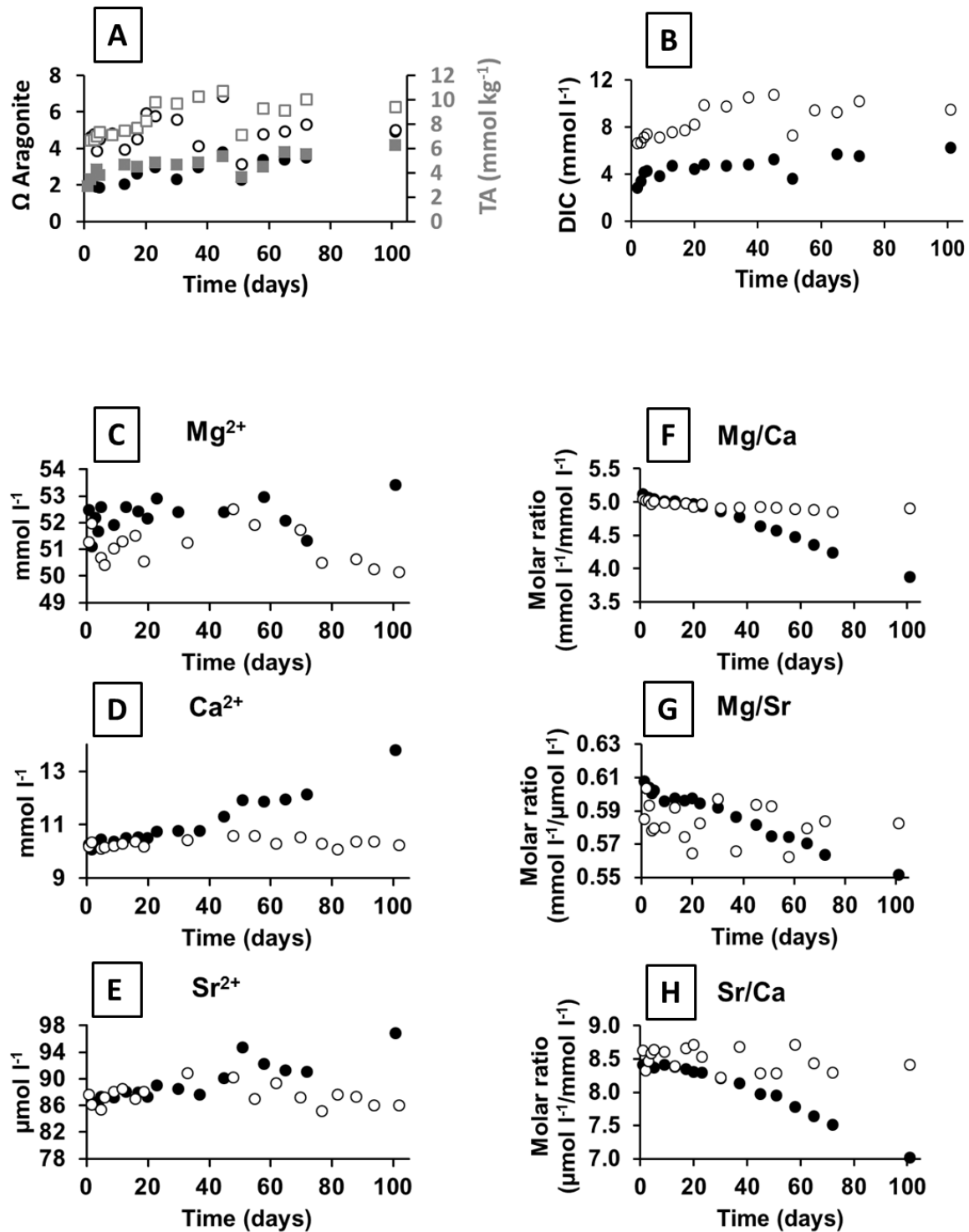
Figure 4. Medium chemistry of the anoxic-sediment incubation: Temporal development of (A) $\Omega_{Aragonite}$ (circles) and Total Alkalinity (TA) (squares), (B) DIC, (C-E) divalent-cation concentrations, and (F-H) divalent-cation ratios. Solid symbols show bulk-medium values, open symbols show control values. Note the continuous variation in the cation-control concentration apparently caused by spurious errors.

Shell surface structure and bacterial abundance

Stereomicroscopic examination prior to- and after the incubation displayed partial loss of surface material at areas of shell samples, that were exposed to both the *S. sediminis* culture and the anoxic sediment (Fig. 5B, 5D). Further SEM- examination of post-incubation samples revealed stepwise corrosion of surficial shell structures compared to the sample incubated in the cell-free control (Fig. 6). Filtered liquid samples from the shell-cleaning procedure of the *S. sediminis* culture and the anoxic sediment contained dense biofilm fragments, visualized by the DAPI staining (Fig. 7), foremost in the bacterial culture, while the cell-free control liquid did not display any bacterial cells.
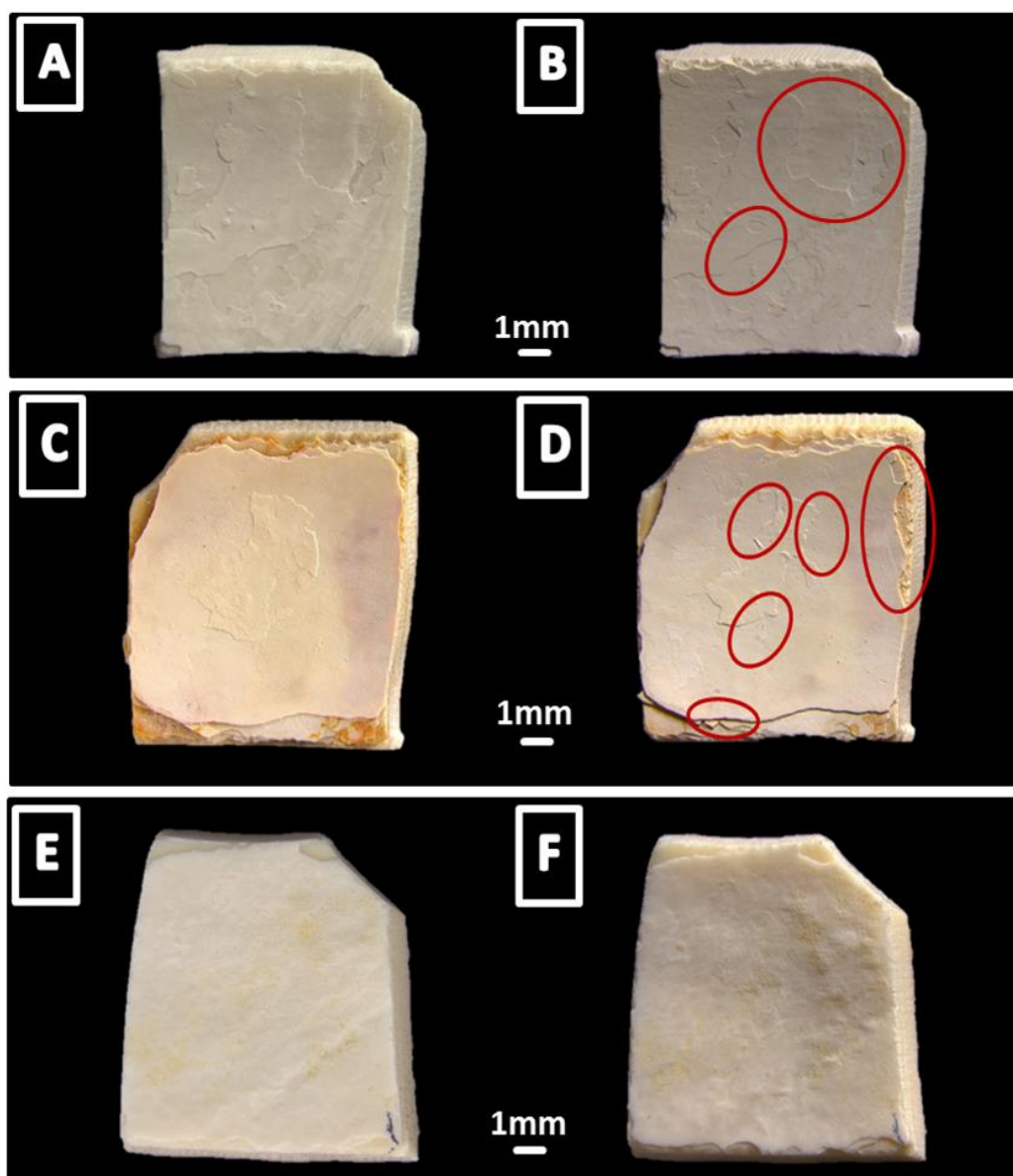
Figure 5. Stereomicroscopic pictures of shell samples prior to- (left) and after the incubation (right). Pictures show samples that were incubated in (A,B) the bacterial culture, (C,D) the anoxic sediment, and (E,F) the cell-free control. Red marks display macroscopically visible surface-alteration features. Mark that light regimes were not 100% reproducible prior to- and after the incubations.
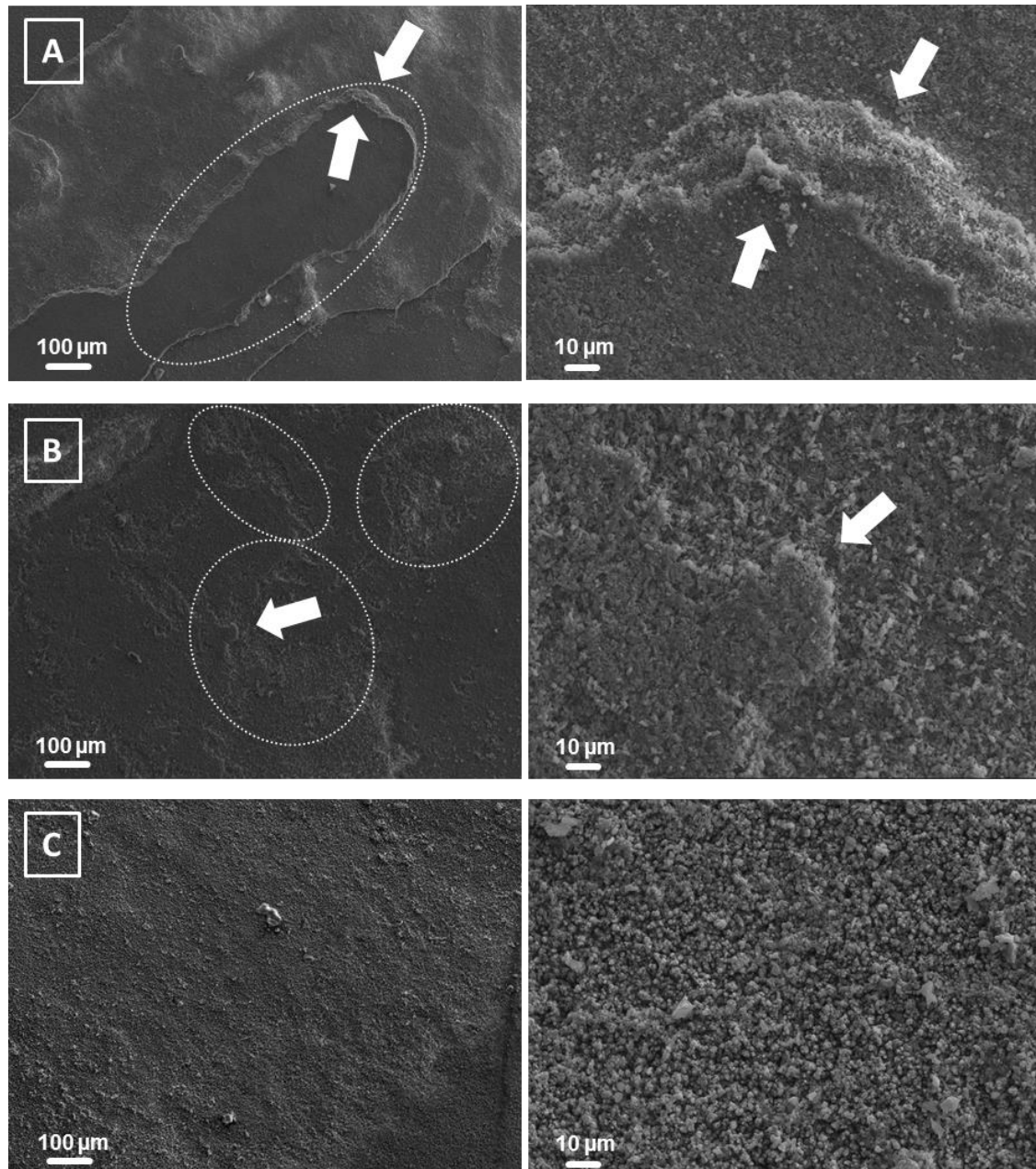
Figure 6. Scanning Electron Microscopy (SEM) pictures of shell samples incubated in (A) the *S. sediminis* culture, (B) the anoxic sediment, and (C) the cell-free control. Dotted circles indicate altered areas, arrows indicate surface-dissolution features.
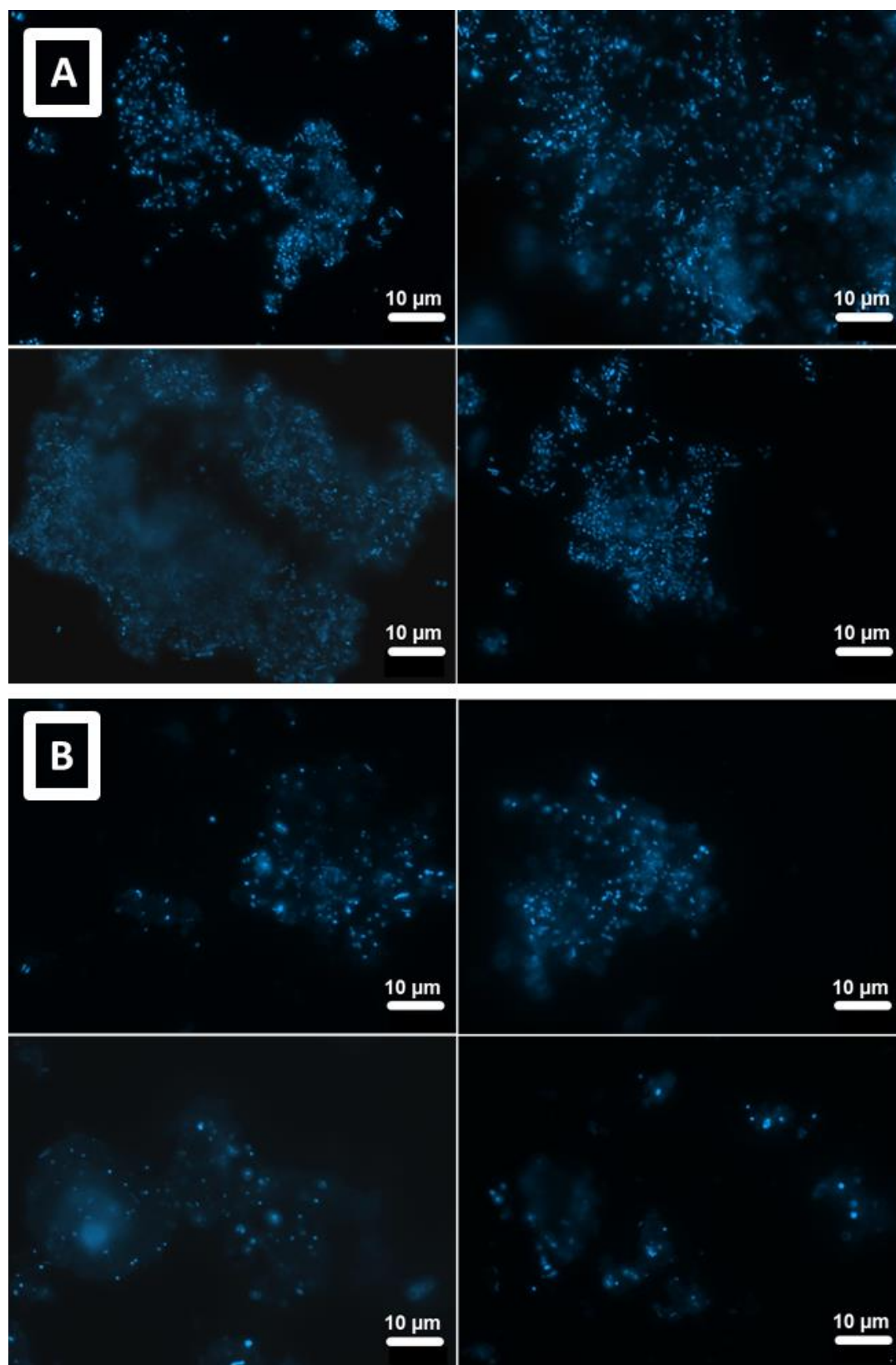
Figure 7. Stereomicroscopic pictures of biofilm fragments isolated from the cleaning procedure of (A) the *S. sediminis* culture, and (B) the anoxic sediment. Cells were stained with 4,6 diamidino-2-phenylindole (DAPI).

Shell elemental composition

Electron Microprobe mapping of the shell sample exposed to *S. sediminis* (Fig. 8A) and the sample exposed to the anoxic sediment (Fig. 8B) displayed a decline of Ca concentrations in outer shell parts relative to inner parts, and relative to the cell-free control sample (Fig. 8C). Concentrations in Ca ranged from 39 wt% of pristine, inner shell parts down to 31 wt% in outer sample parts exposed to the bacterial culture, with the affected area protruding ca. 90 µm from the outer to the inner sample part. No notable change in Ca concentration was quantified in the cell-free control sample over the same distance from outer to inner sample area with values of 38 and 39 wt% and no decrease over the distance (Fig. 8C). Furthermore, the sample incubated in the *S. sediminis*-culture medium displayed an increase in phosphorous concentrations on the outer surface. Nevertheless, these differences were at the limits of the analytical resolution. Examination of samples exposed to the cell-free control did not display any change in phosphorous distribution throughout the samples. EMP mapping of the sample exposed to the anoxic sediment (Fig. 8B) displayed Ca^{2+} loss on outer surface parts relative to inner parts, and the control sample. The Ca concentration ranged from 38 wt% in inner shell parts down to 30 wt% in sediment-exposed shell-parts, with the affected region protruding > 200 µm into the inner regions of the shell sample. The µ-XRF map of the sample exposed to *S. sediminis* (Fig. 9) displayed a Sr^{2+} increase of 23 ppm in the outer shell parts, and a Sr^{2+} increase of up to 46 ppm in the inner shell parts. A Sr^{2+} increase of 23 ppm in the outer shell parts and 57 ppm in the inner shell parts was observed for the sample exposed to the anoxic sediment. The respective areas of the control sample revealed a Sr^{2+} increase of less than 11 ppm in the outer shell parts and 80 ppm in the inner shell parts (Fig. 9). Raman spectroscopy prior to and after the experiment displayed the doublet of bands at approximately 701 and 705 cm^{-1} that is typical for aragonite (Fig. 10).
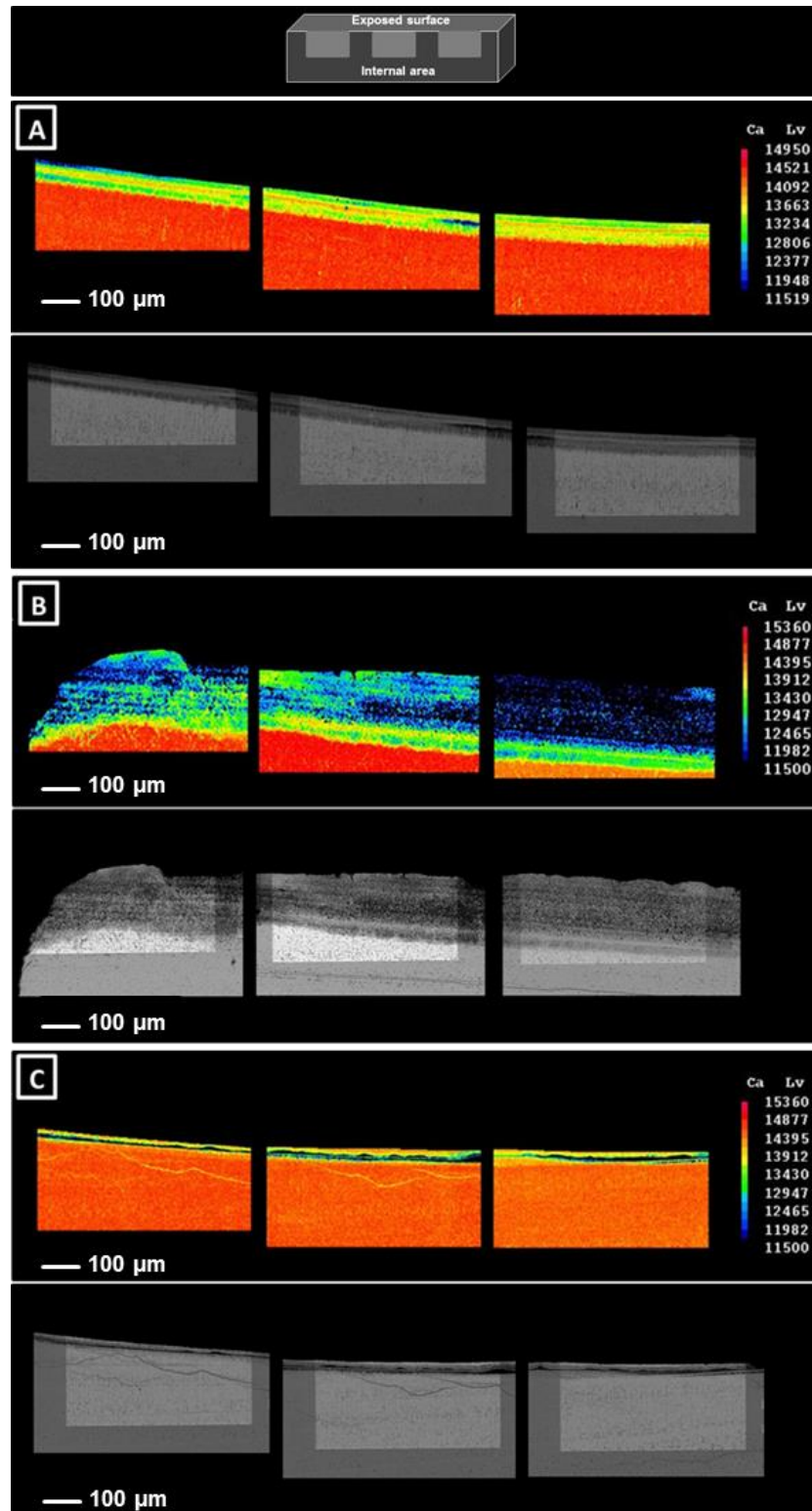
Figure 8. Electron Microprobe (EMP) maps of shell samples incubated in (A) the *S. sediminis* culture, (B) the anoxic sediment, and (C) the cell-free control (note fissure in the control sample leading to rim artifacts that resemble loss in Ca). Samples were sawn perpendicular, the upper sample parts are the surfaces exposed to the incubations, the lower parts are the inner, pristine sample-area. Maps show intensity in counts per second. BSE pictures display the measured areas within the samples.
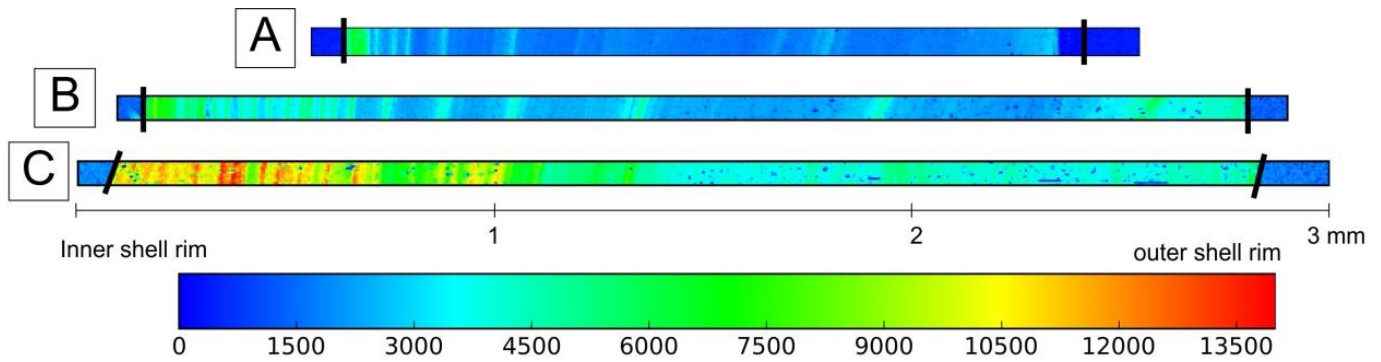
Figure 9. µ-XRF-maps of Sr L-edge along the transects of *A. islandica* shells incubated in (A) the *S. sediminis* culture, (B) the cell-free control and (C) the anoxic sediment. Concentrations are displayed in counts per second. The very left and right parts of the maps display the resin in which the samples were embedded. In sample (A) the periostracum is still present, and is characterized by an absence of strontium.
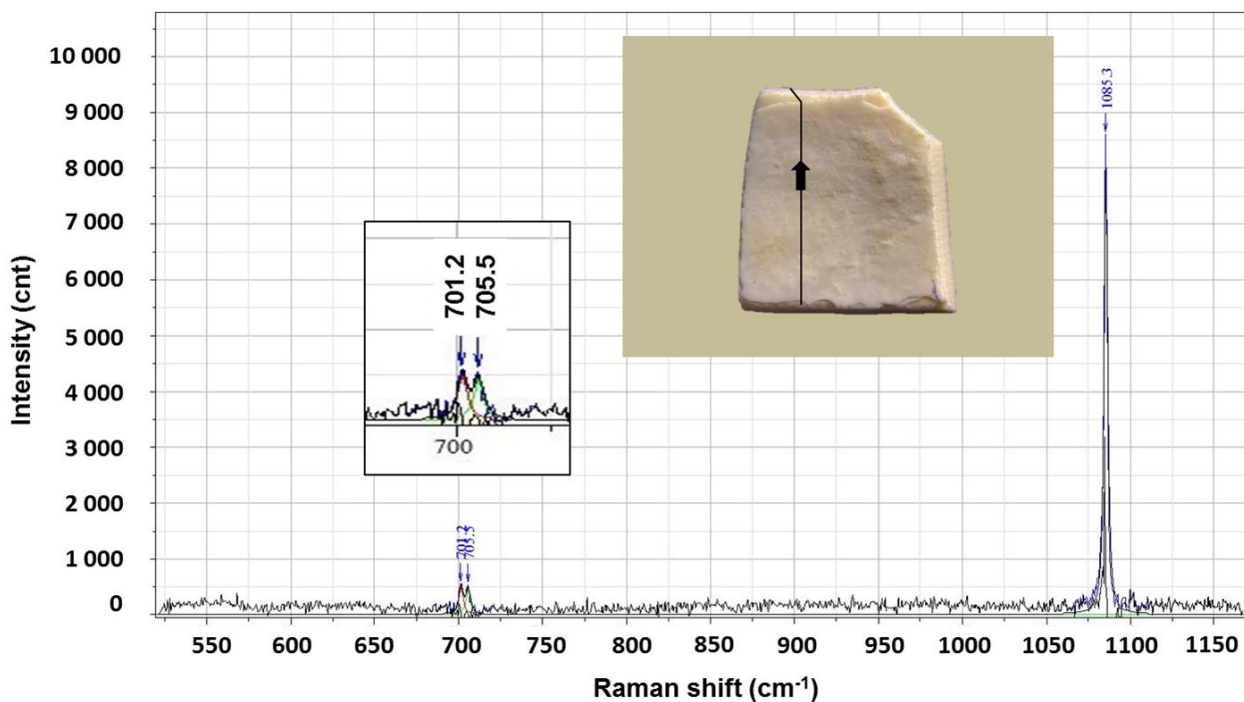
Figure 10. Example of output from a Raman spectroscopic scan conducted on an *A. islandica* shell-sample after incubation in the bacterial culture medium (the conducted transect is indicated on the sample-picture). The doublet displays the bending mode v4 of the carbonate ion in aragonite.

Shell carbon and oxygen isotope ratios

Isotope data measured from subsamples exposed to incubation experiments must be placed against the background variability of seasonal cycles in carbon and oxygen isotope ratios typical for *A. islandica* bivalves. Previous high-resolution analyses of sample material used in this study (Ritter *et al.*, 2017) documents a primary spatial variability of 1.1‰ for oxygen and 4.2‰ for carbon in the bivalves studied. With reference to isotope data analyzed after the incubation experiments, oxygen isotope compositions of shell surfaces directly beneath the periostracum and various other portions of subsamples exposed to the bacterial culture and the anoxic display a range of 2.4‰ and 1.4‰ whilst carbon ranges from 1.0 to 2.9‰ and 0.6 to 3.1‰, respectively (Table 3, Fig. 11). Water samples were not analyzed as both carbon and oxygen in the minute volumes of aragonite that were dissolved or did exchange with the experimental fluid is too small to affect the bulk water or sediment isotope ratios.

Table 3. δ^{13}C and δ^{18}O values of shell samples incubated in the *S. sediminis* culture, anoxic sediment, and the cell-free control for sample surfaces. Unaltered reference samples (no incubation) served as further references.

Sample	Treatment	Comment	$\delta^{13}C_{PDB}$ [‰]	± s	$\delta^{18}O_{PDB}$ [‰]	± s
CHA-M-019 AI17 B15	*S. sediminis*	Periostracum	1.49	0.03	4.09	0.06
CHA-M-051 AI32 B1 1	*S. sediminis*	Contact periostracum - mineral	1.81	0.02	2.03	0.11
CHA-M-019 AI17 B1 6	*S. sediminis*	Contact periostracum - mineral	2.19	0.02	2.36	0.08
CHA-M-051 AI32 B1 1	*S. sediminis*	Beneath contact	1.81	0.01	1.74	0.13
CHA-M-019 AI17 B1 6	*S. sediminis*	Beneath contact	2.94	0.04	2.21	0.06
CHA-M-019 AI17 B15	*S. sediminis*	Mineral	1.95	0.02	2.63	0.05
CHA-M-051 AI32 B1 1	*S. sediminis*	Lower side	1.04	0.04	2.66	0.08
CHA-M-019 AI17 B1 6	*S. sediminis*	Lower side	1.59	0.02	2.87	0.05
CHA-M-051 AI32 B1 1	*S. sediminis*	Sawn area	1.20	0.03	2.76	0.09
CHA-M-051 AI32 B1 1	*S. sediminis*	Sawn area	1.24	0.03	2.73	0.09
CHA-M-019 AI17 B1 6	*S. sediminis*	Sawn area	2.77	0.02	2.57	0.11
CHA-M-014-AI12 B4	Anoxic sediment	Periostracum	2.65	0.05	3.69	0.03
CHA-M-012 AI10 B5	Anoxic sediment	Contact periostracum - mineral	2.77	0.02	2.90	0.04
CHA-M-005 AI3 B7	Anoxic sediment	Contact periostracum - mineral	2.44	0.06	2.52	0.09
CHA-M-012 AI10 B5	Anoxic sediment	Beneath contact	3.08	0.04	2.61	0.10
CHA-M-005 AI3 B7	Anoxic sediment	Beneath contact	2.48	0.03	2.30	0.07
CHA-M-014-AI12 B4	Anoxic sediment	Mineral	3.12	0.03	2.57	0.07
CHA-M-012 AI10 B5	Anoxic sediment	Lower side	2.55	0.02	3.69	0.07
CHA-M-005 AI3 B7	Anoxic sediment	Lower side	0.61	0.06	2.71	0.07
CHA-M-012 AI10 B5	Anoxic sediment	Sawn area	2.90	0.05	2.77	0.05
CHA-M-005 AI3 B7	Anoxic sediment	Sawn area	2.04	0.04	2.33	0.06
CHA-M-004 AI2 B1	Cell-free control	Periostracum	-1.03	0.02	0.89	0.07
CHA-M-048 AI29 B1 6	Cell-free control	Contact periostracum - mineral	2.60	0.01	1.85	0.04
CHA-M-048 AI29 B1 6	Cell-free control	Beneath contact	3.14	0.02	2.40	0.10
CHA-M-004 AI2 B1 6	Cell-free control	Mineral	1.88	0.01	1.07	0.03
CHA-M-048 AI29 B1 6	Cell-free control	Lower side	2.81	0.01	4.13	0.07
CHA-M-048 AI29 B1 6	Cell-free control	Sawn area	2.82	0.03	3.40	0.06
CHA-M-048 AI29 B1 12	Unaltered	Contact periostracum - mineral	2.26	0.05	1.95	0.09
CHA-M-048 AI29 B1 13	Unaltered	Beneath contact	2.24	0.04	2.54	0.03
CHA-M-048 AI29 B1 15	Unaltered	Lower side	1.23	0.01	2.27	0.07
CHA-M-048 AI29 B1 14	Unaltered	Sawn area	1.54	0.02	2.51	0.08
CHA-M-048 AI29 B1 20	Unaltered	Contact periostracum - mineral	2.97	0.03	2.73	0.11
CHA-M-048 AI29 B1 21	Unaltered	Beneath contact	3.37	0.02	2.33	0.09
CHA-M-048 AI29 B1 23	Unaltered	Lower side	2.30	0.04	3.07	0.05
CHA-M-048 AI29 B1 22	Unaltered	Sawn area	2.68	0.02	2.56	0.04
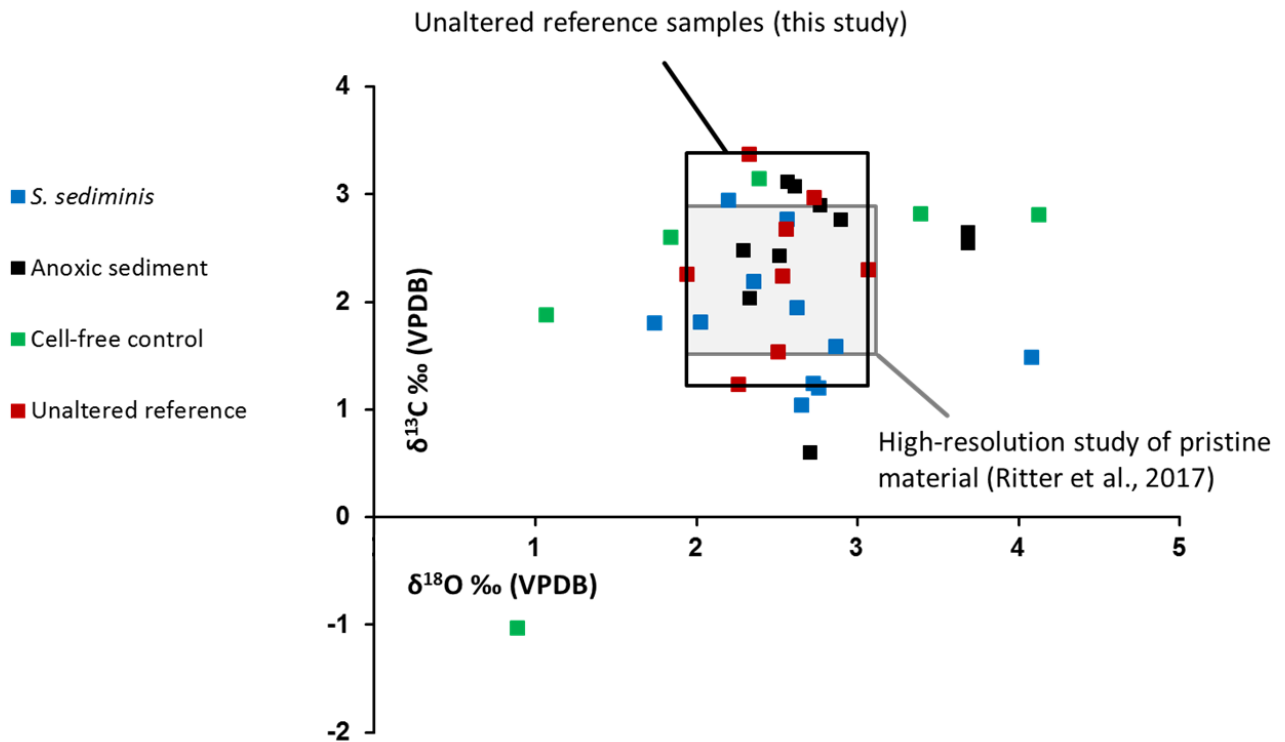
Figure 11. $\delta^{13}C$ and $\delta^{18}O$ values for sample surfaces of shell samples incubated in the *S. sediminis* culture, anoxic sediment, the cell-free control, and unaltered reference samples.

Interpretation and Discussion

Despite the - in comparison to geological time scales - extremely short experimental duration of three months, remarkable patterns in the carbonate chemistry of the liquid phase of both the *S. sediminis*-culture and the anoxic-sediment are found. These alterations are echoed by alterations of the surficial shell ultrastructure and the elemental composition of shell. Surficial aragonite dissolution of bivalve subsamples is amongst the most obvious features induced by bacteria-biomineral interatction. The most difficult data are present in isotope ratios of pristine versus incubated shell subsamples. We consider the observed outcome of the present study noteworthy and will discuss their implications in more detail in the following chapters.

Microbial alteration of the shell's aragonitic structure and geochemistry

Alteration at the species level: *S. sediminis*

The ability to hydrolyze chitin polymers by means of a chitinase, and to furthermore oxidize and ferment the chitin-monomer unit *N*-acetylglucosamine (Yang *et al.*, 2006; Rodionov *et al.*, 2010) makes *S. sediminis* an ideal candidate for carbonate alteration experiments. Chitin is one of the main structural constituents of the mollusk organic matrix from which aragonite biomineral nucleation, growth, and architecture is controlled (Lowenstam and Weiner, 1989; Weiner and Addadi, 2011). The degradation of the resulting intra- and intercrystalline organic framework (Marin *et al.*, 1996) consequently increases the reactive surface for entering pore-water (medium-) fluid as well as bacterial cells and EPS, and with it potentially enhancing the effects of alteration processes. The suggested underlying mechanisms for aragonite dissolution in the *S. sediminis* culture incubation include the hydrolysis of chitin polymers by *S. sediminis* chitinase, followed by fermentation of *N*-acetylglucosamine during cell attachment to the mineral and subsequent shell-surface dissolution through acidic fermentation products.

Results of stereomicroscopic- and SEM analyses displayed structural dissolution features, and are further supplemented by the loss of Ca detected by shell-sample EMP mapping as well as the increased Ca^{2+} concentrations in the *S. sediminis*-culture medium. Yet Sr^{2+} concentrations in the medium decreased over time although, expectedly, values should have increased due to aragonite dissolution. We explain this intuitively contradictory outcome through the effect of divalent cation scavenging by bacterial biofilm EPS (McCalla, 1939). As biofilm fragments were isolated from incubated shell samples, we expect the presence of EPS. Adsorption of divalent cations occurs via electrostatic binding sites within the EPS, with the charge of functional groups allowing for binding of the cations as a function of pH (Liu and Fang, 2002, Comte *et al.*, 2008). The reported pK_a values range from 4.8 for carboxyl- up to 11 for hydroxyl groups. A study by Guibaud *et al*. (2008) additionally suggested EPS-binding affinity to be cation-species specific. The hydration enthalpy differs among Mg, Ca, and Sr ions, with the latter showing the lowest value of -1444.7 $-\Delta H$ kJ mol^{-1} (Burgess, 1978). Given the decreasing Sr^{2+} concentration in the medium over time, preferred binding of Sr^{2+} to EPS functional groups, relative to Ca^{2+} or Mg^{2+}, is feasible and could account for the enrichment of Sr^{2+} on the sample margins detected by the μ-XRF mapping. Exchange of lost shell Ca^{2+} with pore fluid Sr^{2+} from enriched bacterial EPS could have fostered this enrichment. However, no high-resolution analyses of the biofilms are at hand to underpin this hypothesis, and the high Sr^{2+} concentrations at the control inner shell rim speak for a general higher Sr^{2+} content in that region. Furthermore, the cell wall of *Shewanella* sp. has a high adsorption affinity for dissolved Sr^{2+} with a maximum sorptive capacity of reactive surfaces for Sr^{2+} of 0.075 (*S. alga*) and 0.079 mmol·g^{-1} (*S.*

putrefaciens) when cells are coated with Fe(III) oxide (Small *et al.*, 1999). Whilst in this study the addition of Fe(III) to the *S. sediminis*-culture medium could have facilitated a cell wall - cation interaction similar to the observations by Small *et al.* (2009), the described Sr^{2+} scavenging abilities are a function of pH and the process requires protonated functional groups at low pH (5.5 - 5.9) that serve as Sr^{2+} binding sites. However, given that the pH in bacterial EPS can differ substantially from that of the surrounding environment (Hunter and Beveridge, 2005), Sr^{2+} adsorption within the *S. sediminis* EPS is feasible despite the comparably high pH in the *S. sediminis* medium. Adsorption of divalent cations could also account for the observed Mg^{2+} decrease in the medium. The simultaneously observed increase of Ca^{2+} concentrations presumably results from the observed loss of Ca in the shell, and Ca^{2+} adsorption is consequently reflected by the subsequent decrease in Ca^{2+} medium concentration. Moreover, cation complexation by bacterial EPS, here specifically EPS functional groups, could explain why despite the strong increase in TA and $\Omega_{Aragonite}$ no inorganic carbonate precipitation took place within the medium according to microscopic observations.

The undersaturation of the *S. sediminis* incubation medium with respect to Aragonite at the experimental start (Fig. 3) remains unresolved, as solely the inoculated bacterial culture could have had an effect on medium $\Omega_{Aragonite}$, but the undersaturation remained for five days. Furthermore Ca^{2+} concentrations did not reflect the low $\Omega_{Aragonite}$ of the medium. The onset of bacterial fermentation is depicted in the slight pH decrease that is correlated with an increase in TA. The increasing Ca^{2+} concentrations in the medium indicate subsequent shell dissolution, caused by fermentation products, and Ca^{2+} values furthermore suggest a ceasing dissolution process from day 37 on. However, pH and TA increased beyond this point of time, and the pCO_2 reached a peak value of 12,500 µatm (Table 2). It is therefore apparent that pH and TA in the medium were dominated by CO_2 degassing into the headspace, with the latter being foremost by sample equilibration with the atmosphere during the sampling procedure.

Alteration at the community level: anoxic sediment

The microbial biota in marine sediments accounts for diverse metabolic processes (Jørgensen, 2006; Orcutt *et al.*, 2011) that, via the generation of alkaline or acidic metabolites, either facilitate carbonate precipitation or dissolution, respectively. During earliest burial into sediments, biogenic carbonates are exposed to anaerobic bacterial communities such as denitrifiers, Mn- and Fe-oxide reducers, and sulfate-reducing bacteria. Respective respiratory processes account for an alkalinity increase in the environment through generation of HCO_3^-. This in turn facilitates authigenic carbonate nucleation and precipitation (Berner *et al.*, 1970; Castanier *et. al*., 1999; Van Lith *et al.*, 2003). Closed-system model calculations suggest that sulfate reduction does not induce carbonate precipitation but, in contrary, leads to a drop in both pH and saturation index (SI) due to generation

of one mole H^+ per mole sulfur turnover (Meister, 2013). In contrast, experimental approaches demonstrated that SRB in particular can have an enhanced effect on environmental alkalinity, pH and SI, e.g., through the usage of metabolic hydrogen (H_2) and formate produced by bacterial fermentation (Gallagher *et al.*, 2014). At present, both statements are controversially discussed. The sulfate-reduction zone is vertically followed by the methanogenic zone, where CO_2 is withdrawn from the system via archaea-driven methanogenesis (Nealson, 1997; Jørgensen, 2006) implying a further increase in pH. Overall, the majority of anaerobic microbial metabolic processes accounts for an increase in system-alkalinity and pH that has the potential to facilitate carbonate precipitation in marine sediments. While the anoxic-sediment medium of this study displayed distinct increases in TA and $\Omega_{Aragonite}$ over time as it was expected from anaerobic microbial organic matter degradation, stabilization in CO_2 partial pressure, medium divalent-cation concentrations (Fig. 4C, 4D, 4E) and shell-sample constitution (Figs. 5, 6, and 8) indicated that rather carbonate dissolution caused these increases. The increase in Sr^{2+} concentrations in the incubation medium resulted in a decreasing Mg/Sr ratio. A comparably stronger increase in Ca^{2+} concentrations was consequently reflected by a distinct decrease in Mg/Ca and Sr/Ca ratios. In contrast, the anoxic-sediment control displayed no clear trend in divalent-cation concentrations.

Cell aggregations isolated from the incubated shell samples confirmed the attachment of bacterial biofilms to the shell surface, stereomicroscopic examinations of the shell outer surface indicated exfoliation, and SEM pictures displayed a step-wise retreating surface structure. No evidence for a newly formed carbonate phase was found on these surfaces. Additionally, Raman spectroscopy of the sample provided no indication of carbonate polymorphs other than aragonite, thus excluding microbially-induced non-stoichiometric dolomite or high Mg-calcite precipitation. EMP mapping revealed Ca loss on the sample part exposed to the sediment. The EMP intensity maps displayed a decrease in Ca^{2+} concentration towards the shell surface over a depth of > 200 µm. This decrease in Ca^{2+} supports the observed structural changes as well as the increase in $\Omega_{Aragonite}$, and indicates a slow, continuous dissolution process. Data from the sediment-control medium displayed strong variations in all measured medium parameters and an increase in carbonate system parameters over time, the latter reflecting anoxic-sediment habitats dominated by bicarbonate-generating anaerobic metabolic processes. However, the distinct increase in Ca^{2+} and Sr^{2+} concentration over time determined in the anoxic-sediment incubation was not reflected in the sediment-control data.

All sediment samples were taken in the midst of April, when spring bloom in the North Sea supposedly was just developing (Wiltshire *et al.*, 2008), and subsequent sedimentation of organic carbon had probably not reached the seafloor (water depth at sampling station = 17 m). It is therefore plausible that, in exhaust of available labile organic carbon in the sediment, constituents of the shell periostracal, inter-, and intracrystalline organic matter were used as metabolic substrates by

a variety of bacteria. The subsequent increase in reactive surface area would have supported dissolution processes, which in turn resulted in the addition of Ca and Sr ions into the anoxic medium. Metal-ion complexation on the charge of bacterial cell walls is a function of pH (Konhauser and Riding, 2012). The increasing pH in the medium, resulting from carbonate dissolution and anaerobic organic matter degradation, might have led to an increasing net negative charge of cell wall surface and/or EPS functional groups. Both effects would consequently lead to a high affinity for binding of the metal cations. This could furthermore explain the increase of Sr^{2+} counts in the outer sample margins that was detected via µ-XRF mapping and presumably reflects direct microbe-mineral interaction in that area.

Tentative interpretation of carbon and oxygen isotope data

Previously reported $\delta^{13}C$ values for *A. islandica* shells from different origins range between -0.7‰ (Butler *et al.*, 2009) and +4‰ (Schöne, 2005), and $\delta^{18}O$ values between -1.7‰ (Dunca *et al.*, 2009) and +3.6‰ (Schöne *et al.*, 2004). Ritter *et al.* (2017) when studying the bivalves used for this experiment, reported spatially resolved $\delta^{13}C$ values from +1.6 to +3.0‰ and $\delta^{18}O$ values ranging from +2.0 to +3.1‰. Consequently, non-altered natural *A. islandica* shells exhibit a substantial inter- and intra-shell isotopic variability that induces a significant level of complexity when comparing pre- and post-incubation sample isotope geochemistry. Moreover, as has been documented in previous work, the simple sawing or drilling of aragonite, and even scratching material off the surface with a scalpel, may induce a partial neomorphic change to calcite. Neomorphism in turn affects both carbon and oxygen isotope ratios depending on the percent transition from aragonite to calcite (Staudigel and Swart, 2016). All of these issues strongly suggest that an overinterpretation of these data is not encouraged.

In essence, bacterially altered shell subsamples as well as those from the anoxic-sediment experiments display an increased scatter for both carbon and oxygen relative to high-resolution micromilled samples from pristine shells (Ritter et al., 2017). Clearly, the range in oxygen (values of >4‰) is more significantly increased relative to carbon. Remarkably, the most ^{18}O-enriched sample is from a cell-free control experiment. Moreover, when comparing isotope data from different incubation experiments and different sampling sites, no obvious picture emerges (Fig. 10).

Considering these issues, the authors suggest that the present data are potentially interesting and relevant, particularly in the light of previous work suggesting an impact of microbe metabolism on carbonate isotope ratios (Londry and Des Marais, 2003). At present it seems unclear to which degree the choice of a specific sampling site within a subsample (outer shell, inner shell, surface, center), the sampling bias resulting in aragonite-calcite neomorphism, and the primary seasonal variability in aragonite isotope geochemistry must be placed against genuine bacteria-induced patterns. The way

forward must lie in significantly expanded experimental duration (>12 months) and a very detailed and careful sampling strategy of comparable material from comparable shell subsamples.

Conclusions

The presented study identifies the potential of marine benthic bacteria to affect ultrastructural and geochemical properties of *A. islandica* shells over an experimental time span of three months. Processes observed included the partial dissolution of the surficial shell crystal ultrastructure and the alteration of the biomineral's geochemical and (to a less indicative degree) isotopic composition. We further hypothesize that the disintegration of inter-crystalline organic matter opened pathways for reactive fluids to enter the carbonate hard parts, leading to enhanced rates of fluid-carbonate interaction. We suggest that microbially-induced aragonite alteration could play a so far underappreciated role in seafloor and earliest burial diagenetic realms. These alteration processes have - over geological time scales - the potential to compromise aragonitic proxy archives.

References

Abele, D., Strahl, J., Brey, T. and Philipp, E.E.R. (2008) Imperceptible senescence: ageing in the ocean quahog *Arctica islandica*. *Free Radical Research*, **42**, 474-80.

Aloisi, G., Gloter, A., Krüger, M., Wallmann, K., Guyot, F. and Zuddas, P. (2006) Nucleation of calcium carbonate on bacterial nanoglobules. *Geology,* **34**, 2017-2020.

Balci, N., Shanks, W.C., Mayer, B. and Mandernack, K.W. (2007) Oxygen and sulfur isotope systematics of sulfate produced by bacterial and abiotic oxidation of pyrite. *Geochimica et Cosmochimica Acta*, **71**, 3796-3811.

Bathurst, R.G.C. (1975) Carbonate Sediments and Their Diagenesis (Developments in Sedimentology). Elsevier Science, Oxford, 640 pp.

Berner, R.A. (1980) Early Diagenesis: A Theoretical Approach. Princeton University Press, New Jersey, 256 pp.

Berner, R.A., Scott, M.R. and Thomlinson, C. (1970) Carbonate alkalinity in the pore waters of anoxic marine sediments. *Limnology and Oceanography*, **15**, 544-549.

Beveridge, T.J., and Murray, R.G. (1980) Sites of metal deposition in the cell wall of Bacillus subtilis. *Journal of Bacteriology*, **141**, 876-887.

Braissant, O., Decho, A.W., Dupraz, C., Glunk, C., Przekop, K.M. and Visscher, P.T. (2007) Exopolymeric substances of sulfate-reducing bacteria: Interactions with calcium at alkaline pH and implication for formation of carbonate minerals. *Geobiology*, **5**, 401-411.

Burgess, J. (1978) Metal ions in solution. Halsted Press, New York, 481 pp.

Butler, P.G., Wanamaker, A.D., Scourse, J.D., Richardson, C.A. and Reynolds, D.J. (2013) Variability of marine climate on the North Icelandic Shelf in a 1357-year proxy archive based on growth increments in the bivalve *Arctica islandica*. *Palaeogeography, Palaeoclimatology, Palaeoecology*, **373**, 141-151.

Butler, P.G., Scourse, J.D., Richardson, C.A., Wanamaker, A., Bryant, C.L. and Bennell, J.D. (2009) Continuous marine radiocarbon reservoir calibration and the 13 C Suess effect in the Irish Sea: Results from the first multi-centennial shell-based marine master chronology. *Earth and Planetary Science Letters*, **279**, 230-241.

Cai, W.-J., Chen, F., Powell, E.N., Walker, S.E., Parsons-Hubbard, K.M., Staff, G.M., Wang, Y., Ashton-Alcox, K.A., Callender, W.R. and Brett, C.E. (2006) Preferential dissolution of carbonate shells driven by petroleum seep activity in the Gulf of Mexico. *Earth and Planetary Science Letters* **248**, 227-243.

Castanier, S., Le Métayer-Levrel, G., Perthuisot, J.-P. (1999) Ca-carbonates precipitation and limestone genesis – the microbiogeologist point of view. *Sedimentary Geology*, **126**, 9-23

Chafetz, H.S., and Buczynski, C. (1992) Bacterially Induced Lithification of Microbial Mats. *Palaios*, **7**, 277-293

Comte, S., Guibaud, G., and Baudu, M. (2008) Biosorption properties of extracellular polymeric substances (EPS) towards Cd, Cu and Pb for different pH values. *Journal of Hazardous Materials*, **151**, 185-193.

Coughlin, R.T., Tonsager, S. and McGroarty, E.J. (1983) Quantitation of Metal Cations Bound to Membranes and Extracted Lipopolysaccharide of *Escherichia coli*. *Biochemistry*, **22**, 2002-2007.

Davis, K.J., Nealson, K.H. and Lüttge, A. (2007) Calcite and dolomite dissolution rates in the context of microbe-mineral surface interactions. *Geobiology*, **5**, 191-205.

Decho, A.W. (2010) Overview of biopolymer-induced mineralization: What goes on in biofilms? *Ecological Engineering*, **36**, 137-144.

Decho, A.W., Visscher, P.T. and Reid, R.P. (2005) Production and cycling of natural microbial exopolymers (EPS) within a marine stromatolite. *Palaeogeography, Palaeoclimatology, Palaeoecology*, **219**, 71-86.

Dodd, J. (1963) Paleoecological Implications of Shell Mineralogy in Two Pelecypod Species. The Journal of Geology, **71**, 1-11.

Dunca, E., Mutvei, H., Göransson, P., Mörth, C.M., Schöne, B.R., Whitehouse, M.J., Elfman, M. and Baden, S.P. (2009) Using ocean quahog (*Arctica islandica*) shells to reconstruct paleoenvironment in Öresund, Kattegat and Skagerrak , Sweden. *International Journal of Earth Sciences* **98**, 3-17.

Dupraz, C., Visscher, P.T., Baumgartner, L.K. and Reid, R.P. (2004) Microbe-mineral interactions: Early carbonate precipitation in a hypersaline lake (Eleuthera Island, Bahamas). *Sedimentology*, **51**, 745-765.

Froelich, P.N., Klinkhammer, G.P., Bender, M.L., Luedtke, N.A., Heath, G.R., Cullen, D., Dauphin, P., Hammond, D. and Hartman, B. (1979) Early oxidation of organic matter in pelagic sediments of the eastern equatorial Atlantic : suboxic diagenesis*. Geochimica et Cosmochimica Acta* **43**, 1057-1090

Gallagher, K., Dupraz, C. and Visscher, P. (2014) Two opposing effects of sulfate reduction on carbonate precipitation in normal marine, hypersaline, and alkaline environments: COMMENT. *Geology*, **42**, e313 - e 314-42.

Greenfield, L. (1962). Metabolism and concentration of calcium and magnesium and precipitation of calcium carbonate by a marine bacterium. *Annals of the New York Academy of Sciences*, **109**, 23-45

Guibaud, G., Bordas, F., Saaid, A., D'Abzac, P. and Van Hullebusch, E. (2008) Effect of pH on cadmium and lead binding by extracellular polymeric substances (EPS) extracted from environmental bacterial strains. *Colloids and Surfaces B: Biointerfaces*, **63**, 48-54.

Hillgärtner, H., Dupraz, C. and Hug, W. (2001) Microbially induced cementation of carbonate sands: are micritic meniscus cements good indicators of vadose diagenesis? *Sedimentology*, **48**, 117 - 131.

Himmler, T., Brinkmann, F. and Bohrmann, G. (2011) Corrosion patterns of seep-carbonates from the eastern Mediterranean Sea. *Terra Nova*, **23**, 206-212

Hunter, R.C. and Beveridge, T.J. (2005) Application of a pH-Sensitive Fluoroprobe (C-SNARF-4) for pH Microenvironment Analysis in *Pseudomonas aeruginosa* Biofilms. *Applied and Environmental Microbiology*, **71**, 2501-2510.

Immenhauser, A., Schöne, B.R., Hoffmann, R. and Niedermayr, A. (2016) Mollusc and brachiopod skeletal hard parts: intricate archives of their marine environment. *Sedimentology*, **63**, 1-59.

Jørgensen, B.B. (2006) Bacteria and marine Biogeochemistry. In: *Marine Geochemistry* (Eds H.D. Schulz and M. Zabel), pp. 173-207. Springer, Berlin, Heidelberg.

Kawaguchi, T. and Decho, A.W. (2002) A laboratory investigation of cyanobacterial extracellular polymeric secretions (EPS) in influencing CaCO3 polymorphism. *Journal of Crystal Growth*, **240**, 230-235.

Konhauser, K. and Riding, R. (2012) Bacterial Biomineralization. In: *Fundamentals of Geobiology*, (Eds A. Knoll, D. Canfield, and K. Konhauser), 105-130, Blackwell Science, Oxford.

Konhauser, K.O., Fyfe, W.S., Ferris, F.G. and Beveridge, T.J. (1993) Metal sorption and mineral precipitation by bacteria in two Amazonian river systems: Rio Solimoes and Rio Negro, Brazil. *Geology*, **21**, 1103-1106.

Krause, S., Aloisi, G., Engel, A., Liebetrau, V. and Treude, T. (2014) Enhanced Calcite Dissolution in the Presence of the Aerobic Methanotroph *Methylosinus trichosporium*. *Geomicrobiology Journal*, **31**, 325-337.

Liu, H. and Fang, H.H.P. (2002) Characterization of electrostatic binding sites of extracellular polymers by linear programming analysis of titration data. *Biotechnology and Bioengineering*, **80**, 806-811.

Londry, K.L. and Des Marais, D.J. (2003) Stable carbon isotope fractionation by sulfate-reducing bacteria. *Applied and Environmental Microbiology*, **69**, 2942-9.

Lowenstam, H.A. and Weiner, S. (1989) On Biomineralization. Oxford University Press, Oxford, 324 pp.

Lüttge, A., Zhang, L. and Nealson, K.H. (2005) Mineral surfaces and their implications for microbial attachment: Results from Monte Carlo simulations and direct surface observations. *American Journal of Science*, **305**, 766-790.

Marin, F. (2012) The formation and mineralization of mollusk shell. *Frontiers in Bioscience*, **S4**, 1099-1125.

Marin, F., Smith, M., Isa, Y., Muyzer, G., Westbroek, P., Isat, Y., Muyzert, G. and Westbroek, P. (1996) Skeletal matrices, muci, and the origin of invertebrate calcification. *Proceedings of the National Academy of Sciences of the United States of America*, **93**, 1554-9.

McCalla, T.M. (1939) Cation adsorption by bacteria. *Journal of Bacteriology*, 40, 1, 23-32.

Meister, P. (2013) Two opposing effects of sulfate reduction on carbonate precipitation in normal marine, hypersaline, and alkaline environments. *Geology*, **41**, 499-502.

Nealson, K.H. (1997) SEDIMENT BACTERIA: Who ' s There , What Are They Doing , and What ' s New? *Annual Review of Earth and Planetary Sciences*, **25**, 403-34.

Orcutt, B.N., Sylvan, J.B., Knab, N.J. and Edwards, K.J. (2011) Microbial Ecology of the Dark Ocean above, at, and below the Seafloor. *Microbiology and Molecular Biology Reviews*, **75**, 361-422.

Paine, S.G., Linggood, F.V., Schimmer, F. Thrupp, T.C. (1933) The Relationship of Micro-Organisms to the Decay of Stone. *Philosophical Transactions of the Royal Society London, Series B, Biological Sciences*, **222**, 97-127.

Riding, R. (2000) Microbial carbonates: the geological record of calcified bacterial algal mats and biofilms. *Sedimentology,* **47**, 179-214.

Ritter, A.-C., Mavromatis, V., Dietzel, M., Kwiecien, O., Wiethoff, F. , Griesshaber, E., Casella, L.A. Schmahl, W.W., Koelen, J., Neuser, R., Leis, A., Buhl, D., Niedermayr, A., Breitenbach, S.F.M., Bernasconi, S.M. and Immenhauser, A. (2017) Exploring the impact of diagenesis on (isotope) geochemical and microstructural alteration features in biogenic aragonite. Accepted article, doi: 10.1111/sed.12356.

Rodionov, D.A., Yang, C., Li, X., Rodionova, I.A., Wang, Y., Obraztsova, A.Y., Zagnitko, O.P., Overbeek, R., Romine, M.F., Reed, S., Fredrickson, J.K., Nealson, K.H. and Osterman, A.L. (2010) Genomic encyclopedia of sugar utilization pathways in the *Shewanella* genus. *BMC genomics*, **11**, 494.494

Sánchez-Román, M., Rivadeneyra, M.A., Vasconcelos, C. and McKenzie, J.A. (2007) Biomineralization of carbonate and phosphate by moderately halophilic bacteria. *FEMS Microbiology* Ecology, **61**, 273-284.

Schindler, M. and Osborn, M.J. (1979) Interaction of Divalent Cations and Polymyxin B with Lipopolysaccharide. *Biochemistry*, **18**, 4425-4430.

Schöne, B.R. (2013) *Arctica islandica* (Bivalvia): A unique paleoenvironmental archive of the northern North Atlantic Ocean. *Global and Planetary Chan*ge, **111**, 199-225.

Schöne, B.R. (2005) Daily Growth Rates in Shells of *Arctica islandica*: Assessing Sub-seasonal Environmental Controls on a Long-lived Bivalve Mollusk. *Palaios*, **20**, 78-92.

Schöne, B.R., Castro, A., Fiebig, J. and Houk, S.D. (2004) Sea surface water temperatures over the period 1884 – 1983 reconstructed from oxygen isotope ratios of a bivalve mollusk. *Palaeogeography, Palaeoclimatology, Palaeoecology*, **212**, 215-232.

Selvarengan, P., Kubicki, J.D., Guégan, J. and Châtellier, X. (2010) Complexation of carboxyl groups in bacterial lipopolysaccharides: Interactions of H+, with Kdo and galacturonate molecules via quantum mechanical calculations and NMR spectroscopy. *Chemical Geology*, **273**, 55-75.55-75

Shirai, K., Schöne, B.R., Miyaji, T., Radarmacher, P., Krause, R.A. and Tanabe, K. (2014) Assessment of the mechanism of elemental incorporation into bivalve shells (*Arctica islandica*) based on elemental distribution at the microstructural scale. *Geochimica et Cosmochimica Acta*, **126**, 307-320.

Small, T.D., Warren, L.A. and Roden, E.E. (1999) Sorption of Strontium by Bacteria, Fe (III) Oxide, and Bacteria - Fe (III) Oxide Composites. *Environmental Science and Technology*, **33**, 4465-4470.

Sotaert, K, Hofmann, A.F., Middelburg, J.J., Meysman, F.J.R. and Greenwood, J. (2007) The effect of biogeochemical processes on pH. *Marine Chemistry*, **105**, 30-51.

Staudigel, P.T., and Swart, P.K. (2016). Isotopic behavior during the aragonite-calcite transition: Implications for sample preparation and proxy interpretation. *Chemical Geology*, **442**, 130-138.

Sutherland, I.W. (2001) Biofilm exopolysaccharides: A strong and sticky framework. *Microbiology*, **147**, 3-9.

Swart, P.K. (2015) The geochemistry of carbonate diagenesis: The past, present and future. *Sedimentology*, **62**, 1233-1304.

Tucker, M.E. and Bathurst, R.G.C. (1990) Carbonate Diagenesis. Blackwell Scientific Publications, 320 pp.

Uroz, S., Calvaruso, C., Turpault, M.P. and Frey-Klett, P. (2009) Mineral weathering by bacteria: ecology, actors and mechanisms. *Trends in Microbiology*, **17**, 378-387.

Van Lith, Y., Warthmann, R., Vasconcelos, C. and McKenzie, J.A. (2003) Microbial fossilization in carbonate sediments: A result of the bacterial surface involvement in dolomite precipitation. *Sedimentology*, **50**, 237-245.

Vasconcelos, C. and McKenzie, J. (1997) Microbial mediation of modern dolomite precipitation and diagenesis under unoxic conditions (Lagoa Vermelha, Rio de Janeiro, Brazil). *Journal of Sedimentary Research*, **67**, 378-390.

Walker, J.C. (1984) Suboxic diagenesis in banded iron formations. *Nature*, **309**, 340-342.

Watabe, N. (1983) Shell repair. In: The Mollusca Vol.4 (Eds A.S.M. Saleuddin and K.M. Wilbur), pp. 235-287. Academic Press.

Watabe, N. (1965) Crystal-Matrix Relationships in the Inner Layer of Mollusk Shells. *Journal of Ultrastructure Research*, **12**, 351-370.

Weiner, S. and Addadi, L. (2011) Crystallization Pathways in Biomineralization. *Annual Review of Materials Research*, **41**, 21-40.

Weiner, S. and Addadi, L. (1991) Acidic macromolecules of mineralized tissues: the controllers of crystal formation. *Structural Chemistry*, **16**, 252-256.

Williams, D.F, Arthur, M.A., Jones, D.S. and Healy-Williams, N. (1982) Seasonality and mean annual sea surface temperatures from isotopic and sclerochronological records. *Nature*, **296**, 432-434.

Wilson, P.A. and Opdyke, B.N. (1996) Equatorial sea-surface temperatures for the Maastrichtian revealed through remarkable preservation of metastable carbonate. *Geology*, **24**, 555-558.

Wiltshire, K.H., Malzahn, A.M., Wirtz, K., Greve, W., Janisch, S., Mangelsdorf, P., Manly, B.F.J. and Boersma, M. (2008) Resilience of North Sea phytoplankton spring bloom dynamics: An analysis of long-term data at Helgoland Roads. *Limnology and Oceanography*, **53**, 1294-1302.

Wright, D.T. and Wacey, D. (2005) Precipitation of dolomite using sulphate-reducing bacteria from the Coorong Region, South Australia: Significance and implications. *Sedimentology*, **52**, 987-1008.

Yang, C., Rodionov, D.A., Li, X., Laikova, O.N., Gelfand, M.S., Zagnitko, O.P., Romine, M.F., Obraztsova, A.Y., Nealson, K.H. and Osterman, A.L. (2006) Comparative genomics and experimental characterization of N-acetylglucosamine utilization pathway of *Shewanella oneidensis*. *Journal of Biological Chemistry*, **281**, 29872-29885.

Zeebe, R. and Wolf-Gladrow, D. (2001) CO_2 in Seawater: Equilibrium, Kinetics, Isotopes. *Elsevier Oceanography Series*, **65**, Amsterdam, pp. 346.

Zhao, J.S., Manno, D., Beaulieu, C., Paquet, L. and Hawari, J. (2005) *Shewanella sediminis* sp. nov., a novel Na+- requiring and hexahydro-1,3,5-trinitro-1,3,5-triazine-degrading bacterium from marine sediment. *International Journal of Systematic and Evolutionary Microbiology*, **55**, 1511-1520.

Chapter 3

Effects of heterotrophic bacterial activity on coral aragonite during early diagenesis

Skadi M. Lange[a][*], Stefan Krause[a], Vanessa Fichtner[b], Ann-Christine Ritter[c], Thomas Huthwelker[d], Sebastian Büsse[e], Stanislav N. Gorb[e], Harald Strauss[b], Adrian Immenhauser[c] and Tina Treude[f,g][*]

[a] *GEOMAR Helmholtz-Centre for Ocean Research Kiel, Department of Biogeochemistry, Wischhofstr. 1-3, 24148 Kiel, Germany*

[b] *University of Münster, Department of Geology and Paleontology, Corrensstr. 24, 48149 Münster, Germany*

[c] *Ruhr-University Bochum, Department of Geology, Mineralogy, and Geophysics, Universitätsstr. 150, 44801 Bochum, Germany*

[d] *Paul Scherrer Institute, 5232 Villigen - PSI, Switzerland*

[e] *Kiel University, Zoological Institute: Functional Morphology and Biodynamics, Am Botanischen Garten 9, 24118 Kiel, Germany*

[f] *Department of Earth, Planetary, and Space Sciences, University of California, Los Angeles, 595 Charles E. Young Drive, Los Angeles, California 90095-1567, USA*

[g] *Department of Atmospheric and Oceanic Sciences, University of California, Los Angeles, 595 Charles E. Young Drive, Los Angeles, California 90095-1567, USA*

Abstract

Marine sediments are chemically imprinted by aerobic and anaerobic bacterial communities and their respective metabolic redox processes. Consequently, benthic heterotrophic bacteria have the potential to alter sediment-deposited biogenic carbonates during earliest to early diagenesis. To investigate the alteration effects of heterotrophic bacterial activity on biogenic carbonates, aragonitic hard parts of the scleractinian coral *Porites* sp. were incubated in benthic oxic and anoxic bacterial cultures and anoxic sediment slurries over varying time spans and at differing incubation temperatures. All incubation media showed a strong increase in pH, total alkalinity and $\Omega_{Aragonite}$ over time. Decreasing Ca^{2+} and Sr^{2+} concentrations in one oxic bacterial culture medium led to a respective increase in medium Mg/Ca and Mg/Sr ratio and a decrease in the Sr/Ca ratio. Increasing Ca^{2+} and Sr^{2+} concentrations in the anoxic bacterial incubation had the opposite effect on the respective divalent cation ratios. Despite the distinct changes in media carbonate chemistry, changes in surficial, geochemical and isotopic alteration on coral samples were subtle. Analysis of *Porites* C_{org} content revealed a low organic share in the bulk carbonate. Apparently, bacterially-mediated carbonate alteration is a function of time, (growth-) temperature, and the availability of organic carbon in the respective carbonate species.

Introduction

Coral aragonitic skeletons are elaborate recorders of paleoenvironmental conditions, archiving ocean temperature, chemistry, and circulation over their lifetime through their geochemical and isotopic composition (e.g. Beck et al., 1992; Druffel, 1997; Cohen and Mc Connaughey, 2003). Specifically ocean temperature is directly related to coral calcification and elemental composition: The inverse correlation between sea-surface temperature (SST) and coral uptake of Sr^{2+} to Ca^{2+} during biomineralization results in a robust skeletal Sr/Ca thermometer for past ocean temperature reconstruction (Weber et al., 1973, Smith et al., 1979; Alibert and Mc Culloch, 1997; Swart et al., 2002; Inoue et al., 2007). The Sr/Ca thermometry is further supplemented when correlated to coral $\delta^{18}O$, reflecting SST and oxygen isotopic composition of oceanic water masses (Beck et al., 1992; Gagan et al., 1998; Al-Rousan et al., 2003). Furthermore, coral Mg/Ca ratio serves as an accurate proxy for SST reconstruction (Mitsuguchi et al., 1996), albeit that the accuracy of Mg/Ca proxy application may be compromised by vital, non-SST effects on coral Mg^{2+} uptake (Fallon et al., 1999; Gagnon et al., 2007).

Many coral skeletons are not precipitated in isotopic equilibrium with the surrounding environment (Weber and Woodhead, 1972; Swart, 1983, Adkins et al., 2003), and non-equilibrium calcification may furthermore lead to heterogeneity of skeletal trace-elemental distribution (Harriss and Amy, 1964; Allison et al., 2001; Sinclair et al., 2006). Algal symbionts (zooxanthellae) in hermatypic corals favor the formation of calcium carbonate ($CaCO_3$) during coral calcification by local photosynthetic removal of CO_2 from the system, and supply of energy for the transport of bicarbonate (HCO_3^-) and Ca^{2+} (Chalker and Taylor, 1978). However, photosynthetic activity during skeletogenesis can lead to variability in Ca^{2+} uptake (Al-Horani, 2005) thereby potentially compromising coral Sr/Ca ratios (Cohen et al., 2002). Bioerosion through endolithic microorganisms and/or external microborers affects coral skeletons during life history and after death (Le Campion-Alsumard et al., 1995; Tribolet, 2007; Glynn and Manzello, 2015). *Post mortem*, coral skeletons are subject to early diagenetic processes, such as organic matter degradation and carbonate dissolution, crystal lattice exchange, and $CaCO_3$ polymorph replacement. These processes have the potential to substantially alter carbonate structure, geochemistry and isotopic composition, thereby compromising the reliability of proxy applications. Consequently, research on diagenetic impact on marine carbonates is conducted intensely, but is foremost considering abiotic alteration factors (e.g. Bathurst, 1975; Berner, 1980; Enmar et al., 2000; Hendy et al., 2007; Swart, 2015). Studies on the biotic share in diagenetic processes include microbial alteration of carbonate isotopic composition (Walker, 1984), mediation of dolomite diagenesis (Vasconcelos and McKenzie, 1997), as well as micritization of skeletal- and non-skeletal carbonates (Tucker and Bathurst, 1990) and shallow carbonate arenites (Hillgärtner et

al., 2001). The post-depositional alteration potential of marine benthic bacterial communities on carbonate structure and geochemistry, however, has scarcely been taken into consideration. Marine sediments provide a habitat for highly diverse microbial communities that shape their environment through intertwined metabolic redox reactions. These reactions are governed by the availability of electron acceptors with different energy yields for the organisms that account for a distinct vertical bacterial distribution within the sediments (Froelich et al., 1979; Jørgensen, 2006; Orcutt et al., 2011) (Table 1).

Table 1. Microbial metabolic redox reactions with carbonate-alteration potential, and associated Gibbs free energies (modified after Orcutt et al., 2011).

Pathway	Reaction	$\Delta G°$ (kJ/mol)
Oxic respiration	$CH_2O + O_2 \rightarrow CO_2 + H_2O$	-770
Denitrification	$CH_2O + 4/5\ NO_3^- \rightarrow 1/5\ CO_2 + 2/5\ N_2 + 4/5\ HCO_3^- + 3/5\ H_2O$	-463
MnO_2 reduction	$CH_2O + 3CO_2 + H_2O + 2MnO_2 \rightarrow 2\ Mn^{2+} + 4HCO_3^-$	-557
Fe(III) oxide reduction	$CH_2O + 7CO_2 + 4Fe\ (OH)_3 \rightarrow 4Fe^{3+} + 8HCO_3^- + 3H_2O$	-697
Sulfate reduction	$CH_2O + ½\ SO_4^{2-} \rightarrow HCO_3^- + 1/2H_2S$	-98
Anaerobic oxidation of methane (AOM)	$CH_4 + SO_4^{2-} \rightarrow HCO_3^- + HS^- + H_2O$	-16.6
Methanogenesis from H_2/CO_2	$H_2 + ¼\ HCO_3^- + ¼\ H^+ \rightarrow ¼\ CH_4 + ¾\ H_2O$	-57
Methanogenesis from acetate	$CH_3COOH \rightarrow CH_4 + CO_2$	-4.2
Fermentation from ethanol	$CH_3CH_2OH + H_2O \rightarrow CH_3COOH + 2H_2$	-181
Fermentation from lactate	$CH_3CH_2COO^- + 3H_2O \rightarrow CH_3COOH + HCO_3^- + 3H_2$	-1.075
Acetogenesis	$H_2 + ½\ CO_3^{2-} + ¼\ H^+ \rightarrow ¼\ CH_3COO^- + H_2O$	-90

The resulting alkaline or acidic bacterial metabolic products induce a respective micro-zonation that may foster carbonate precipitation or dissolution, respectively. In the upper zone of the sediment, exposure to acidified niches originating from oxic respiration and generation of CO_2 potentially leads to $CaCO_3$ dissolution. Aerobic metabolic activity is vertically followed by anaerobic, HCO_3^-, generating metabolic processes (i.e. foremost denitrification, Mn(IV), Fe(III), and sulfate reduction) that lead to an increase in alkalinity and thereby foster secondary carbonate precipitation. Bacterial cells and biofilms were reported to either induce carbonate precipitation, foremost associated with sulfate reduction (Dupraz et al., 2004; Wright and Wacey, 2005; Aloisi et al., 2006; Sánchez-Román et al., 2007, Krause et al., 2012) or, in contrast, inhibit precipitation through sorption of organic molecules, such as extracellular polymeric substances (EPS), to carbonates (Decho, 2010). Direct attachment of bacterial cells and biofilms to carbonates can induce weathering of carbonate surficial structures

(Paine, 1933; Decho et al., 2005; Uroz et al., 2009; Krause et al., 2014a). Furthermore, bacterial cell-wall lipopolysaccharides (LPS) and EPS in biofilms contain functional groups that scavenge and bind divalent-cations from the environment (Schindler and Osborn, 1979; Coughlin et al., 1983; Selvarengan et al., 2010).

Within a previous study, evidence for bivalve shell surface dissolution and subsequent changes in aragonitic shell elemental composition through anaerobic benthic bacterial activity was provided (Lange et al., in revision): There, shell samples were incubated for three months in seawater media containing a *Shewanella sediminis* HAW-EB3 culture or an anoxic sediment slurry. Samples from both incubations showed surficial dissolution features after the incubation, that were reflected by a strong increase in media total alkalinity (TA), dissolved inorganic carbon (DIC) and the saturation state of aragonite ($\Omega_{Aragonite}$) over time. Furthermore, a decrease in Ca concentrations was observed on exposed sample parts and was reflected by a Ca^{2+} concentration increase in the incubation media.

In the present study, aragonitic hard parts of the scleractinian coral *Porites* sp. were tested for their susceptibility to bacterial carbonate alteration. *Porites* are hermatypic corals containing photosynthetic endosymbionts of the single-celled algae *Symbiodynium*. Due to their ample distribution and longevity, *Porites* aragonitic skeletons are frequently used archives for SST reconstruction (Weber and Woodhead, 1972; Alibert and McCulloch, 1997; Quinn et al., 1998; Felis et al., 2003). The coral samples were incubated in three experimental set-ups: The first set-up comprised oxic natural seawater media containing the benthic bacterial strain *Alcanivorax borkumensis* SK2[T], an aerobic, heterotrophic, hydrocarbonoclastic bacterium first isolated from sediment slurries off the island Borkum, North Sea (Yakimov et al., 2005). Recent experiments showed the capability of *A. borkumensis* to precipitate high Mg-calcite through means of a carbonic anhydrase (Krause et al., 2014b). In the second set-up, coral samples were incubated in anoxic natural seawater medium containing the benthic strain *Shewanella sediminis* HAW-EB3. The facultative anaerobe, heterotrophic bacterium has the ability to oxidize and ferment N-acetylglucosamine, an integral component of the aragonitic inter- and intracrystalline organic matrix. The third set-up comprised anoxic slurries of natural seawater and marine sediment, the latter containing the respective natural benthic bacterial communities. Research questions based on previously obtained results were: (i) Are the observed alteration features on shell samples and the underlying mechanisms applicable to coral surface structure, geochemistry, and isotopic composition (ii) Will the extended reaction area (i.e. coral pore space) enhance the degree of bacterially-mediated carbonate alteration? (iii) Are bacterially-mediated alteration processes a function of (growth-) temperature and/or experimental duration?

Methods

Bacterial culturing and seawater medium

Both the *Shewanella sediminis* and the *Alcanivorax borkumensis* strain are representative for ubiquitously distributed benthic heterotrophic bacteria, with the potential to interact with biogenic carbonates: While *S. sediminis* chitinase activity can degrade the chitinous constituents of the mineral organic matrix, thereby opening pathways that facilitate dissolution processes, *A. borkumensis* may provoke carbonate precipitation through carbonic anhydrase activity. Bacterial cultures were obtained from the Leibniz Institute DSMZ - German Collection of Microorganisms and Cell Cultures (Braunschweig, Germany). The *S. sediminis* culture was grown at 10°C in DSMZ medium 514 with the following composition (g l^{-1}): peptone, 5; yeast extract, 1; Fe(III) citrate, 0.1; NaCl, 19.45; $MgCl_2 \bullet 6H_2O$, 12.6; Na_2SO_4, 3.24; $CaCl_2 \bullet 2H_2O$, 2.39; KCl 0.55; $NaHCO_3$, 0.16; KBr, 0.08; $SrCl_2$, 0.034; H_3BO_3, 0.022; NaF, 0.0024; $(NH_4)NO_3$, 0.0016; $Na_2HPO_4 \bullet 2H_2O$, 0.01; and 2.9 µl Na-silicate. Sterile culturing vials and media were purged with N_2/CO_2 gas (80%/20%) prior to inoculation of the cultures. The initial pH of the sterile media was adjusted to 7.3. Two *A. borkumensis* cultures were grown under oxic conditions at 10°C and 20°C, respectively, with the very same medium composition and additional 1% pyruvate as carbon source. From the third generation on, the *S. sediminis* culture was inoculated to anoxic sterile natural seawater containing 100 mg l^{-1} additional Fe (III) citrate and 1000 mg l^{-1} yeast. Both *A. borkumensis* cultures were inoculated to oxic sterile natural sweater containing 100 mg l^{-1} additional Fe (III) citrate, 1000 mg l^{-1} yeast, and 1% pyruvate. The seawater media were autoclaved prior to inoculation and media pH was adjusted to 7.4. At the experimental start, 900 ml of sterile seawater media each were transferred to sterile 2 l gas-tight flat flange beakers. For incubation of the *S. sediminis* culture, the beakers were closed with sterile butyl rubbers and the seawater medium, with additional 200 ml sterile Resazurin as a redox indicator, was purged with N_2 to establish anoxic conditions. The beaker had an N_2 headspace of 0.2 bar above atmospheric pressure. Subsequently, 10 ml of the *S. sediminis* culture were inoculated to the media. The respective cell-free control was incubated under the very same conditions without the bacterial culture, and the incubations were kept at 10°C in the dark throughout the experiment. The flat flange beakers for the *A. borkumensis* incubations were closed with sterile cotton plugs after inoculation of 10 ml of the cultures each. The two *A. borkumensis* cultures and their correspondent cell-free controls were kept at 10°C and 20°C respectively throughout the experiment. While the 10°C incubation reflected the temperature regime at the natural habitat, the growth optimum for *A. borkumensis* is at 20°C and potentially allowed for enhanced development of the culture over the same experimental time span.

The seawater was sampled off Heligoland (54° 06´ N, 008° 00´ E) during RV Heincke cruise HE-411, subsequently stored in an intermediate bulk container (IBC) at 10°C, and constantly aerated with an EHEIM compact 600 aquarium pump (EHEIM, Deizisau, Germany). For the experiments, aliquots of the seawater were sterilized (UV water sterilizer, Wiegandt GmbH, Krefeld, Germ) and filtered through a 0.2 μm Whatman Polycap™ 75 AS Filter (GE Healthcare Life Sciences, Buckinghamshire, UK).

Anoxic sediment slurries

The anoxic sediment incubation represented natural sediment containing the corresponding anaerobic bacterial communities with the aforementioned carbonate-alteration potential. The sediments were obtained with RV Suedfall from Piep, Büsum (German Bight, 54° 50´ N, 8° 89´ E) at 17 m water depth. Sediments from the German Bight are characterized by an alternating mixture of clay, silt and sand, with a carbonate share about 1 to15%, and a share in quartz of up to 90% in the mean. Sediment sampling was conducted with a Van-Veen grab. Following extrication of organic debris the sediments were transferred to sterile 1 l Duran flasks, and flasks were closed with sterilized butyl rubbers. The sediment samples were subsequently stored at 10°C in the dark. Due to a low measured C_{org} content of only 1 wt% (Carlo-Erba NA-1500 Elemental Analyzer), the sediments were enriched with organic carbon to represent organic-rich sediments that provide sufficient organic carbon as electron donor for heterotrophic metabolic activity. For enrichment with organic carbon, algal cultures (DT´s Premium Blend Phytoplankton) were lyophilized, subsequently sonicated and weighed. Prior to the incubations, 1.2 g of algae per 100 g sediment wet weight was added to both, the sediment and the control sediment, to increase their initial C_{org} content to 3 wt% (Carlo-Erba NA-1500 Elemental Analyzer). Slurries were prepared from sediment and sterile seawater (2:1 mixture), and to each of the slurries 200 μl sterile Resazurin was added as a redox indicator. The slurries were transferred to sterile 2 l gas-tight flange beakers and the beakers were closed gas-tight with butyl rubbers. The beakers were subsequently flushed with N_2 gas to drive O_2 out of the system and ensure anoxic conditions. Both incubations had a N_2 headspace of 0.2 bar above atmospheric pressure and were kept at 10°C in the dark throughout the experiment. Controls contained slurries (2:1 mixture) without coral samples.

Coral samples

Porites sp*.* specimens were sampled alive in approx. 5-7 m depth during field work at the fringing reef, Gulf of Aqaba, in 1993. The corals were stored at room temperature prior to this study. Before the experiment, the corals were sawn parallel to their respective growth direction. Slices were further divided into subsamples of approx. 1 x 1 x 2 cm. Subsamples were chosen from the

apparently pristine, inner skeleton parts that contained neither alteration features (e.g. boring traces), nor organic remains that were visible on the outside regions of the coral.

Incubation procedure

Sterilized plastic skimming ladles were disposed of handles, and sewing threads of different lengths were attached to the handles to allow for free sample distribution in the media or on the sediment surface. Coral-sample edges were fixed with sterile plastic cable ties and knotted to the threads. Ladles were attached to the uppermost inner part of 2 l flat flange beakers containing either media or sediments, and beakers were closed with either sterile cotton plugs (oxic incubations) or butyl rubbers (anoxic incubations). For more details of the experimental setup see Lange *et al.* (in revision). Prior to the incubation start, anoxic set ups were purged with N_2 to a headspace of 0.2 bars to ensure anoxic conditions. 10 ml of bacterial cultures were inoculated to the oxic and anoxic media. To each of the anoxic incubations, 200 ml Resazurin was added as a redox indicator. Oxic incubations were kept at 10°C and 20°C, all anoxic incubations were kept at 10°C in the dark. During the incubation period, beakers were pivoted smoothly every other day. Sampling of seawater or medium was conducted with N_2 flushed syringes and the withdrawn volumes (12 ml per sample point) were replaced with N_2 gas. The samples were transferred to sterile N_2 purged 50 ml Duran flasks, from which the aliquots for subsequent analyses of medium carbonate chemistry were taken. Due to extensive cell growth, the oxic incubations were stopped on day 25 to prevent cell death after the stationary growth phase. Two third of the *S. sediminis* medium was exchanged on day 62 due to extensive growth of the culture. Sediment incubations were running for three months. After the incubations, coral samples were rinsed with sterile seawater (cleaning for upcoming analyses) and subsequently ultra-purified water (prevention of salting out seawater and resulting analytic bias). The latter was adjusted to pH with NH_4^+ solution. Samples were dried in parafilm-sealed Petri dishes at 40°C and subsequently stored at room temperature for analyses. Liquids from the coral-cleaning procedure (approx. 2 ml each), including the biofilms, were preserved in formaldehyde solution (final concentration 2%) at 4°C.

Cell staining and -analysis

For cell staining, the afore preserved liquid samples were vortexed, and 100 µl of each sample was transferred to 5 ml 1x sterile PBS and filtered on a 0.2 µm Whatman™ nucleopore™ polycarbonate membrane filter (GE Healthcare, 37586 Dassel). The filters were dried at room temperature, embedded in 1% low-melt agarose and dried at 37°C. Staining of the filters was conducted with 4,6 diamidino-2-phenylindole (DAPI) solution (1µl ml^{-1}) for 15 minutes in the dark, and filters were

transferred to microscope slides. The slides were examined and photographed with a Zeiss Axio Imager.M2 stereomicroscope, using a DAPI filter-set, imaging was carried out with the ZEN pro 2012 software (Carl Zeiss Microscopy GmbH, Jena, Germany).

Media carbonate system and seawater chemistry

Media sampling was conducted daily to weekly. Carbonate system parameters measured were pH, and Total Alkalinity (TA). The saturation state of aragonite ($\Omega_{Aragonite}$) was calculated after Zeebe and Wolf-Gladrow (2001). The pH was measured with a Schott Instruments Lab 850 pH sensor (SI analytics GmbH, Mainz, Germany). The sensor was calibrated with reference solution buffers (L4794, L 4796, L 4799, SI analytics GmbH, Mainz, Germany) according to the Physikalisch-Technische Bundesanstalt (PTB) and the National Institute of Standards and Technology (NIST). The pH measuring was conducted directly after sampling on the whole 12 ml aliquot in opened Duran flaks. To allow for uniform equilibration of all samples with the environment, the measuring time was restricted to 20 seconds each. TA measurements were conducted in an open-cell titration vessel after Pavlova (Pavlova et al., 2008), using a Metrohm 876 Dosimat plus (Ω Metrohm, Florida, USA). Of each sample, 0.5 ml subsamples were titrated with 0.01 M HCl. During the titration, samples were continuously purged with N_2 for withdrawal of released CO_2. Calibration of the samples was conducted with a IAPSO seawater standard. Minor- and trace-element concentrations were determined with 1 ml medium samples treated with 0.1 ml HNO_3 Suprapur[©] (1/100 v/v) prior to analyses. Concentrations were measured by inductively coupled plasma atomic emission spectroscopy (ICP-AES - JY 170 ULTRATRACE, HORIBA, Kyoto, Japan). The detection limit was 2 mg l^{-1} for Ca^{2+}, 6 mg l^{-1} for Mg^{2+} and 25 µg l^{-1} for Sr^{2+}, with a precision of 2%.

Coral structure and elemental composition

Raman spectroscopy was conducted on each of the dried coral samples prior to- and after the experiment to analyze carbonate polymorphism. Analyses were conducted with a LabRAM HR800 spectrometer (Horiba Jobin Yvon GmbH, Bensheim, Germany) at room temperature. The carbonate was excited along a transect of 1 cm, with the 473 nm line of a Nd-YAG laser. Scattered radiation from the samples was measured in a 90° scattering geometry. The Raman spectra were obtained at an interval of 0.65 cm^{-1} (0 - 4000 cm^{-1}) and a slid width of 100 mm. Scanning electron microscopy (SEM) and electron-microprobe (EMP) mapping were conducted with a JEOL JXA 8200 Electron Probe Microanalyzer (JEOL Ltd., Tokyo, Japan). SEM was applied to determine alteration features on the biofilm-free coral-sample surfaces. For SEM micrographs, samples were air-dried and sputter coated using a platinum/gold target. Images were acquired at 15 kV and a 19 µA filament current. Changes

in porosity were determined via μ-computed tomography (μ-CT) imaging. Samples were mounted on a holder and scanned with a Skyscan 1172 (Bruker, Kontich, Belgium) prior to- and after the experiment. Scanning was conducted with an acceleration voltage of 100 kV and a current of 100 μA, applying a Cu filter. X-ray projections were captured over a full 360° rotation. The resulting images were processed with the NRecon reconstruction program (Bruker, Kontich, Belgium). Prior to calculation, the first 10 pictures of scanned slices of 5 μm, each were cropped. The highest standard deviation in picture size was 0.43% pixels. Calculation of percentage pore-space per area of each slice prior to- and after the incubations was done with ImageJ. The sample incubated in the 10°C cell-free control was used as a control for all samples incubated in either bacterial cultures, or the anoxic sediment. Scans of the 10°C *A. borkumensis* incubation were excluded from the analyses as the areas scanned pre- and post-incubation were not identical, and are therefore not included in the analyses.

EMP mapping was conducted for the calculation of sample minor- and trace element concentrations. Prior to mapping, samples were sawn into quarters, embedded in epoxy resin (Araldite® 2020, Huntsman, Texas, USA), and dried overnight at 50°C. The sawn sample surface was ground using Hermes water grinding papers (P1200, P2400 and P4000) at a pressure of 25N and cleaned with pressurized air after each grinding procedure. Following grinding with P4000, samples were exposed to a subsonic bath for 5 - 10 seconds each, to extricate remaining fibers from the sample pore space. Samples were carbon coated prior to analyses. EMP maps (JEOL JXA 8200 Electron Probe Microanalyzer, with a precision of 2%) were obtained by wavelength dispersive spectrometry (WDS) mode, and repeated to gather 8 accumulations of the respectively selected area. Prior to- and after each mapping, standards were measured (Calcite, KAN1, VG-2, Strontianite A2_modernCoral). For quantitative wavelength dispersive analyses the element concentrations were measured along a mapping area of 100 μm parallel to the exposed rim of the sample x 150 μm in the direction of non-exposed, inner sample parts. Mg (TAP, Ka), Sr (TAP, Strontianite), Ca (PETJ), P (PETH) and S (PETH) were measured simultaneously. The beam current was 50 nA with a beam spot size of 3 μm, the accelerating voltage was 15 kV.

Micro X-ray Fluorescence (μ-XRF) mapping was conducted at the PHOENIX-beamline (Paul Scherrer Institute, Switzerland). Prior to the analyses, the samples were cut parallel to the growth direction and mounted on a glass holder. The thin sections were polished to a thickness of 200 μm. Element mapping was conducted along an average length of 500 μm from the outer sample rim to the central part of the skeleton segment. During measurements a fixed Si (111)-monochromator (Bruker AXS GmbH, Karlsruhe, Germany) with an energy resolution higher than 0.5 eV was used. Fluorescence signals were collected with a detector equipped with four elements of silicon drift diodes (VORTEX, USA). To display the Sr^{2+} distribution in the samples, the Sr^{2+} L-edge electrons were excited with a beam-energy of 2600 eV. Simultaneous detection of phosphorus K-edge electrons allowed for

discrimination between phosphorus-rich resin (Körapox 439, Kömmerling, Pirmasens, Germany) and phosphorus-poor coral carbonate. The element maps were generated with a spatial resolution of 5 μm. Due to space limitation on the sample mounting device, only one control was used representatively for all incubations. To avoid analytic bias caused by different incubation conditions, an unaltered reference control sample was chosen for the analyses.

Carbon and oxygen isotope analyses

For coral carbon- (δ^{13}C) and oxygen (δ^{18}O) isotope analyses, sub-samples were retrieved from one incubated coral block per incubation type. Sample material was first scratched off with a scalpel from the outmost sample surface and the inner sample region directly under the surface ("subsurface"). Subsequently, the coral samples were drilled with a Proxxon precision drill (Proxon, Föhren, Germany) to a depth of approx. 1 mm depth where further material was retrieved. From the sample exposed to the 10°C *A. borkumensis* incubation, two surface subsamples were taken from different sample areas to allow for repeat determination due to EMP mapping results. All subsamples were transferred to glass vials. The vials were closed gastight and transferred into an autosampling device at 70°C. Subsequently, a few drops of phosphoric acid were added to the sample. Carbon- and oxygen isotope values were measured from the liberated CO_2 gas using a Thermo Finnigan MAT253 mass spectrometer (Thermo Fisher Scientific Inc., Waltham, USA) interfaced to a GasBench. Carbon and oxygen isotope results are given in ‰ relative to the VPDB standard. For correction of the measured data an additional in-house standard was measured to the samples.

Results

Oxic incubation media

In the 10°C *A. borkumensis* incubation, carbonate-system parameters increased over time. The pH increased from initial 6.5 to 8.3, Total Alkalinity increased from 2.4 to 29.2 mmol kg^{-1}, and $\Omega_{Aragonite}$ from 0.1 to 16.09 (Fig. 1A, B)). The Mg^{2+} and Ca^{2+} concentrations showed no specific trend, with values between 51.7 and 50.9 mmol l^{-1}, and 5.1 and 5.2 mmol l^{-1}, respectively, while the Sr^{2+} concentration showed a 5% decrease from 85.5 to 81.3 μmol l^{-1} (Fig. 1C, D, E). The resulting Mg/Ca ratio stayed between values of 5.0 and 5.2, the Mg/Sr ratio increased from 0.6 to 0.62, and the Sr/Ca ratio decreased from 8.5 to 8.2 (Fig. 1F, G, H). The pH values in the 10°C cell-free control went from initial 7.7 to 7.9, with a drop to 7.4 on day 8. Total Alkalinity remained at values of 2.0 to 2.2 mmol kg^{-1}, and $\Omega_{Aragonite}$ went from 1.2 to 2.2 (Fig. 1A, B). Divalent-cation concentrations in the control remained stable: The Mg^{2+} concentration had values from 50.2 to 49.5 mmol l^{-1}, Ca^{2+} values were between 9.6 and 9.8 mmol l^{-1}, and the Sr^{2+} concentration between 82.7 and 83.2 μmol l^{-1} (Fig. 1C, D,

E). The resulting Mg/Ca ratio had values around 5.1, the Mg/Sr ratio was around 0.61 to 0.6, and the values of the Sr/Ca ratio were between 8.47 and 8.52 (Fig. 1F, G, H).

In the 20°C *A. borkumensis* incubation, the pH increased from 6.6 to 8.3, TA increased markedly from 2.4 to 40.1 mmol kg^{-1}, $\Omega_{Aragonite}$ from 0.1 to 74 (Fig. 2A, B). The Mg^{2+} concentration decreased from an initial 50.5 mmol l^{-1} to 47.2 mmol l^{-1} and increased to 50.1 mmol l^{-1} on day 23, at the end of the experiment (Fig. 2C). The Ca^{2+} and Sr^{2+} concentrations decreased from 9.9 to 9.4 mmol l^{-1} and from 83.1 to 77.2 µmol l^{-1}, respectively (Fig. 2D, E). The Mg/Ca ratio increased from an initial 5.1 to 5.3, and the Mg/Sr ratio from 0.6 to 0.7. The Sr/Ca ratio decreased from 8.4 to 8.2 (Fig. 2F, G, H). The pH in the 20°C cell-free control ranged between 7.7 and 7.6, Total Alkalinity increased from 2.3 to 2.6 mmol kg^{-1} on day 20 and decreased to 2.5on day 24. The $\Omega_{Aragonite}$ value remained at 1 throughout the experiment (Fig. 2, B). The Mg^{2+} concentration had values between 51.0 and 52.0 mmol l^{-1}, Ca^{2+} values were stable around 10.3 mmol l^{-1}. The Sr^{2+} concentration ranged from 83.0 to 84.0 µmol l^{-1} (Fig. 2C, D, E). The Mg/Ca ratio remained stable between 5 and 5.1, the Mg/Sr ratio stayed at 0.6, and the Sr/Ca ratio was between 7.9 and 8.0 throughout the experiment (Fig. 2F, G, H).
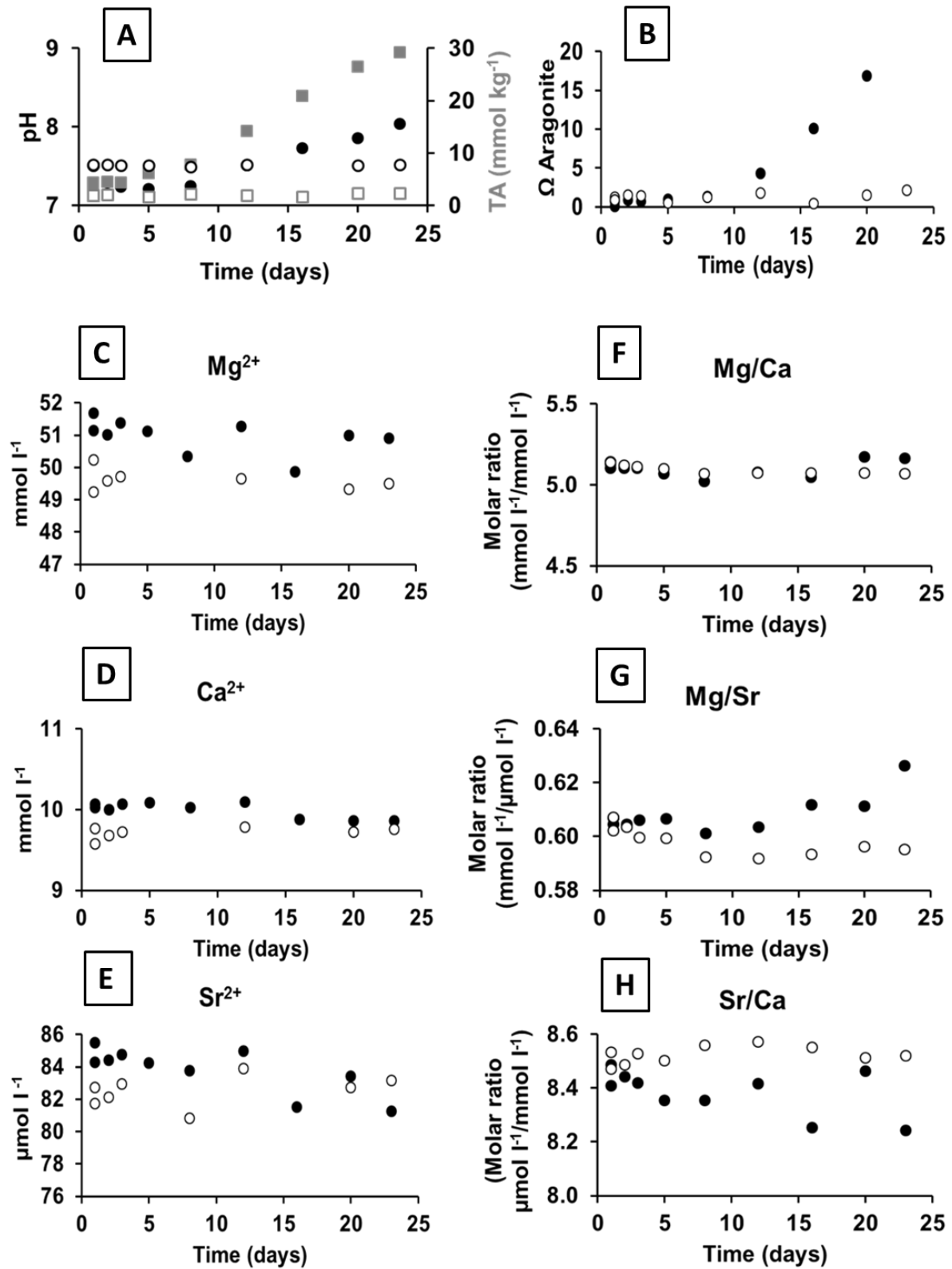
Figure 1. Medium chemistry of the 10°C *A. borkumensis* incubation: Temporal development of (A) pH (circles) and Total Alkalinity (TA) (squares), (B) $\Omega_{Aragonite}$, (C-E) divalent-cation concentrations, and (F-H) divalent-cation ratios. Solid symbols show bulk-medium values, open symbols show control values.
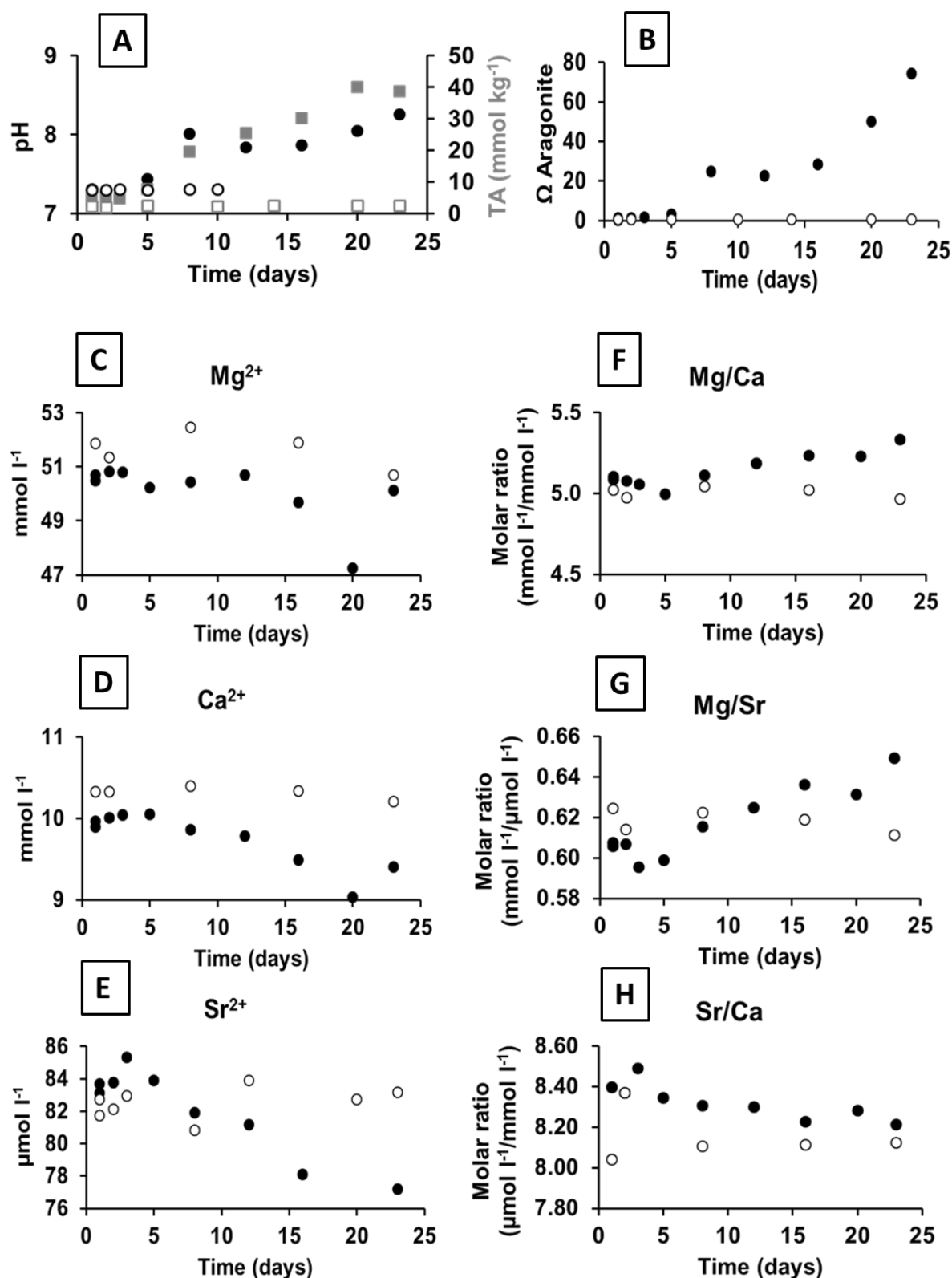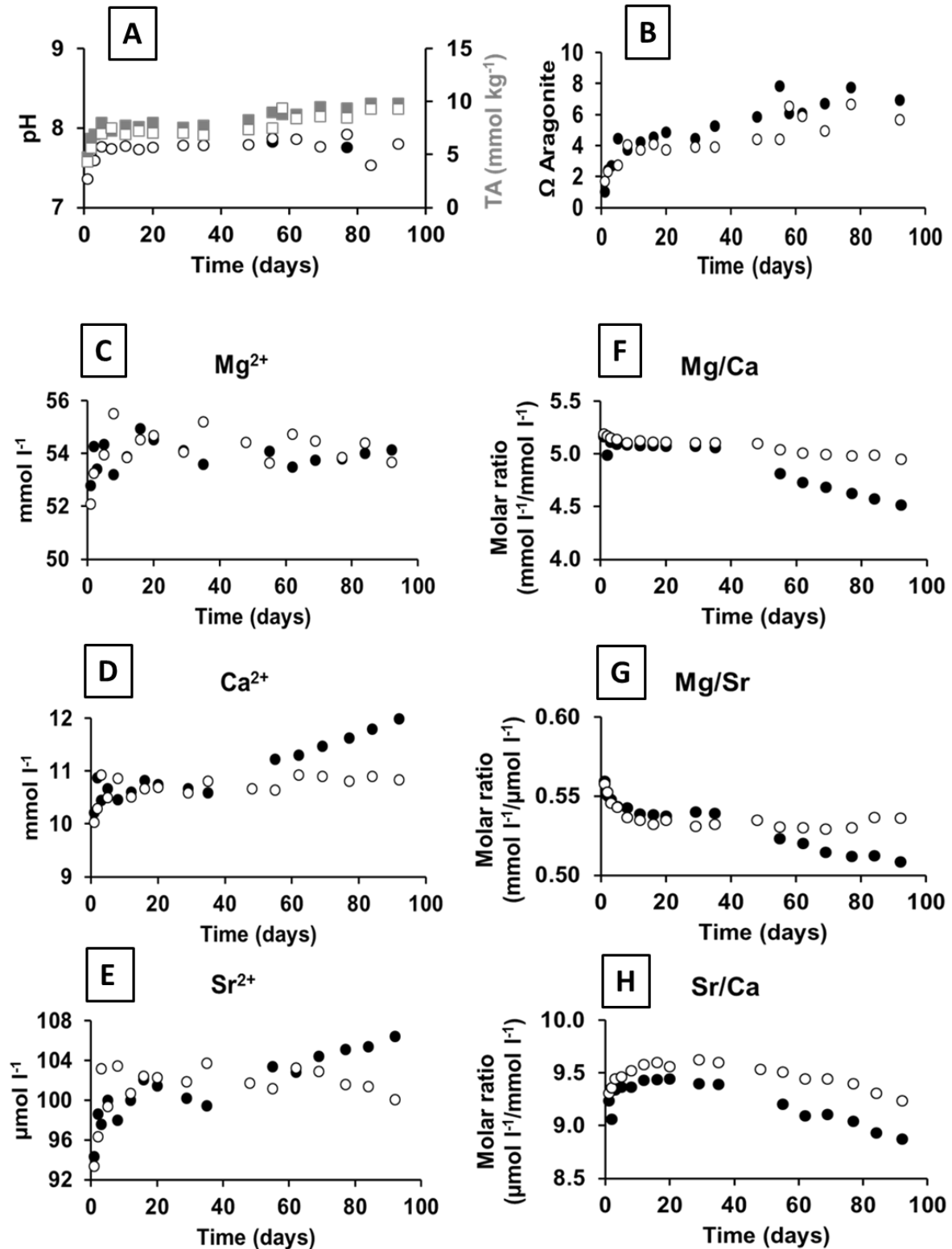
Figure 2. Medium chemistry of the 20°C *A. borkumensis* incubation: Temporal development of (A) $\Omega_{Aragonite}$ (circles) and Total Alkalinity (TA) (squares), (B-D) divalent-cation concentrations, and (E-G) divalent-cation ratios. Solid symbols show bulk-medium values, open symbols show control values.

Anoxic incubation media

In all anoxic incubations, the added resazurin indicator did not change from colorless (anoxic conditions) to pink (partially or fully oxic conditions) confirming constant anoxic conditions. In the *S. sediminis* incubation, the carbonate system parameters changed notably during the incubation period: The pH increased from 7.2 to 7.7, and after the medium exchange from 7.1 to 7.8 (Fig. 3A). Total Alkalinity increased from an initial 3.7 to 16.4 mmol kg^{-1} on day 55, $\Omega_{Aragonite}$ increased from 0.5 to 8.2 (Figs. 3A, B). After medium exchange the values for pH increased from 7.1 to 7.7, TA increased from 12.2 to 35.3 mmol kg^{-1}, and $\Omega_{Aragonite}$ from 3.2 to 16.5 (Fig. 3A, B). The Mg^{2+} concentration decreased from initial 51.8 to 49.9 mmol l^{-1} and further to 49.1 mmol l^{-1} after the medium exchange (Fig. 3C). The Ca^{2+} and Sr^{2+} concentrations increased from 10.0 to 10.8 mmol l^{-1} and 82.9 to 89.1 µmol l^{1}, respectively, prior to medium exchange. After the medium exchange the Ca^{2+} and Sr^{2+} concentrations remained stable with values between 10.0 and 9.9 mmol l^{-1}, and 83.4 and 83.2 µmol l^{-1}, respectively (Fig. 3D, E). Prior to the medium exchange, the Mg/Ca ratio decreased from an initial 5.2 to 4.7, and remained stable at 5.0 after the exchange. The Mg/Sr ratio decreased from 0.62 to 0.57 prior to the medium exchange and remained stable at 0.6 afterwards, and the Sr/Ca ratio remained stable throughout the experiment at a avalue of 8.3 (Fig. 3F, G, H). The pH in the cell-free control slightly increased from 7.2 to 7.3, TA ranged around 2.5 mmol kg^{-1} throughout the experiment, and $\Omega_{Aragonite}$ remained stable around 1 (Fig. 3A, B). The Mg^{2+} concentration was between 50.0 and 51 mmol l^{-1}, Ca^{2+} values remained stable between 9.9 and 10.2 mmol l^{-1}, and Sr^{2+} concentration had values from 80 to 81 µmol l^{-1} (Fig. 3C, D, E). The Mg/Ca ratio in the cell-free control was 5.0 to 5.1, the Mg/Sr ratio remained stable around 0.6, and the Sr/Ca ratio was between 8.0 and 8.1 (Fig. 3F, G, H).

In the anoxic sediment incubation, the pH increased from 7.4 to 7.7, TA increased from 4.8 to 9.9 mmol kg^{-1}, and $\Omega_{Aragonite}$ increased from 1.0 to 7.0 (Fig. 4A,B). Divalent cation concentrations also increased with time: The Mg^{2+} concentration increased from 52.8 to 54.1 mmol l^{-1}, the Ca^{2+} concentration from 10.2 to 12.0 mmol l^{-1}, and the Sr^{2+} concentration from 94.3 to 106.4 mmol l^{-1} (Fig. 4C, D, E). The Mg/Ca ratio decreased from 5.2 to 4.5, the Mg/Sr ratio decreased from 0.6 to 0.5, and the Sr/Ca ratio decreased from 9.2 to 8.9 (Fig. 4F, G, H). The pH values in the anoxic sediment control increased from an initial 7.4 to 7.8, TA increased from 5.8 to 12.0 mmol kg^{-1}, $\Omega_{Aragonite}$ increased from 3.6 to 6.6 (Fig. 4A, B). The Mg^{2+}, Ca^{2+} and Sr^{2+} concentrations increased from 52.1 to 53.7 mmol l^{-1}, 10.0 to 10.8 mmol l^{-1}, and from 93.3 to 100.1 mmol l^{-1}, respectively (Fig. 4C, D, E). The Mg/Ca ratio decreased from 5.2 to 5.0, the Mg/Sr ratio from 0.6 to 0.5, and the Sr/Ca ratio from an initial 9.3 to 9.2 at the end of the experiment (Fig. 4F, G, H).
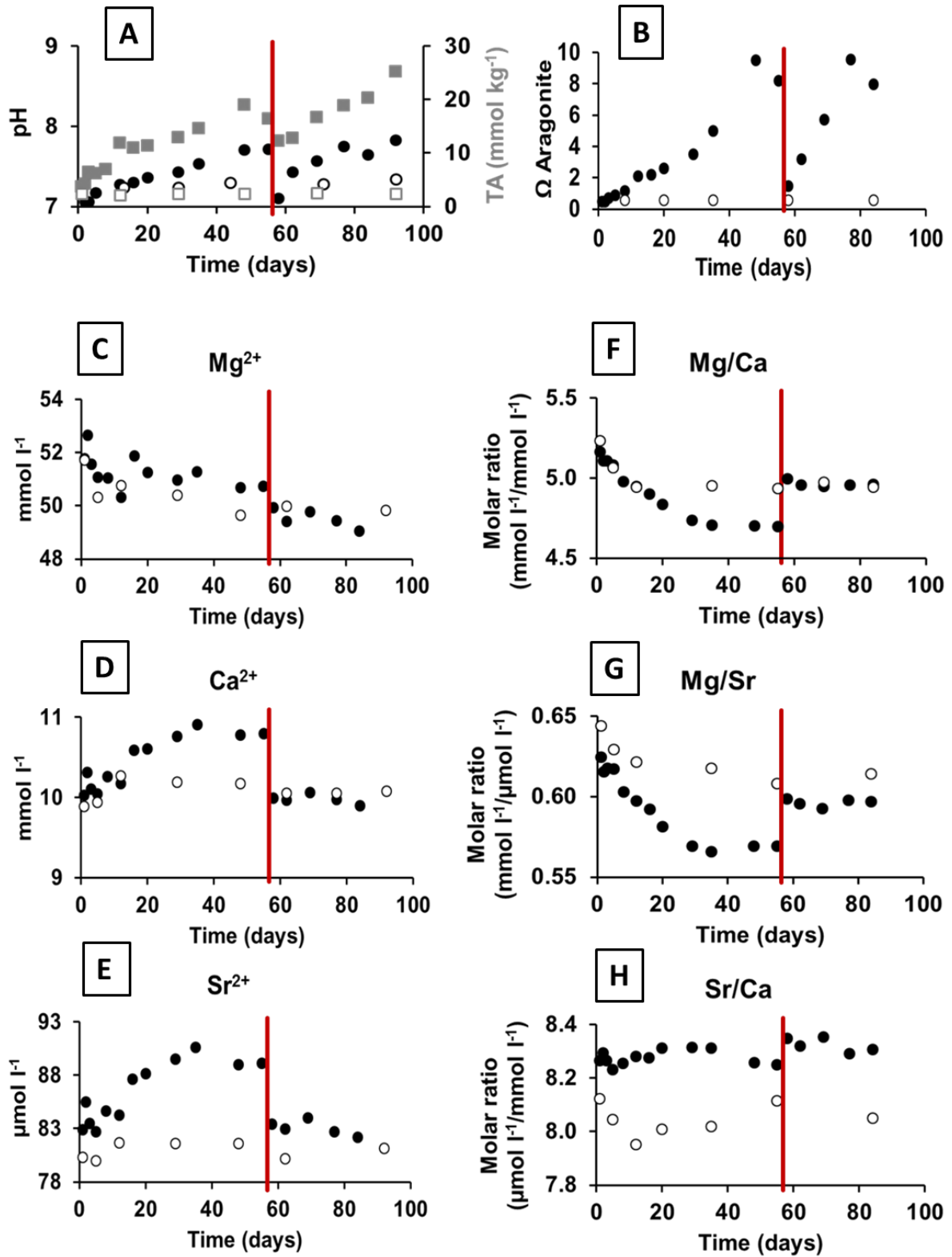
Figure 3. Medium chemistry of the *S. sediminis* incubation: Temporal development of (A) pH (circles) and Total Alkalinity (TA) (squares), (B) $\Omega_{Aragonite}$, (C-E) divalent-cation concentrations, and (F-H) divalent-cation ratios. Solid symbols show bulk-medium values, open symbols show control values. Red bars mark medium exchange on day 58.

Figure 4. Medium chemistry of the anoxic-sediment incubation: Temporal development of (A) pH (circles) and Total Alkalinity (TA) (squares), (B) $\Omega_{Aragonite}$, (C-E) divalent-cation concentrations, and (F-H) divalent-cation ratios. Solid symbols show bulk-medium values, open symbols show control values.

Coral structure and bacterial abundance

The SEM micrographs of samples from all incubations displayed intact surface structures with no distinct signs of secondary carbonate precipitation or surface dissolution (Fig. 5). Semi-quantitative pore-space calculation from μ-CT scans showed an increase in pore space on the coral sample exposed to the 20°C *A. borkumensis* incubation (pre-experiment 38.16 ± 0.94%, post-experiment 33.94 ± 1.14%), and a decrease in pore space was observed in the 10°C cell-free control sample (pre-experiment 35.66 ± 0.45%, post- experiment 34.76 ±0.39%) (Table 2). The pore-space on the sample exposed to the *S. sediminis* incubation decreased from 43.37 ± 1.61% (pre- experiment) to 40.48 ± 0.15% (post-experiment). No noticeable change in pore space on the sample incubated in the anoxic sediment (pre-experiment 37.31 ± 0.48%, post-experiment 35.60 ± 2.24%).

Filtered liquids from the cleaning procedure of samples incubated in the bacterial cultures and the anoxic sediment incubation contained dense cell aggregates, visualized by the DAPI staining (Fig. 6), with the highest density in the *S. sediminis* culture. In the A. borkumensis culture, biofilm fragments were visible. No cells were detected in the sample from the cell-free controls.
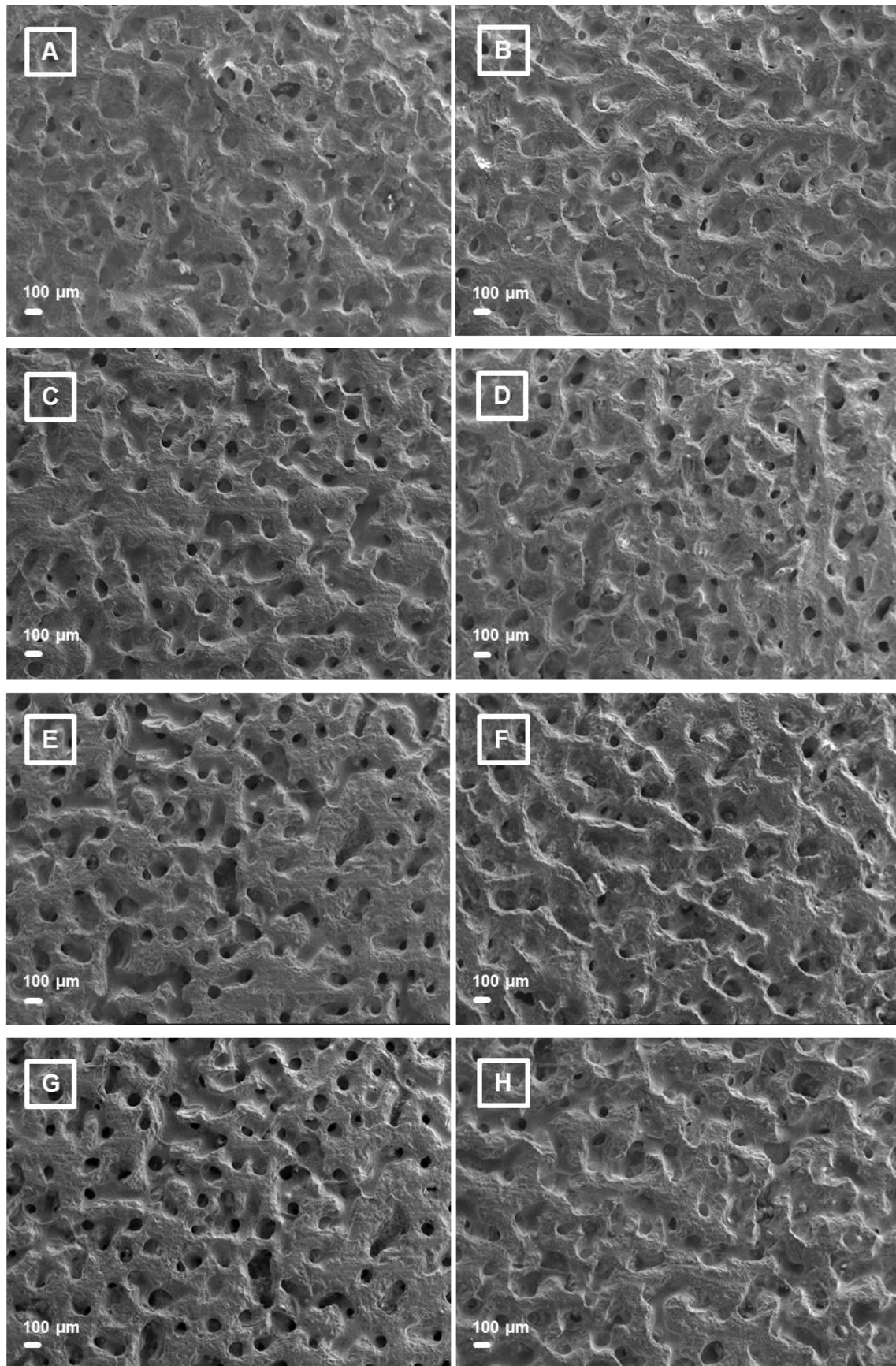
Figure 5. Scanning Electron Microscopy (SEM) micrographs of coral samples incubated in (A) the 10°C *A. borkumensis* incubation, (B) the 10°C cell-free control, (C) the 20°C *A. borkumensis* incubation, (D) the 20°C cell-free control, (E) the *S. sediminis* culture, (F) the cell-free control, and (G) the anoxic sediment. (H) Non-incubated reference sample.

Table 2. Percentage of pore space on coral samples prior to- and after incubation determined by X-ray microtomography scans and subsequent semi-quantitative analyses. Note that the sample incubated in the 10°C A. borkumensis culture was not comparable and is therefore not listed.

|	Pre-incubation		Post-incubation	
Sample	Pores (px)	Pore space (%)	Pores (px)	Pore space (%)
A. borkumensis 20°C				
K_005_C36_119	2780219	37.95	1901339	34.43
K_005_C36_120	2757078	37.66	2021220	36.46
K_005_C36_121	2791357	38.35	1939014	34.83
K_005_C36_122	2745142	37.71	1843554	33.23
K_005_C36_123	2697639	36.98	1898635	33.98
K_005_C36_124	2784206	38.13	1877527	33.61
K_005_C36_125	2822398	38.54	1824033	32.81
K_005_C36_126	2946800	40.31	1818003	32.68
K_005_C36_127	2835957	38.76	1921190	34.30
K_005_C36_128	2704701	37.19	1845275	33.04
Mean	2786550	38.62	1888979	33.94
SD	72005	0.33	62035	1.14
S. sediminis				
K_006_850_119	3020448	47.87	1906911	40.26
K_006_850_120	2717243	42.89	1927482	40.48
K_006_850_121	2707655	42.77	1928639	40.48
K_006_850_122	2672502	42.33	1950720	40.75
K_006_850_123	2722781	43.02	1913284	40.30
K_006_850_124	2715300	42.85	1930286	40.52
K_006_850_125	2708717	42.80	1922670	40.44
K_006_850_126	2695492	42.60	1940055	40.65
K_006_850_127	2732126	43.16	1932062	40.53
K_006_850_128	2754456	43.44	1923899	40.41
Mean	2744672	43.37	1927601	40.48
SD	99270	1.61	12422	0.15
Anoxic sediment				
K_005_C-24_119	1927459	37.96	1779045	34.77
K_005_C-24_120	1922074	37.79	1773208	34.72
K_005_C-24_121	1919451	37.62	1787995	34.92
K_005_C-24_122	1877435	36.90	1778300	34.81
K_005_C-24_123	1856890	36.49	1788518	34.94
K_005_C-24_124	1888171	37.17	1786974	34.93
K_005_C-24_125	1882183	37.09	1793664	35.02
K_005_C-24_126	1924066	37.81	1791675	34.99
K_005_C-24_127	1907809	37.35	2144853	41.97
K_005_C-24_128	1879086	36.91	1787840	34.95
Mean	1898462	37.31	1821207	35.60
SD	24717	0.48	113899	2.24
Control				
K_005_C13_119	1672227	34.88	1861010	35.23
K_005_C13_120	1723729	35.87	1855203	35.12
K_005_C13_121	1692539	35.26	1824226	34.46
K_005_C13_122	1698659	35.39	1814701	34.38
K_005_C13_123	1740789	36.23	1798670	34.14
K_005_C13_124	1747741	36.34	1863181	35.09
K_005_C13_125	1724405	35.85	1858088	35.13
K_005_C13_126	1708245	35.46	1847348	34.97
K_005_C13_127	1701459	35.42	1823363	34.54
K_005_C13_128	1720358	35.88	1828321	34.52
Mean	1713015	35.66	1837411	34.76
SD	22903	0.45	22446	0.39
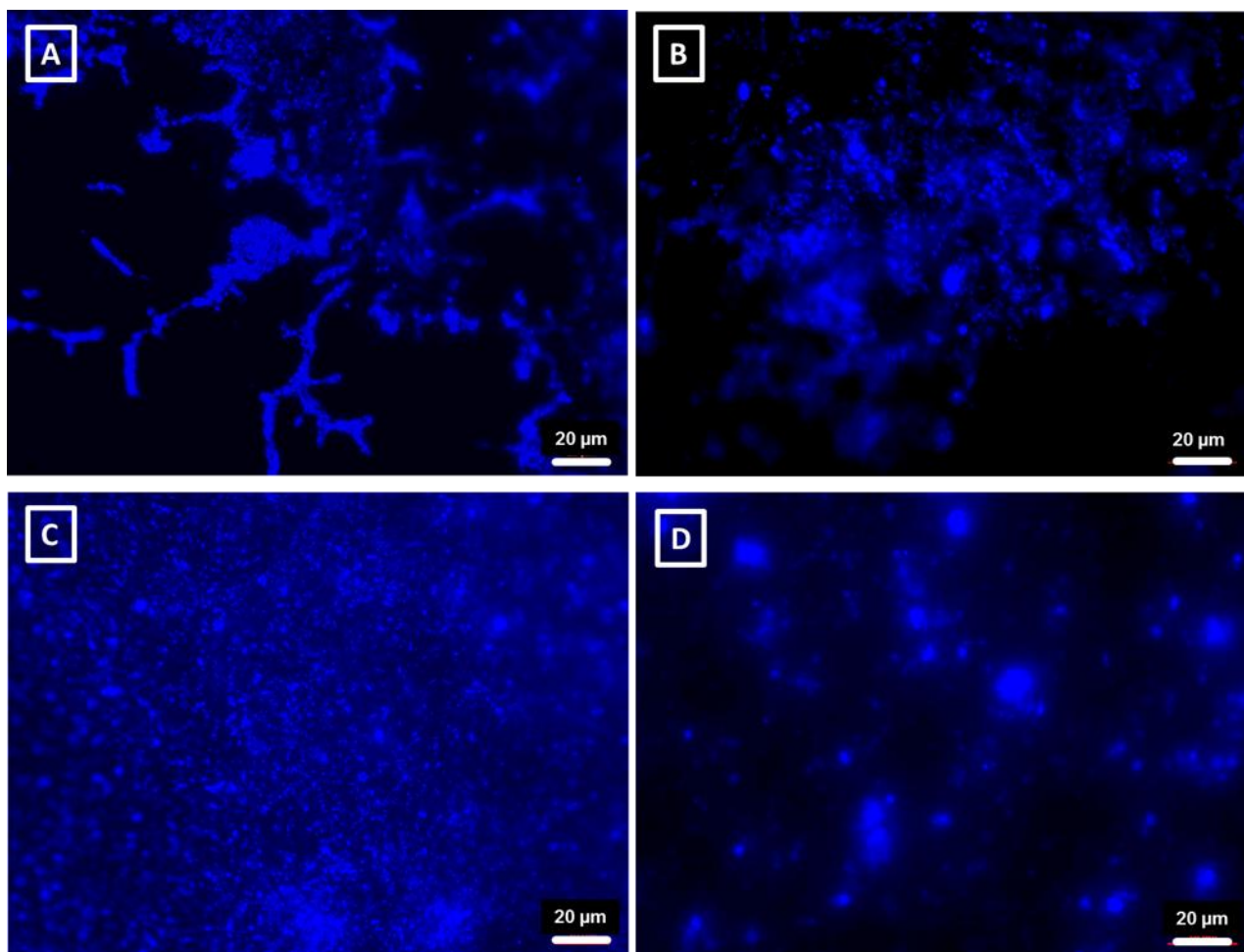
Figure 6. Cell aggregates and biofilms in the liquid retrieved from the cleaning procedure of coral samples incubated in (A) the 10°C *A. borkumensis* incubation, (B) the 20°C *A. borkumensis* incubation, (C) the *S. sediminis* incubation, and (D) the anoxic sediment incubation. Cells were stained with 4,6 diamidino-2-phenylindole (DAPI).

Coral elemental composition

The EMP maps displayed a decrease of Ca and Sr in the outermost sample areas exposed to the 10°C *A. borkumensis* incubation (Fig. 7A). While the Ca^{2+} concentration decreased from 20 wt% in inner, pristine sample areas to 6 wt% on the exposed sample rim, the loss in Sr concentration was visible, but below detection limit (0.2×10^{-5}) as was the loss in Sr in the rim of the sample exposed to the 20°C *A. borkumensis* incubation (0.2×10^{-3}) (Fig. 7A, C). In both samples the supposedly affected area protruded < 5 μm into the respective sample. Signs of phosphorous concentration increase were detected in the sample rim exposed to the 10°C *A. borkumensis* incubation. Samples exposed to the *S. sediminis* culture or the anoxic sediment displayed no changes in element concentrations relative to the respective controls (Fig. 8A-D). Strontium concentrations determined by means of μ-XRF analyses displayed average values of 20 to 30 wt% in all incubated samples and controls and the

unaltered reference. A minimum concentration of 10 wt% was determined at all sample pores, and peak values reached were 20 – 30 wt% in the incubated samples and 30wt% in the unaltered reference (Fig.9, 10). No other carbonate polymorph than aragonite was detected in the RAMAN analyses (Fig. 11).
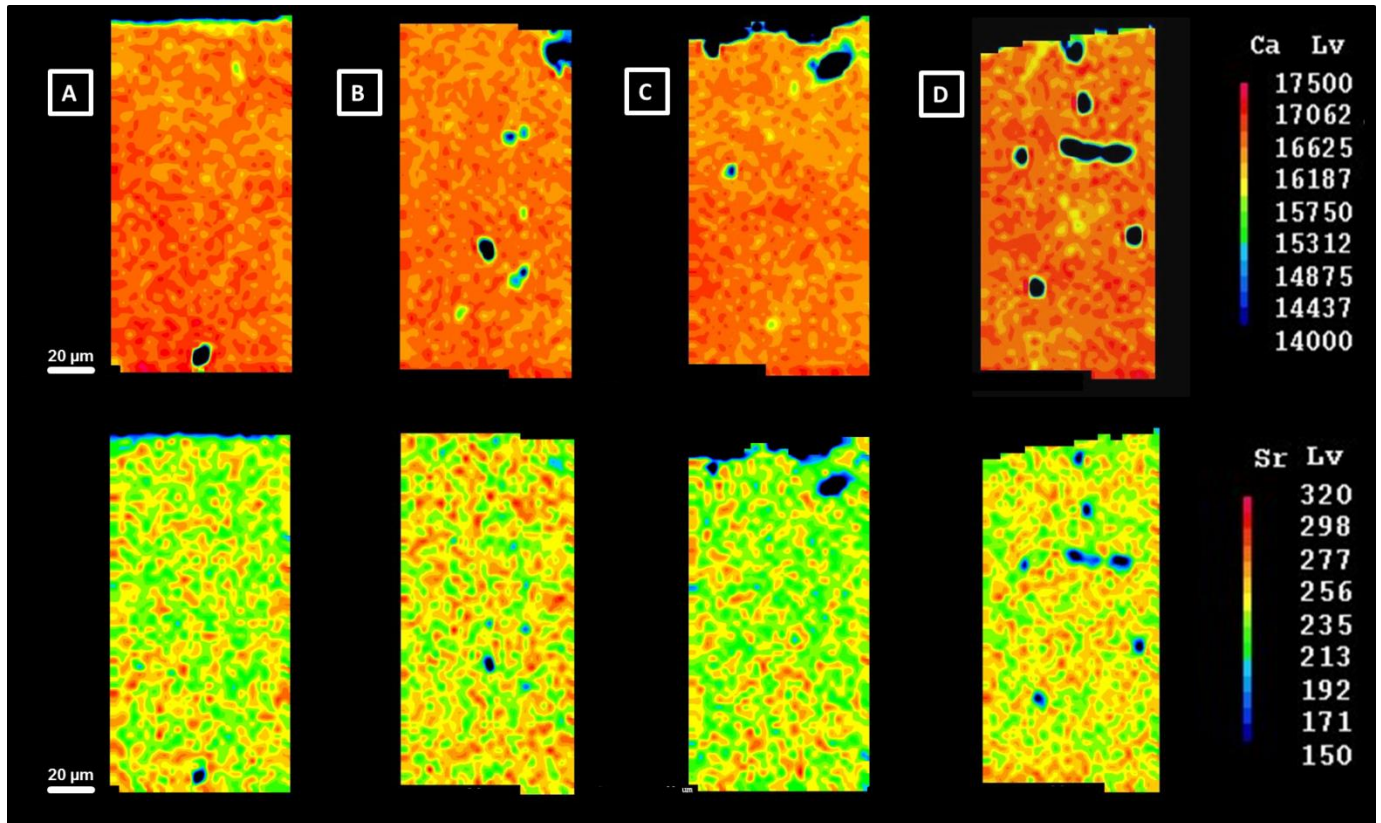
Figure 7. Electron Microprobe Ca and Sr maps of coral samples incubated in oxic incubation set-ups: (A) in the 10°C *A. borkumensis* incubation, (B) the 10°C cell-free control, (C)in the 20°C *A. borkumensis* incubation and (D) the 20°C cell-free control . Samples were sawn perpendicular, the upper sample parts are the surfaces exposed to the incubations, the lower parts are the inner, pristine sample-area. Maps show intensity in counts per second.
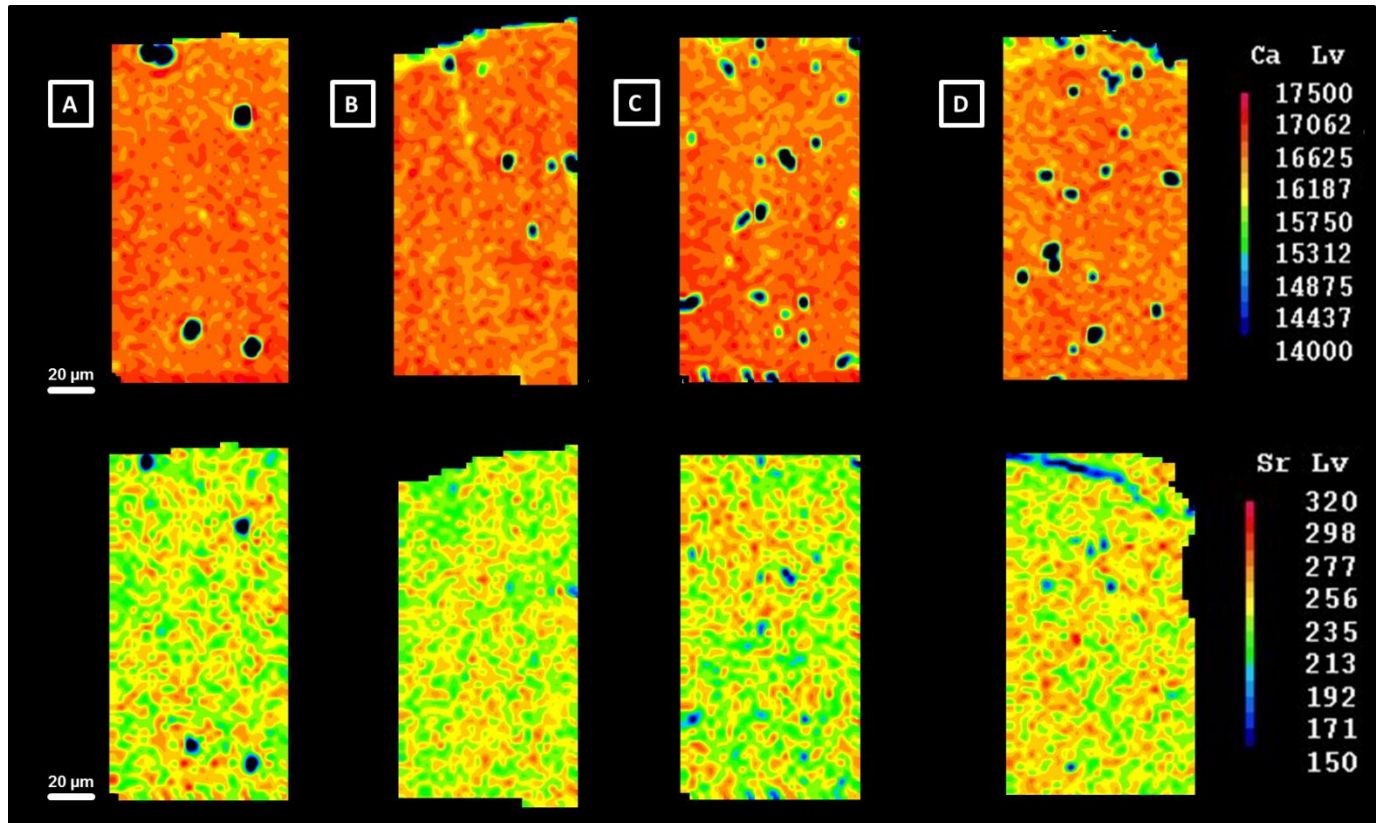
Figure 8. Electron Microprobe Ca and Sr intensity maps of coral samples incubated in anoxic incubation set-ups: (A) in the *S sediminis* culture, (B) in the cell-free control, (C) in the anoxic sediment. (D) Non-incubated reference sample. Samples were sawn perpendicular, the upper sample parts are the surfaces exposed to the incubations, the lower parts are the inner, pristine sample-area. Maps show intensity in counts per second.
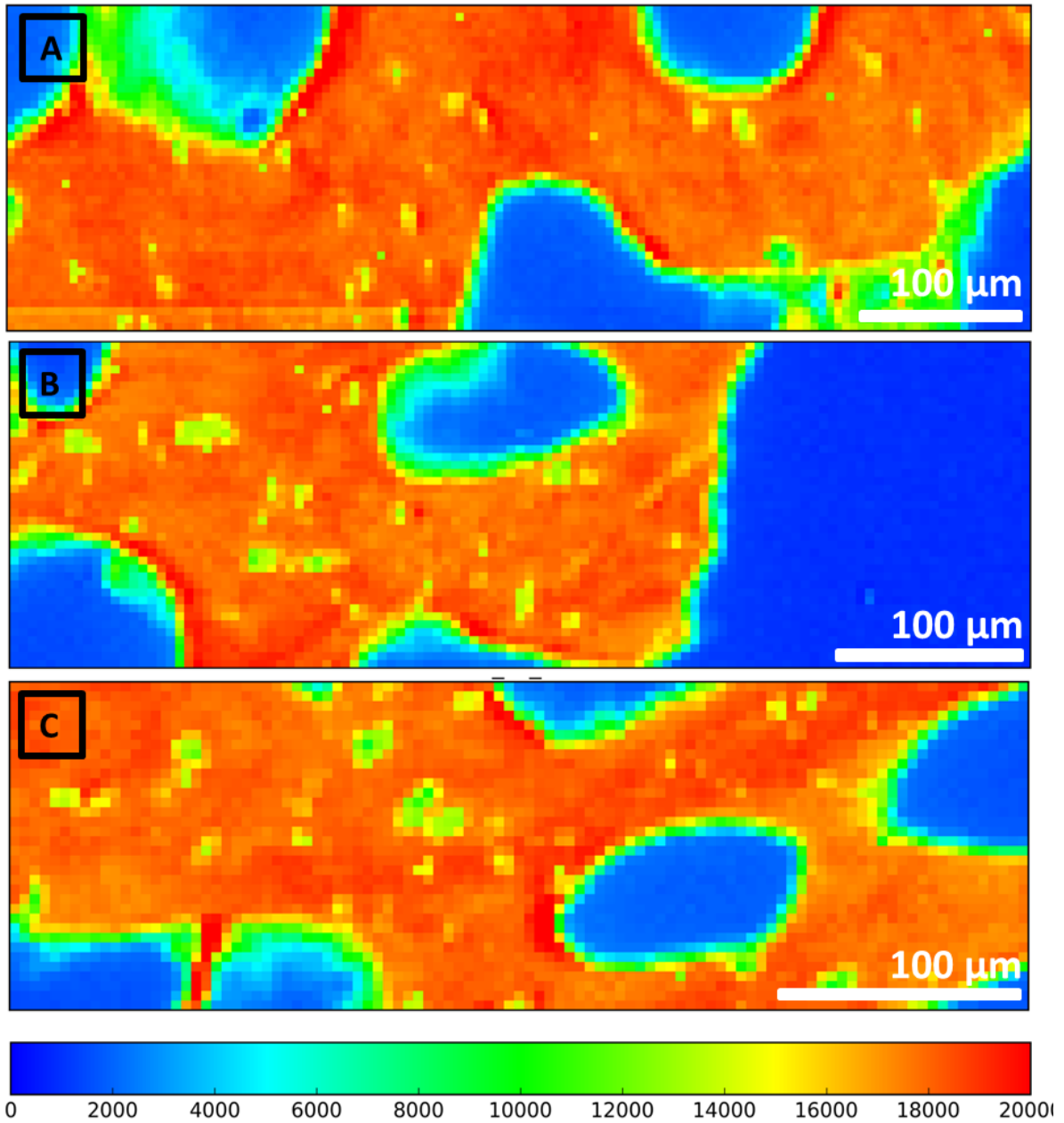
Figure 9. µ-XRF-maps of strontium L-edge along the transects of coral samples incubated in oxic incubation set-ups: (A) the 10°C *A. borkumensis* incubation, and (B) the 20°C *A. borkumensis* incubation. (C) Non-incubated reference sample. Concentrations are displayed in counts per second. Note, that for all incubations only one unaltered reference sample was analyzed.
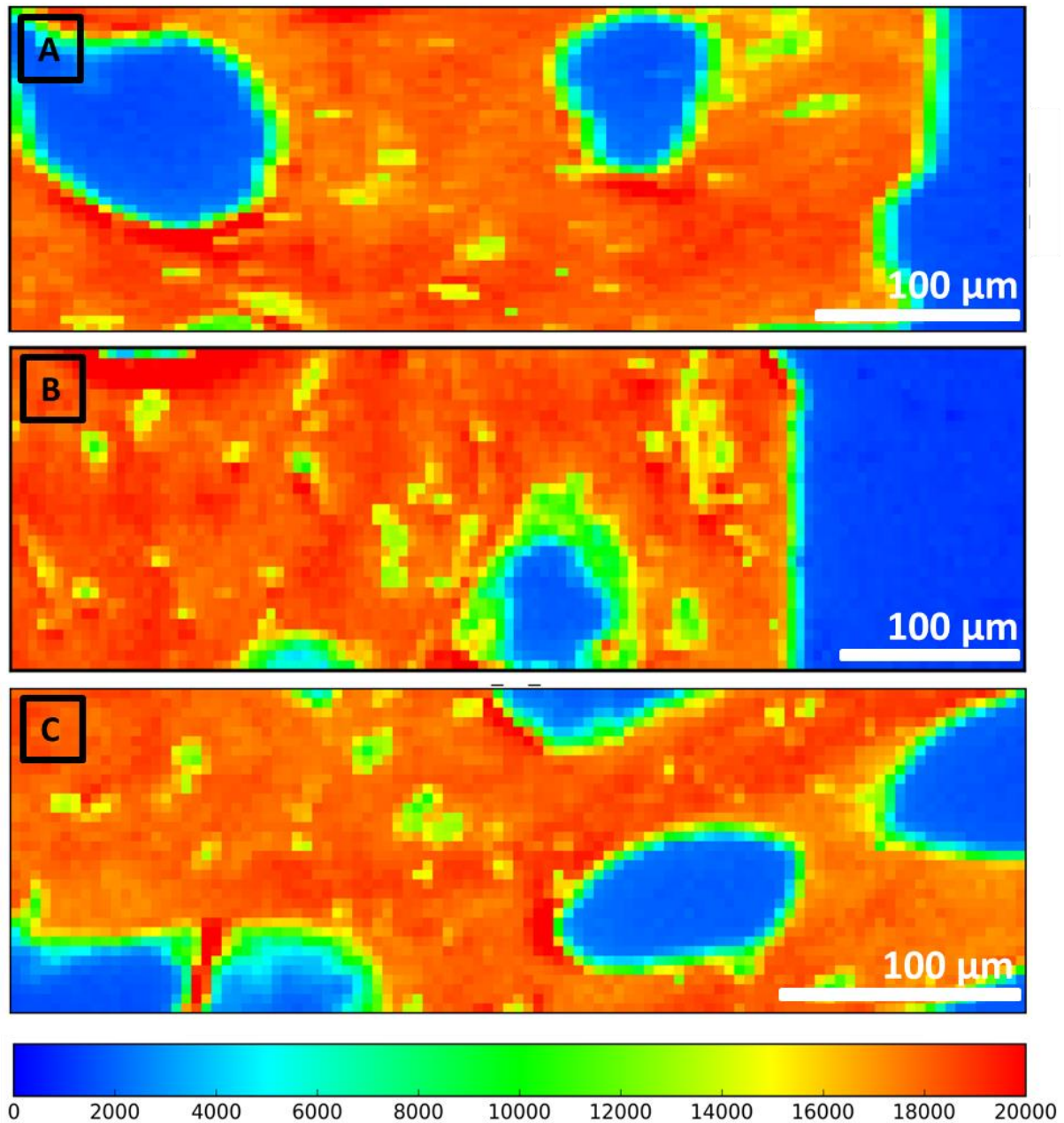
Figure 10. µ-XRF-maps of strontium L-edge along the transects of coral samples incubated in anoxic incubation set-ups: (A) the *S. sediminis* culture, and (B) the anoxic sediment. (C) Non-incubated reference sample. Concentrations are displayed in counts per second. Note, that for all incubations only one unaltered reference sample was analyzed.
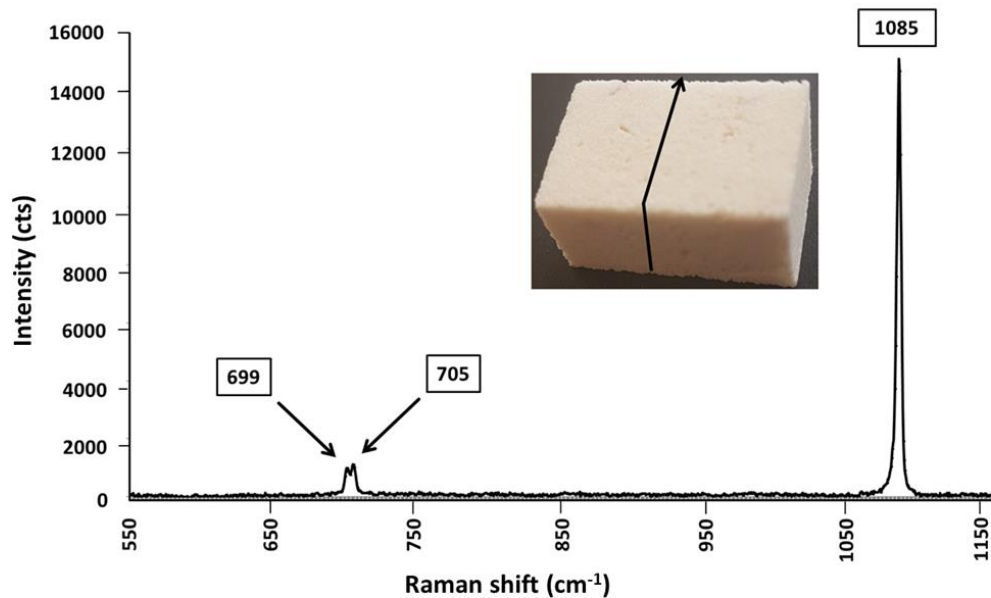
Figure 11. Example of output from a Raman spectroscopic scan conducted on coral sample after incubation in the 10°C *A. borkumensis* bacterial culture medium (the conducted transect is indicated on the sample-picture). The doublet displays the bending mode v4 of the carbonate ion in aragonite.

Coral carbon and oxygen isotopy

The carbon isotope ratios in the coral sample exposed to the 10°C *A. borkumensis* culture were ^{13}C-enriched in the two subsamples taken from the sample surface (-0.39 ± 0.03 and -0.94 ± 0.04‰) relative to the subsurface (-1.17 ± 0.03‰) and to 1 mm sample depth (-2.43 ± 0.02‰) (Table 3). In the 10°C cell-free control, $\delta^{13}C$ values were -1.84 ± 0.04‰ (surface), -2.00 ± 0.03‰ (subsurface), and -1.63 ± 0.04‰ (1 mm depth). Carbon isotope data for the sample exposed to the *A. borkumensis* 20°C incubation were -1.77 ± 0.04‰ on the surface, -1.69 ± 0.02‰ on the subsurface, and -2.22 ± 0.04‰ at 1 mm depth, and values in the 20°C cell-free control were -1.99 ± 0.04‰ (surface), -1.77 ± 0.05‰ (subsurface), and -2.43 ± 0.03‰ (1 mm depth). The $\delta^{13}C$ values of in the sample exposed to the *S. sediminis* culture was -1.80 ± 0.04‰ (surface), -2.14 ± 0.04‰ (subsurface), and -2.39 ± 0.03‰ (1 mm depth), while in the respective cell-free control values ranged from -1.26 ± 0.02‰ on the sample surface to -1.76 ± 0.04‰ on the subsurface, and -1.49 ± 0.02‰ at 1 mm depth. In samples exposed to the anoxic sediment, carbon isotope compositions were -1.55 ± 0.03‰ on the surface, -

1.78 ± 0.02‰ on the subsurface, and -1.74 ± 0.04‰ at 1 mm sample depth. The three unaltered reference samples had δ^{13}C values of -1.94 ± 0.04, -1.98 ± 0.02, and -1.66 ± 0.02‰ on the sample surfaces, -1.88, ± 0.03, -2.38 ± 0.03, and -1.58 ± 0.03‰ on the subsurfaces, and -1.77 ± 0.04, -2.21 ± 0.03, and -1.44 ± 0.03‰ at 1 mm sample depth. Based on the δ^{13}C values in the *A. borkumensis* 10°C sample, a t-test was applied for comparison of mean variances between the sample, cell-free control samples and unaltered reference samples. The results showed no significant difference ($p > 0.05$).

The oxygen isotope data in the sample exposed to the 10°C *A. borkumensis* incubation were -3.39 ± 0.11 and -3.22 ± 0.06‰ on the two subsamples taken from the surface, respectively, -3.15 ± 0.10‰ on the subsurface, and -3.80 ± 0.04‰ at 1mm sample depth (Table 3). In the 10°C cell free control values ranged from -1.7 ± 0.04‰ (surface), to -3.24 ± 0.06‰ (subsurface) and -3.75 ± 0.07‰ (1 mm depth). The δ^{18}O data for the 20°C *A. borkumensis*-incubation sample were -3.33 ± 0.07‰ on the sample surface, -2.88 ± 0.04‰ on the subsurface, and -2.90 ± 0.05‰ at 1 mm sample depth, while in the sample incubated in the 20°C cell-free control had δ^{18}C values of -3.05 ± 0.06‰ (surface), -3.39 ± 0.05‰ (subsurface), and -3.42 ± 0.06‰ (1 mm depth). The sample exposed to the *S. sediminis* culture had δ^{18}O values of -3.34 ± 0.06‰ (surface), -3.42 0.05‰ (subsurface), and -3.64 ± 0.07‰ (1 mm depth), and the δ^{18}O in the respective control sample was -3.38 ± 0.03‰ on the surface, -3.18 ± 0.05‰ on the subsurface, and -3.86 ± ‰ at 1mm sample depth. Samples exposed to the anoxic sediment incubation displayed moderate enrichment in δ^{18}O with increasing depth, with a surface value of -3.50 ± 0.06‰, -3.34 ± 0.05‰ on the subsurface, and -3.27 ± 0.04‰ at 1 mm depth. The unaltered control samples had surface δ^{18}O values of -3.62 ± 0.11, -3.18 ± 0.07, and -3.36 ± 0.07‰, values on the subsurface were -3.47 ± 0.04, -3.14 ± 0.06, and -3.11 ± 0.04‰, and the values at 1 mm sample depth were -4.01 ± 0.08, -3.42 ± 0.03, and -3.57 ± 0.05‰.

Table 3. δ^{13}C and δ^{18}O values of coral samples incubated in the 10°C and 20°C *A. borkumensis* culture, the *S. sediminis* culture, the respective controls, and the anoxic sediment. Unaltered reference samples serve as additional controls. Sampling was conducted on the exposed outmost sample surface, the area underneath the surface ("inside"), and at ca. 1 mm sample depth.

Incubation	Sample region	$\delta^{13}C_{VPDB\text{-}carbonate}$ [‰]	$\delta^{18}O_{VPDB\text{-}carbonate}$ [‰]
A. borkumensis 10°C	surface 1	-0.94 ± 0.04	-3.22 ± 0.06
	surface 2	-0.39 ± 0.03	-3.39 ± 0.11
	subsurface	-1.17 ± 0.03	-3.15 ± 0.10
	1 mm depth	-2.43 ± 0.02	-3.80 ± 0.04
A. borkumensis 10°C cell-free control	surface	-1.77 ± 0.04	-3.33 ± 0.06
	subsurface	-2.00 ± 0.03	-3.24 ± 0.06
	1 mm depth	-1.63 ± 0.04	-3.75 ± 0.07
A. borkumensis 20°C	surface	-1.77 ± 0.04	-3.33 ± 0.07
	subsurface	-1.69 ± 0.02	-2.88 ± 0.04
	1 mm depth	-2.22 ± 0.04	-2.90 ± 0.05
A. borkumensis 20°C cell-free control	surface	-1.99 ± 0.04	-3.05 ± 0.06
	subsurface	-1.77 ± 0.05	-3.39 ± 0.05
	1 mm depth	-2.43 ± 0.04	-3.42 ± 0.06
S. sediminis	surface	-1.80 ± 0.04	-3.34 ± 0.06
	subsurface	-2.14 ± 0.04	-3.42 ± 0.07
	1 mm depth	-2.39 ± 0.04	-3.64 ± 0.07
S. sediminis cell-free control	surface	-1.26 ± 0.02	-3.38 ± 0.03
	subsurface	-1.76 ± 0.04	-3.18 ± 0.05
	1 mm depth	-1.49 ± 0.02	-3.86 ± 0.06
Anoxic sediment	surface	-1.55 ± 0.03	-3.50 ± 0.06
	subsurface	-1.78 ± 0.02	-3.34 ± 0.05
	depth	-1.74 ± 0.04	-3.27 ± 0.04
Unaltered control 1	surface	-1.94 ± 0.04	-3.62 ± 0.11
	subsurface	-1.88 ± 0.03	-3.47 ± 0.04
	1 mm depth	-1.77 ± 0.04	-4.01 ± 0.08
Unaltered control 2	surface	-1.98 ± 0.02	-3.18 ± 0.07
	subsurface	-2.38 ± 0.03	-3.14 ± 0.06
	1 mm depth	-2.21 ± 0.03	-3.24 ± 0.03
Unaltered control 3	surface	-1.66 ± 0.02	-3.36 ± 0.07
	subsurface	-2.58 ± 0.03	-3.11 ± 0.04
	1 mm depth	-1.44 ± 0.03	-3.57 ± 0.05

Discussion

Within the present study, the media of bacterial culture- and sediment incubations underwent distinct increases in pH, TA and $\Omega_{Aragonite}$, with the latter indicating $CaCO_3$ oversaturation in all incubations. As no similar effect was observed in the control media, the increases could have been induced by either coral dissolution, or bacterial activity that was increasing alkalinity and could consequently have facilitated secondary carbonate precipitation in the incubations. The latter assumption was supported by cation withdrawal from the oxic incubation media over time, but no related changes on sample surface structures were observed by SEM, and DAPI-stained samples from

the cleaning procedure displayed no signs of secondary carbonate nucleation. Semi-quantitative pore space analyses did not show distinct changes in sample porosity. Element mapping and carbon isotope analyses reflected the natural variation in the respective characteristics of incubated samples, control samples, and unaltered references. It is therefore apparent, that the observed changes in the incubation media derived from bacterial activity. The present results display rather weak effects (if at all) of heterotrophic bacterial activity on coral aragonitic carbonate under the given experimental conditions. In the following we will discuss these observations in more details.

Microbial alteration of coral structure and geochemistry

Oxic incubations

Alcanivorax borkumensis cultures were incubated with coral specimens at two different temperatures: The 10°C incubation reflected the temperature of the organism´s natural habitat (i.e. 11-12°C, Ellet and Jones, 1994), the 20°C incubation was an approximation to *A. borkumensis* optimum growth conditions (20-30°C, Yakimov, et al., 1998). Media of both the 10°C and the 20°C incubation displayed a strong increase in TA and $\Omega_{Aragonite}$, with higher values in the 20°C incubation compared to the 10°C regime (Figs. 1A, B; 2A, B). A recent study showed that *A. borkumensis* is capable of precipitating biofilm-associated high-Mg calcite (Krause et al., 2014b). Divalent cation concentrations and ratios, foremost in the 20°C medium, indicated bacterial withdrawal of Mg^{2+}, Ca^{2+} and Sr^{2+} from the media and subsequent carbonate precipitation. Loose cell-aggregates and biofilm fragments were visible in samples retrieved from the coral-cleaning procedure of both *A. borkumensis* culture media. In case of secondary carbonate precipitation, semicrystalline spherulites or dumbbell-shaped structures should have been present in the samples, but no signs for precipitation were detected (Fig. 6). The cation withdrawal presumably was based on cation binding through EPS and bacterial cell walls: Divalent cation complexation by EPS electrostatic binding sites was reported by Liu and Fang (2002), and the EPS of bacterial biofilms mediates carbonate precipitation through interaction of metabolically induced alkalinity gradients and the cation-scavenging ability of EPS functional groups (Pentecost, 1985; Decho, 2010). Furthermore, an increase in medium pH induces a net negative charge of bacterial cell walls (Konhauser and Riding, 2012) that enhances the bacterial capacity for cation adsorption (Yee and Fein, 2001). For equilibrium conditions, the anionic bacterial surface ligands in the 20°C culture would facilitate enhanced cation binding, and the pH and TA increase in the medium would have amplified the precipitation process. Consequently, $CaCO_3$ precipitation by *A. borkumensis* following colonization of coral sample surfaces was plausible, with the decreasing cation concentrations in the 20°C culture medium displaying the onset of precipitation. In the 10°C *A. borkumensis* incubation, Mg^{2+} and Ca^{2+} concentrations remained

stable, while Sr^{2+} was withdrawn from the media, and specificity for cation species of EPS electrostatic binding sites has been suggested by Guibaud et al. (2008). It is therefore possible that Sr^{2+} was the cation species foremost scavenged by the bacterial EPS. Furthermore, having the lowest hydration enthalpy of the herein examined cation species, Sr^{2+} is preferentially prone to bind to cell wall functional groups, relative to Mg^{2+} or Ca^{2+}. The observed growth-temperature related differences in cation scavenging suggest a hierarchy in cation scavenging prior to precipitation, where Sr^{2+} is the first cation complexed by the bacteria, followed by Ca^{2+} and Mg^{2+}. The stained cell-aggregates and biofilm fragments displayed no signs of secondary precipitation (Fig. 6) and no other polymorph than aragonite was detected by RAMAN analyses (Fig. 11). While analysis of the µCT scans of the sample exposed to the 20°C *A. borkumensis* incubation revealed a pore-space increase of approx. 5% after the incubation (Table 2), the SEM micrograph showed no obvious dissolution characteristics (Fig. 5), and no related decrease in cation concentrations was detected through EMP mapping or µ-XRF analyses of the respective sample (Figs. 7, 9) However, EMP maps displayed a decrease in Ca concentration in coral samples from the 10°C *A. borkumensis* incubation (Fig. 7) and an increase in phosphorous concentration was observed at sample sites close to the areas of decreasing cation concentration. The determined deviations, specifically in phosphorous concentration, were close to- or below detection limit, and rim artefacts, due to the phosphorous content in the embedding resin in general cannot be ruled out. However, as the cell-wall outer membrane of gram-negative bacteria consists of phospholipids, and bacterial biofilm EPS contains phosphodiester bound DNA, the increase in phosphorous concentration could reflect bacterial sample-surface colonization in the respective areas. If that was the case, cell death in the exceedingly growing culture could have led to a related release of weak acids that in turn would have induced initial dissolution on the coral surface, and subsequent opening of pathways for reactive fluids and bacterial cells.

Anoxic incubations

The increase in pH, TA and $\Omega_{Aragonite}$, together with the increasing Ca^{2+} and Sr^{2+} concentrations in the *S. sediminis* culture medium prior to medium exchange, hinted at carbonate dissolution. As the Sr/Ca ratio in the medium remained stable during the incubation, the dissolution rate was probably constant (Fig. 3). *S. sediminis* is capable of chitin hydrolysis and subsequent fermentation of the chitin monomer N-acteylglucosamine (Yang et al., 2006; Rodionov et al., 2010). Chitin is an integral part of the aragonitic organic matrix that provides a template for biomineralization processes (Watabe, 1985; Weiner and Addadi, 1991; Ehrlich, 2010), and a predominantly chitin containing organic matrix was isolated from aragonitic parts of the scleractinian coral *Pocillopora damicornis* (Wainwright 1963). Hence, degradation of the coral organic matrix through *S. sediminis* chitinase

activity could have induced partial dissolution of coral samples during the present experiments. However, recent studies on scleractinian corals, including those of the genus Porites, reported the mucopolysaccharide glycosaminoglycan to be the dominant organic matrix constituent in various species (e.g. Constantz and Weiner, 1988; Fricain et al., 2000; Puverel et al., 2005), and the exact coral-matrix composition is yet unresolved for many genera. In addition, no deacetylase activity has been reported for *S. sediminis* to date. Furthermore, the C_{org} content measured in the bulk aragonite of coral samples was low (i.e. 0.04%) and samples chosen for the incubations were free of outer organic remains that could have provided a carbon source for the bacteria. While SEM micrographs showed no signs of secondary carbonate precipitation on the coral sample (Fig. 5), a pore-space decrease of approx. 7% after the incubation was determined by analysis of the μ-CT scans (Table 2). EMP mapping displayed no change in Ca or Sr concentrations in the exposed sample area that would reflect either secondary precipitation or dissolution (Fig. 8). Hence, both pore-space increase and the increase in Ca^{2+} and Sr^{2+} concentrations in the medium remain unresolved, unless dissolution has taken place in areas other than those examined (e.g. deeper pore regions) that would account for the latter. The observed decrease in Mg^{2+} concentration in the medium might reflect the extensive growth of the *S. sediminis* culture: An early study by Webb (1968) reported a high affinity of gram negative bacteria for Mg^{2+} uptake, specifically during their exponential growth phase. Considering the function of Mg^{2+} as the co-factor for DNA polymerase, and given the increasing *S. sediminis* cell density, selective bacterial Mg^{2+} uptake would be plausible.

In the anoxic sediment incubation, TA values were high, but only slightly increased throughout the experiment. Hence, the comparably strong increase in $\Omega_{Aragonite}$ apparently is related to the increasing Ca^{2+} concentration over time (Fig. 4). The simultaneous increase in Sr^{2+} concentration hinted at aragonite dissolution. However, analysis of the μ-CT scans did not support this observation (Table 2), and neither EMP nor μXRF mapping displayed a decrease in coral aragonite Ca and Sr concentration in sample parts exposed to the anoxic sediment (Figs. 8, 10). Apparently the availability of labile organic carbon in the fertilized sediments made it unnecessary for the bacteria to approach the hard to obtain coral organic carbon. The majority of anaerobic bacterial organic matter degradation leads to an alkalinity increase in the sediment, where respiratory HCO_3^- is generated by denitrifiying bacteria, Mn- and Fe-reducing bacteria, and sulfate reducers. The latter are furthermore regarded as major contributors to elevated environmental pH and alkalinity values due to their additional withdrawal of the bacterial fermentation products hydrogen and formate from the system (Gallagher et al., 2014). The entirety of these processes is reflected by the changes in medium TA and $\Omega_{Aragonite}$, and, apparently, lead to the same trends in the sediment-control incubation. However, the increase of Ca^{2+} and Sr^{2+} concentrations observed in the sediment was not observed in the sediment control. Given that both incubations derived from the very same bulk sediment, a similar share in carbonate

constituents can be assumed. Dissolution of sediment-derived carbonate (i.e. aragonite) should therefore have been reflected in medium divalent cation concentrations of both the anoxic sediment, and the anoxic sediment control.

Isotopic composition

Skeletons of hermatypic corals in general display a high variability in carbon isotopic composition, caused by rates of symbiotic photosynthesis to respiration. If photosynthetic rates are high, enhanced ^{12}C fixation through zooxanthellae leads to the subsequent use of ^{13}C for coral calcification (for a comprehensive review, see Swart, 1983). The present dataset reflects this variability to a certain degree. However, coral samples exposed to the 10°C *A. borkumensis* incubation showed increasing δ ^{13}C values from the pristine, deeper sample parts to the exposed surface parts, relative to the cell-free control and unaltered samples. The δ ^{13}C values recently reported for modern Porites species in the Gulf of Aqaba range from -1.25‰ to -3.37‰ (Al-Rousan and Felis, 2012), and both subsamples taken from the surface of the 10°C *A. borkumensis* sample exceeded the maximum reported value by far (-0.94 ± 0.04‰ and -0.39 ± 0.03‰). Furthermore, deviations from the presumable pristine areas at 1 mm depth to the exposed/outmost surface lie between 0.23 and -0.23‰ in the cell-free control sample and the unaltered reference samples, values in the 10°C *A. borkumensis* sample deviate between 1.49 and 2.04‰. However, the p value > 0.05 obtained from the t-test displayed no significant difference between *A. borkumensis* sample and any of the control samples. The δ^{18}O values of incubated and control coral samples lie at the lower end of values reported for *Porites* species (-2.74 to -3.81‰; Grottoli, 1999 and -1.85 to -3.30‰, Al-Rousan et al., 2002), but no trends in the spatial isotope distribution from pristine inner, to exposed outer areas was observed. Hence, bacterial activity during the experiment apparently was not reflected in the samples´ oxygen isotopic composition.

Conclusions

The present data did not confirm an alteration pattern that is simply transferrable from bivalve (Lange et al., inrevision) to coral aragonite, nor did the comparably large sample surface of the coral compared to the bivalve lead to enhanced coral carbonate alteration by bacteria from any incubation set-up. The crucial factor appears to be the relatively low fraction of available organic carbon in the coral samples (with a mean of 0.04%) compared to the bivalve shell samples (with a mean of 3% including periostraca, and 0.4% in the bulk aragonite). Based on the medium divalent cation data, the degree of alteration (i.e. carbonate precipitation) potential in the oxic incubation with *A. borkumensis* increased with growth temperature. However, this was not supported by structural,

geochemical, or isotopic coral-sample analyses, which is probably owed to the short incubation time of only 25 days. Given the changes in carbonate chemistry of all incubation media, but the cell free-controls, over time, it could be hypothesized that coral aragonite might be prone to bacterial alteration within a longer experimental duration. The apparent Mg^{2+} uptake of *S. sediminis* over time further suggests a susceptibility of organic-rich calcitic structures to bacterially-mediated alteration. The observed subtle changes within a short time span could, over geological timescales, have an enhanced effect on coral structure and geochemistry. Within the present study, however, none such alterations were detected, which leads to the final conclusion that organic-poor coral aragonites selected in this study appear to be less susceptible to microbial alterations compared to the more organic-rich shells of *A. islandica*.

References

Adkins, J.F., Boyle, E.A., Curry, W.B., and Lutringer, A. (2002) Stable isotopes in deep-sea corals and a new mechanism for "vital effects". *Geochimica et Cosmochimica Acta*, **67**, 6, 1129-1143.

Alibert, C., and McCullock, M.T. (1997) Strontium/calcium ratios in modern *Porites* corals from the Great Barrier Reef as a proxy for sea surface temperature: Calibration of the thermometer and monitoring of ENSO. *Paleoceanography*, **12**, 3, 345-363.

Allison, N., Finch, A.A., Sutton, S.R., and Newville, M. (2001) Strontium heterogeneity and speciation in coral aragonite: Implications for the strontium paleothermometer. *Geochimica et Cosmochimica Acta*, **65**, 16, 2669-2676.

Al-Horani, F.,A. (2005) Effects of changing seawater temperature on photosynthesis and calcification in the scleractinian coral *Galaxea fascicularis*, measured with O_2, Ca^{2+} and pH microsensors. *Scientia Marina*, **69**, 3, 347-354.

Aloisi, G., Gloter, A., Krüger, M., Wallmann, K., Guyot, F. and Zuddas, P. (2006) Nucleation of calcium carbonate on bacterial nanoglobules. *Geology*, **34**, 2017-2020.

Al-Rousan, S., Al-Moghrabi, S., Pätzold, J., and Wefer, G (2003). Stable oxygen isotopes in *Porites* corals monitor weekly temperature variations in the northern Gulf of Aqaba, Red Sea. *Coral Reefs*, **22**, 4, 346-356.

Bathurst, R.G.C. (1975) Carbonate Sediments and Their Diagenesis (Developments in Sedimentology). Elsevier Science, Oxford, 640 pp.

Beck, W.J., Edwards, L.R., Ito, E., Taylor, F.W., Recy, J., Rougerie, F., Joannot, P., and Henin, C (1992) Sea-Surface Temperature from Coral Skeletal Strontium/Calcium Ratios. *Science*, **257**, 644-647.

Berner, R.A. (1980) Early Diagenesis: A Theoretical Approach. Princeton University Press, New Jersey, 256 pp.

Chalker, B.E., and Taylor, D.L. (1978) Rhythmic variations in calcification and photosynthesis associated with the coral *Acropora cervicornis* (Lamarck). *Proceedings of the Royal Society London B.*, **201**, 179-189.

Cohen, A.L., Owens, K.E., Layne, G.D., and Shimizu N. (2002) The Effect on Algal Symbionts on the Accuracy of Sr/Ca Paleotemperatures from Coral. *Science*, **296**, 331 – 333.

Cohen, A.L, and McConnaughey, T.A. (2003) Geochemical Perspectives on Coral Mineralization. *Reviews in Mineralogy and Geochemistry*, **54**, 1.

Constantz, B. and Weiner, S., (1988). Acidic Macromolecules Associated With the Mineral Phase of Scleractinian Coral Skeletons. *The Journal of Experimental Zoology*, **248**, 253-258.

Coughlin, R.T., Tonsager, S. and McGroarty, E.J. (1983) Quantitation of Metal Cations Bound to Membranes and Extracted Lipopolysaccharide of *Escherichia coli*. *Biochemistry*, **22**, 2002-2007.

Decho, A.W., Visscher, P.T. and Reid, R.P. (2005) Production and cycling of natural microbial exopolymers (EPS) within a marine stromatolite. *Palaeogeography, Palaeoclimatology, Palaeoecology*, **219**, 71-86.

Decho, A.W. (2010) Overview of biopolymer-induced mineralization: What goes on in biofilms? *Ecological Engineering*, **36**, 137-144.

Druffel, E. M. (1997) Geochemistry of corals: Proxies of past ocean chemistry, ocean circulation, and climate. *Proceedings of the National Academy of Sciences of the United States of America*, **94**, 16, 8354-8361.

Dupraz, C., Visscher, P.T., Baumgartner, L.K. and Reid, R.P. (2004) Microbe-mineral interactions: Early carbonate precipitation in a hypersaline lake (Eleuthera Island, Bahamas). *Sedimentology*, **51**, 745-765.

Ellet, D.J. and Jones, S.R. (1994) Surface temperature and salinity time-series from the Rockall Channel 1948-1992. Fisheries Research Data Report, **36**, Lowentoft.

Enmar, R., Stein, M. Bar-Matthews, M., Sass, E., Katz, A., and Lazar, B. (2000) Diagenesis in live corals from the Gulf of Aqaba. I. The effect on paleo-oceanography tracers. *Geochimica et Cosmochimica Acta*, **64**, 18, 3123-3132.

Fallon, S.J., McCulloch, M.T., van Woesik, R., and Sinclair, D.J. (1999). Corals at their latitudinal limits: laser ablation trace element systematics in *Porites* from Shirigai Bay, Japan. *Earth and Planetary Science Letters*, **172**, 221-238.

Felis, T., Pätzold, J., and Loya, Y. (2003) Mean oxygen-isotope signatures in *Porites* spp. Corals: inter-colony variability and correction for extension-rate effects. *Coral reefs* **22**, 328-336.

Fricain, J.C., Alouf, J., Bareille, R., Rouais, F., and Rouvillain, J.L. (2002). Cytocompatibility study of organic matrix extracted from carribean coral Porites astroides. *Biomaterials*, **23**, 673-679.

Froelich, P.N., Klinkhammer, G.P., Bender, M.L., Luedtke, N.A., Heath, G.R., Cullen, D., Dauphin, P., Hammond, D. and Hartman, B. (1978) Early oxidation of organic matter in pelagic sediments of the eastern equatorial Atlantic : suboxic diagenesis*. Geochimica et Cosmochimica Acta*, **43**, 1057-1090

Gagan, M.K., Ayliffe, L.K., Hopley, D., Cali, J.A., Mortimer, G.E., Chappell, J., McCulloch, M.T., and Head, M. J (1998). Temperature and Surface-Ocean Water Balance of the Mid-Holocene Tropical Western Pacific. *Science*, **279**, 1014-1018.

Gagnon, A.C., Adkins, J.F., Fernandez, D.P., and Robinson, L.F. (2007). Sr/Ca and Mg/Ca vital effects correlated with skeletal architecture in a scleractinian deep-sea coral and the role of Rayleigh fractionation. *Earth and Planetary Science Letters*, **261**, 1-2, 280-295.

Gallagher, K., Dupraz, C. and Visscher, P. (2014) Two opposing effects of sulfate reduction on carbonate precipitation in normal marine, hypersaline, and alkaline environments: COMMENT. *Geology*, **42**, e313 - e 314-42.

Grottoli, A.G. (1999) Variability of stable isotopes and maximum linear extension in reef-coral skeletons at Kaneohe Bay, Hawaii. *Marine Biology*, **135**, 437-449

Guibaud, G., Bordas, F., Saaid, A., D'Abzac, P. and Van Hullebusch, E. (2008) Effect of pH on cadmium and lead binding by extracellular polymeric substances (EPS) extracted from environmental bacterial strains. *Colloids and Surfaces B: Biointerfaces*, **63**, 48-54.

Harriss, R.C., and Almy, Jr., C.C. (1964) A preliminary investigation into the incorporation and distribution of minor elements in the skeletal material of scleractinian corals. *Bulletin of Marine Science*, **14**, 3, 418-423(6).

Hendy, E.J., Gagan, M.K., Lough, J. M., McCulloch, M., and deMenocal, P.B (2007) Impact of skeletal dissolution and secondary aragonite on trace element and isotopic climate proxies in Porites corals. *Paleoceanography*, **22**, PA 4101.

Hillgärtner, H., Dupraz, C. and Hug, W. (2001) Microbially induced cementation of carbonate sands: are micritic meniscus cements good indicators of vadose diagenesis? *Sedimentology*, **48**, 117 - 131.

Inoue, M., Suzuki, A., Nohara, M., Hibino, K., and Kawahata, H. (2007) Empirical assessment of coral Sr/Ca and Mg/Ca ratios as climate proxies using colonies grown at different temperatures. *Geophysical Research Letters*, **34**, L12611.

Jørgensen, B.B. (2006) Bacteria and marine Biogeochemistry. In: *Marine Geochemistry* (Eds H.D. Schulz and M. Zabel), pp. 173-207. Springer, Berlin, Heidelberg.

Konhauser, K. and Riding, R. (2012) Bacterial Biomineralization. In: *Fundamentals of Geobiology*, (Eds A. Knoll, D. Canfield, and K. Konhauser), 105-130, Blackwell Science, Oxford.

Krause S., Liebetrau, V., Gorb, S., Sánchez-Román, M., McKenzie, J.A., and Treude T. (2012) Microbial nucleation of Mg-rich dolomite in exopolymeric substances under anoxic modern seawater salinity: New insight into an old enigma. *Geology*, **40**, 587-590.

Krause, S., Aloisi, G., Engel, A., Liebetrau, V. and Treude, T. (2014a) Enhanced Calcite Dissolution in the Presence of the Aerobic Methanotroph Methylosinus trichosporium. *Geomicrobiology Journal*, **31**, 325-337.

Krause, S., Liebetrau, V., Eisenhauer, A., and Treude, T. (2014b) Carbonic anhydrase - a geological relevant enzyme? Goldschmidt Conference abstract.

Lange, S.M., Krause, S., Ritter, A.-C., Fichtner, V., Immenhauser, A., Strauss, H., and Treude, T. (2017) Anaerobic microbial activity affects earliest diagenetic pathways of bivalve shells. In revision for *Sedimentology*.

Le Campion-Alsumard, T., Golubic, S., and Hutchings, P. (1995) Microbial endoliths in skeletons of live and dead corals: Porites lobate (Moorea, French Polynesia). *Marine Ecology Progress Series*, **117**, 149-157.

Liu, H. and Fang, H.H.P. (2002) Characterization of electrostatic binding sites of extracellular polymers by linear programming analysis of titration data. *Biotechnology and Bioengineering*, **80**, 806-811.

Lynn, P.W., and Manzello, D.P. (2015) Bioerosion and coral reef growth: a dynamic balance. In: *Coral reefs in the Anthropocene* (Ed Charles Birkeland) Pp 67-97, Springer Netherlands.

Mitsuguchi, T., Matsumoto, E., Abe, O., Uchida, T., and Isdale, P.J. (1997). Mg/Ca Thermometry in Coral Skeletons.*Science*, **274**, 961-963.

Orcutt, B.N., Sylvan, J.B., Knab, N.J. and Edwards, K.J. (2011) Microbial Ecology of the Dark Ocean above, at, and below the Seafloor. *Microbiology and Molecular Biology Reviews*, **75**, 361-422.

Paine, S.G., Linggood, F.V., Schimmer, F. Thrupp, T.C. (1933) The Relationship of Micro-Organisms to the Decay of Stone. *Philosophical Transactions of the Royal Society London, Series B, Biological Sciences*, **222**, 97-127.

Puverel, S., Tambutté, E., Zoccola, D., Domart-Coulon, I., Bouchot, A., Lotto, S., Allemend, D., and Tambutté, S. (2005). Antibodies against the organic matrix in scleractinians: a new tool to study coral biomineralization. *Coral Reefs*, **24**, 149-156.

Rodionov, D.A., Yang, C., Li, X., Rodionova, I.A., Wang, Y., Obraztsova, A.Y., Zagnitko, O.P., Overbeek, R., Romine, M.F., Reed, S., Fredrickson, J.K., Nealson, K.H. and Osterman, A.L. (2010) Genomic encyclopedia of sugar utilization pathways in the Shewanella genus. *BMC genomics*, **11**, 494.494

Sánchez-Román, M., Rivadeneyra, M.A., Vasconcelos, C. and McKenzie, J.A. (2007) Biomineralization of carbonate and phosphate by moderately halophilic bacteria. *FEMS Microbiology Ecology*, **61**, 273-284.

Schindler, M. and Osborn, M.J. (1979) Interaction of Divalent Cations and Polymyxin B with Lipopolysaccharide. *Biochemistry*, **18**, 4425-4430.

Selvarengan, P., Kubicki, J.D., Guégan, J.-P., and Chatellier, X. (2010) Complexation of carboxyl groups in bacterial lipopolysaccharides: Interactions of H^+, Mg^{2+}, Ca^{2+}, Cd^{2+}, and UO^{2+}_2 with Kdo and galacturonate molecules via quantum mechanical calculations and NMR spectroscopy. *Chemical Geology*, **273**, 55-75.

Sinclair, D.J., Williams, B., and Risk, M. (2006) A biological origin for climate signals in corals – Trace element "vital effects" are ubiquitous in Scleractinian coral skeletons. *Geophysical Research Letters*, **33**, L17707.

Smith, S.V., Buddemeier, R.W., Redalje, R.C., and Houck, J.E. (1979) Strontium-Calcium Thermometry in Coral Skeletons. *Science*, **204**, 4391, 404-407.

Swart, P.K. (1983) Carbon and Oxygen Isotope Fractionation in Scleractinian Corals: a Review. *Earth-Science Reviews*, **19**, 51-80.

Swart, P.K., Elderfield, H., and Greaves, M..J. (2002) A high-resolution calibration of Sr/Ca thermometry using the Caribbean coral *Montastreaea annularis*. *Geochemistry, Geophysics, Geosystems,* **3**, 11.

Swart, P.K. (2015) The geochemistry of carbonate diagenesis: The past, present and future. *Sedimentology*, **62**, 1233-1304.

Tribollet, A. (2007) The boring microflora in modern coral reef ecosystems: a review of its roles In: *Current Developments in Bioerosion*, Springer, Berlin Heidelberg.

Tucker, M.E. and Bathurst, R.G.C. (1990) Carbonate Diagenesis. Blackwell Scientific Publications, 320 pp.

Uroz, S., Calvaruso, C., Turpault, M.P. and Frey-Klett, P. (2009) Mineral weathering by bacteria: ecology, actors and mechanisms. *Trends in Microbiology*, **17**, 378-387.

Vasconcelos, C. and McKenzie, J. (1997) Microbial mediation of modern dolomite precipitation and diagenesis under unoxic conditions (Lagoa Vermelha, Rio de Janeiro, Brazil*). Journal of Sedimentary Research*, **67**, 378-390.

Wainright, S.A. (1963) Skeletal organization in the coral, *Pocillopora damicornis*. *Journal of Cell Science,* **s3-104**: 169 – 183.

Walker, J.C.G. (1984) Suboxic diagenesis in banded iron formations. *Nature*, **309**, 340-342.

Watabe, N. (1965) Crystal-Matrix Relationships in the Inner Layer of Mollusk Shells. *Journal of Ultrastructure Research*, **12**, 351-370.

Webb, M. (1968) The Influence of Certain Trace Metals on Bacterial Growth and Magnesium Utilization. *Journal of General Microbiology*, **51**, 325-335.

Weber, J.N. (1973) Incorporation of strontium into reef coral skeletal carbonate. *Geochimica et Cosmochimica Acta*, **37**, 2173-2190.

Weber, J.N., and Woodhead, P.M.J. (1972). Temperature dependence of oxygen-18 concentration in reef coral carbonates. *Journal of Geophysical Research*, **77**, 463-473.

Weiner, S. and Addadi, L. (1991) Acidic macromolecules of mineralized tissues: the controllers of crystal formation. *Structural Chemistry*, **16**, 252-256.

Wright, D.T. and Wacey, D. (2005) Precipitation of dolomite using sulphate-reducing bacteria from the Coorong Region, South Australia: Significance and implications. *Sedimentology*, **52**, 987-1008.

Yakimov, M.M., Golyshin, P.N., Lange, S., Moore, E.R.B., Abraham, W.R., Lünsdorf, H., and Timmis, K.N. (1998) *Alcanivorax borkumensis* gen. nov., sp. nov., a new, hydrocarbon-degrading and surfactant-producing marine bacterium. *International Journal of Systematic Bacteriology*, **48**, 339-348.

Yang, C., Rodionov, D.A., Li, X., Laikova, O.N., Gelfand, M.S., Zagnitko, O.P., Romine, M.F., Obraztsova, A.Y., Nealson, K.H. and Osterman, A.L. (2006) Comparative genomics and experimental characterization of N-acetylglucosamine utilization pathway of Shewanella oneidensis. *Journal of Biological Chemistry*, **281**, 29872-29885.

Yee, N. and Fein, J. (2001) Cd adsorption onto bacterial surfaces: A universal adsorption edge? *Geochimica et Cosmochimica Acta*, **65**, 13, 2037-2024.

Zeebe, R. and Wolf-Gladrow, D. (2001) CO_2 in Seawater: Equilibrium, Kinetics, Isotopes. Elsevier Oceanography Series, 65, Amsterdam, pp. 346.

Chapter 4

Effects of heterotrophic bacterial activity on foraminiferal tests

Skadi M. Lange[1],*, Stefan Krause[1], Nicolaas Glock[1], and Tina Treude[2,3*]

[1] GEOMAR Helmholtz Centre for Ocean Research Kiel, Department of Biogeochemistry, Wischhofstr. 1-3, 24148 Kiel, Germany

[2] Department of Earth, Planetary, and Space Sciences, University of California, Los Angeles, 595 Charles E. Young Drive, Los Angeles, California 90095-1567, USA

[3] Department of Atmospheric and Oceanic Sciences, University of California, Los Angeles, 595 Charles E. Young Drive, Los Angeles, California 90095-1567, USA

Advanced draft

Abstract

Foraminiferal tests are frequently applied archives for paleoenvironmental research, and past sea-surface temperature can be deduced from combined analyses of test Mg/Ca and $\delta^{18}O$. However, both planktonic and benthic foraminifera undergo post-mortem deposition in marine sediments. Here, products of microbial metabolic redox processes induce conditions in the proximal environment that either foster $CaCO_3$ precipitation or -dissolution. The structural and geochemical imprint of these processes on foraminiferal tests may compromise the interpretation of these archives. Within the present study, bulk planktonic and benthic foraminiferal tests were incubated in oxic and anoxic bacterial culture media or anoxic sediment slurries over a time span of two months. While tests incubated in the anoxic bacterial incubations or the anoxic sediment showed no signs of alteration, the tests incubated in an oxic medium, containing a culture of the carbonic anhydrase bearing bacterial strain *Alcanivorax borkumensis* SK2[T], were substantially overgrown by secondary carbonate precipitates. The respective incubation medium displayed a distinct increase in foremost TA and $\Omega_{Calcite}$ and withdrawal of Mg^{2+}, Ca^{2+} and Sr^{2+} over time. In the cell-free control incubation, no corresponding development was observed, and control tests were not affected. The distinct alteration of foraminiferal tests by *A. borkumensis* during only two months indicate a potential of carbonic anhydrase bearing bacteria in general to compromise the explanatory power of these archives.

Introduction

Foraminifera are ubiquitously distributed in the marine realm, and while these highly diverse protist organisms cover planktonic as well as benthic habitats, the majority of modern Foraminifera experience a benthic lifestyle (Gupta, 1999). The habitats of benthic foraminifera comprise a wide range of sediment depths of varying organic content, with the correlation between organic carbon (C_{org}) flux and abundance being species-dependent (Altenbach, 1999; Murray, 2006). Besides foraminiferal diversity and ample distribution, their prominent fossil record makes them subject to a wide range of paleoenvironmental studies (e.g. Savin and Douglas, 1973; Belanger et al., 1981; Graham et al., 1981; Nägler et al., 2000; Martin et al., 2002; Creech et al., 2010) and the adaptation capability of some foraminiferal species to oxygen minimum zones is foremost of interest in the reconstruction of past ocean bottom water oxygenation (Loubere et al., 1993; Abu-Zied et al., 2008). Furthermore, the incorporation of Mg^{2+} in tests is a function of temperature, therefore the magnesium to calcium ratio (Mg/Ca) of foraminiferal test allows for sea-surface temperature (SST) reconstruction (Nürnberg et al., 1996; Elderfield and Ganssen, 2000) from which in turn paleo-ocean salinity and ocean circulation patterns can be deduced by analytic combination with the test´s oxygen isotopic ($\delta^{18}O$) composition (Lea et al., 2000). However, biological factors, such as the gametogenesis during the sexual foraminiferal reproduction cycle or physiological control during mineralization, can lead to variations of the Mg^{2+} uptake in foraminiferal tests (Nürnberg et al., 1996; Hastings, 1998). Furthermore, the Mg concentration in foraminiferal tests is taxon- to species specific (Blackmon and Todd, 1959; Lea, 2003), and highly inhomogeneous (Eggins et al., 2003). For example, the Mg/Ca ratio in tests of symbiont-bearing foraminifera differs significantly from that of symbiont-free species (Sadekov et al., 2005). Specifically benthic foraminiferal tests are subject to microbial endolithic boring after settling in the sediment (Golubic et al., 1984; Peebles and Lewis, 1988). Additionally, early diagenesis can abiotically alter trace-element concentration and isotopic signature of both benthic and planktonic foraminiferal tests during lifetime and post mortem, e.g. through cation exchange (Towe and Hemleben, 1976), cementation (Mitchell et al., 1997), and non-stoichiometric re-precipitation (Kozdon et al., 2013). Post-mortem, foraminifera are subject to a redox zonation in marine sediments. The availability and energetic yield of electron acceptors for metabolic redox processes determines the distribution of microbial communities in marine sediments: In the oxic zone of the sediment, aerobic organic matter degradation generates CO_2 and consequently an acidic proximal environment. The energetically next favorable electron acceptor for metabolic redox reactions is NO_3^-, vertically followed by Mn(IV), Fe (III), and SO_4^{2-} (Froelich et al., 1979; Jorgensen, 2006; Orcutt et al., 2011). The related anaerobic reductive metabolisms generate metabolic HCO_3^-, thereby fostering alkaline (micro-) environmental conditions, and further increase

in alkalinity is induced by methanogens that withdraw CO_2 from the system for methanogenesis. Hence, benthic microbial metabolism and the respective metabolic products either create environmental conditions that potentially support carbonate dissolution or precipitation, and could thereby substantially alter the properties of biogenic carbonates after deposition in marine sediments.

In two previous studies, bivalve or coral aragonitic hard parts, respectively, were incubated in bacterial culture media and anoxic sediments (Lange et al., in revision). Results showed distinct bacterial alteration effects in bivalve-shell surface structure and geochemistry, while no comparable impact was observed on coral samples. The main underlying factor apparently was the low share of organic carbon in the coral carbonate (0.04%) compared to that of the bivalve shell (3%). Foraminiferal tests have a C_{org} share of about 1%. Given, that the thickness of foraminiferal tests varies between only 20 and 50 µm, the organic constituents are comparably easy to approach for bacteria. Furthermore, the high surface to volume area of bulk tests would expectedly increase the reactive surface for bacterial activity.

To investigate the susceptibility of foraminiferal tests to bacterial-induced alteration, in the present study bulk foraminiferal tests were exposed to a culture of the aerobic bacterial strain *Alcanivorax borkumensis* SK2[T], the anaerobic bacterial strain *Shewanella sediminis* HAW-EB3, and an anoxic sediment slurry. A recent study by Krause et al. (2014) reported carbonic-anhydrase activity for *A. borkumensis,* which induced increasing alkalinity, supersaturation with respect to $CaCO_3$ and the subsequent precipitation of high-Mg calcite. *S. sediminis* hydrolyzes chitin polymers by means of a chitinase and subsequently oxidizes and ferments the resulting monomer N-acteylglucosamine (Yang et al., 2006; Rodionov et al., 2010). This could consequently lead to degradation of the carbonate-associated organic matrix and to subsequent $CaCO_3$ dissolution. Thereby, both bacterial cultures account for a potential to alter biogenic carbonate archives.

The experiments within this study were conducted to answer the following research questions: (i) Are foraminferal calcitic tests prone to post-mortem aerobic and anaerobic microbial alteration in sediments, with regard to test structure and/or -geochemistry? (ii) If so, will the alteration characteristics compromise paleoenvironmental (i.e. foremost paleotemperature) interpretation of these archives?

Methods

Seawater sampling and treatment

Natural North Sea water for the incubations was sampled during R/V Heincke cruise HE-411 south-east of Heligoland (54° 06´ N, 008° 00´ E). The seawater was subsequently stored in a bulk container (IBC) at 10°C and oxygenated with an EHEIM compact 600 aquarium pump (EHEIM, Deizisau, Germany). Prior to the experimental start, seawater aliquots were sterilized with an UV water sterilizer (Wiegandt GmbH, Krefeld, Germany), and filtered through a 0.2 μm Whatman Polycap™ 75 AS Filter (GE Healthcare Life Sciences, Buckinghamshire, UK).

Anoxic sediment slurries

Anoxic sediment samples were obtained with a multicorer on board R/V Alkor during cruise AL 473 in the central Baltic Sea (Gotland Deep, 57°34.6 N, 20°58.4 E), at 101 m water depth in spring 2016. Samples were extricated from organic debris and stored at 0.9°C in sediment cores closed with sterilized butyl rubbers. For slurry preparation, the North Sea water with a salinity of 33 was diluted to a salinity of 11.5, equivalent to the Gotland Deep sampling station where the sediments were retrieved: Prior to the incubation, 500 ml seawater were diluted with 9 aliquots of 100 ml deionized, sterile water. After every dilution step, pH and TA were controlled.

Foraminifera sampling and preparation

Foraminiferal samples were obtained during Meteor cruise M77/1 off the coast of Peru (11° 13.3 S, 78° 35.6 E) at a water depth of 640 m and a sediment depth of 0-1 cm with a multicorer in November 2008. After extraction from the obtained sediment cores, the samples were transferred to Whirl-Pak™ plastic bags and kept at a temperature of 4°C for further proceeding. The surface sediment samples corresponding to the top centimeter were washed over a 63 μm mesh sieve. The samples, a mix of hard-shelled planktonic and, foremost, benthic specimens were subdivided into grain-size fractions of 63-125, 125-250, 250-315, 315-355, 355-400, and >400 μm and kept in glass vials at room temperature for further proceeding. For the experiment, specimens with a size of >400 μm were chosen for determination of possible surface-alteration effects. The tests were divided in 6 groups of 55 mg each and transferred to sterile petri dishes. Prior to incubation, the tests were soaked in 70% ethanol for 1 week to ensure that no life bacterial cells from the tests were present in the experiment. Tests were subsequently dried at 40°C, and stored in sterile plastic vials. Gaze with a mesh size of 100 μm was sewn into sachets of 3x3 cm size. One corner of each sachet was left open to allow for transfer of the tests to the sachets. Filling of the sachets was done with sterile Eppendorf

pipette cell-saver tips (Eppendorf, Hamburg, Germany), and the open sachet corners were closed with the remaining sewing thread. The filled sachets were transferred to sterile petri dishes, soaked in 70% ethanol for three days, dried at 40°C, and stored at room temperature for further proceeding.

Bacterial culturing and incubation procedure

Shewanella sediminis HAW-EB3 and *Alcanivorx borkumensis* SK2^T cultures were obtained from the Leibniz Institute DSMZ - German Collection of Microorganisms and Cell Cultures (Braunschweig, Germany). The *S. sediminis* culture was inoculated in DSMZ medium 514 with the following composition (g l^{-1}): peptone, 5; yeast extract, 1; Fe(III) citrate, 0.1; NaCl, 19.45; MgCl$_2$ • 6H$_2$O, 12.6; Na$_2$SO$_4$, 3.24; CaCl$_2$ • 2H$_2$O, 2.39; KCl 0.55; NaHCO$_3$, 0.16; KBr, 0.08; SrCl$_2$, 0.034; H$_3$BO$_3$, 0.022; NaF, 0.0024; (NH$_4$)NO$_3$, 0.0016; Na$_2$HPO$_4$ • 2H$_2$O, 0.01; and 2.9 µl Na-silicate. Anoxic conditions were established by purging of sterile culturing vials and -medium with N$_2$/CO$_2$ gas (80%/20%), medium pH was adjusted to 7.8. The culture was grown at 10°C in the dark. From the third generation on, the culture was transferred to a sterile seawater-medium in sterile, butyl-rubber sealed glass vials. The medium was purged with N$_2$ and contained 100 mg l^{-1} additional Fe (III) citrate, 1000 mg l^{-1} yeast, and 200 µl Resazurin as redox/oxygen indicator. The DSMZ medium 514 was further used for growth of the *A. borkumensis* culture with addition of 1% pyruvate. Culturing was carried out in sterile culturing vials under ambient oxic conditions at 20°C. From the third generation on, the cultures were transferred to sterile glass vials containing sterile seawater with additional 100 mg l^{-1} Fe (III) citrate, 1000 mg l^{-1} yeast, and 1% pyruvate.

For the *S. sediminis* incubation, flasks were containing 900ml sterile seawater medium with an N$_2$ headspace of 0.2 bar above atmospheric pressure. Ten ml of the *S. sediminis* culture were inoculated into the medium in sterile butyl-rubber sealed 1 l Duran flasks at the experimental start. Controls contained the same seawater medium without bacterial cells. For the experimental duration, both incubations were kept at 10°C in the darkTen ml *A.Borkumensis* culture were inoculated into the medium in sterile 1 l Duran flasks. Flasks were closed with sterile cotton plugs after inoculation of the bacterial culture. The control contained the sterile-seawater medium without bacterial cells. Each of the bacterial-culture media and the respective controls contained one sachet with foraminiferal tests hanging in the media. Both the incubation and control were kept at 20°C throughout the experimental duration. Due to extensive cell growth, two third of the *A. borkumensis* medium were exchanged on day 48 to prevent cell death in the culture. After contamination of the initial controls, the control runs were repeated for all incubations and sampling of the control media was conducted on a two-week basis.

The final anoxic sediment slurries contained 300 mg sediment with a sterilized aliquot of 600 ml seawater-deionized water mix each, and 200 µl sterile Resazurin was added to each of the

incubations as a redox/oxygen indicator. Slurries were transferred to two sterile 1 l Duran flasks, closed with sterile butyl rubbers, and purged with N_2 gas to ensure anoxic conditions. The anoxic-sediment incubation contained a sachet with foraminifera, deposited on the sediment surface, the control contained a 900 mg aliquot of the slurry without foraminiferal tests. Both incubation set ups had an N_2 headspace of 0.2 bars above atmospheric pressure. The incubations were kept at 10°C in the dark throughout the experimental duration and the flasks were smoothly pivoted every other day. After the incubation period, the sachets with the foraminferal tests were carefully rinsed with sterile seawater, followed by ultra-purified water with a pH adjusted to ca. 8 with NH_4^+-solution. Sachets and tests were dried in parafilm-sealed Petri dishes at 40°C. The dried tests were discharged of the sachets, and were stored in petri dishes at room temperature for upcoming analyses.

Media carbonate system and seawater geochemistry

Sampling for all seawater medium parameters was conducted on a regular basis (daily to weekly). Medium pH was measured with a Schott Instruments Lab 850 pH sensor (SI analytics GmbH, Mainz, Germany). The pH meter was calibrated with reference solution buffers (L4794, L 4796, L 4799, SI analytics GmbH, Mainz, Germany) according to the Physikalisch-Technische Bundesanstalt (PTB) and the National Institute of Standards and Technology (NIST). For total alkalinity measurements, open-cell titration of 0.5 ml samples with 0.01 M HCl in a titration vessel after Pavlova (Pavlova *et al.*, 2008) was conducted, using a Metrohm 876 Dosimat plus (Ω Metrohm, Florida, USA). The TA measurements were calibrated with IAPSO seawater standard. During titration, the vessel was continuously purged with N_2 to strip released CO_2 from the samples. The saturation state of aragonite ($\Omega_{Aragonite}$) was calculated after Zeebe and Wolf-Gladrow (2001). For measurements of dissolved inorganic carbon (DIC) 1.8 ml samples were treated with 10 µl $HgCl_2$ saturated solution in a 2ml glass vial, crimp sealed and stored at 4°C for further processing. DIC concentration was determined as CO_2 with a multi N/C 2100 analyzer (Analytik Jena, Jena, Germany). The detection limit was 0.1 ppm with a precision of 2%. For minor- and trace-element concentrations 1 ml medium samples were acidified with 0.1 ml HNO_3 Suprapur[©] (1/100 v/v) in a 2 ml cryo vial and stored at 4°C for further processing. Divalent-cation concentrations were measured by inductively coupled plasma atomic emission spectroscopy (ICP-AES - JY 170 ULTRATRACE, HORIBA, Kyoto, Japan). The detection limit was 2 mg l^{-1} for Ca^{2+}, 6 mg l^{-1} for Mg^{2+} and 25 µg l^{-1} for Sr^{2+}, with a precision of 2%.

**Test structure and elemental composition**

All incubated tests and non-incubated reference samples were examined by means of scanning electron microscopy (SEM) and electron-microprobe (EMP) mapping post-incubation. For SEM analyses, sample surfaces were air-dried and sputter-coated using a platinum/gold target. SEM images were acquired at 15 kV and a 19 µA filament current. EMP mapping was applied to determine element distribution in relation to the surface structures observed by SEM. The mapping was conducted with a JEOL JXA 8200 Electron Probe Microanalyzer (JEOL Ltd., Tokyo, Japan). Prior to the mapping the tests were embedded in epoxy resin (Araldite® 2020, Huntsman, Texas, USA) and dried over night at 50°C. The resin was ground on the next day, using Hermes water grinding papers (P1200, P2400 and P4000) at a pressure of 25N. Each grinding step was followed by cleaning and drying of the samples with deionized water and pressurized air, respectively. Sample polishing was conducted with different grain sizes of alumo-silica and diamond paste, and the sample surfaces were subsequently cleaned in a supersonic bath for a few seconds. The maps were obtained by wavelength dispersive spectrometry (WDS) mode, and repeated to gather 8 accumulations of the selected area. Standards (Calcite, KAN1, VG-2, Strontianite A2_modernCoral) were measured prior and after mapping to calculate element concentrations. For quantitative wavelength dispersive analyses the element concentrations were subsequently measured along a mapping area of 600 µm parallel to the exposed rim of the sample x 300 µm in the direction of non-exposed, inner sample parts, simultaneously measuring Mg (TAP, Ka), Sr (TAP, Strontianite), Ca (PETJ), P (PETH) and S (PETH). The measurements were conducted at a beam current of 50 nA with a beam spot size of 3 µm. Accelerating voltage was set to 15 kV.

Results

Oxic bacterial culture medium

The pH in the *A. borkumensis* culture medium increased from initial 7.2 to 8.4 on day 48 (before medium exchange). After the medium exchange the pH increased from 7.7 to 8.0. Total alkalinity increased from 4.2 to 17.0 mmol kg^{-1} on day 48, and increased from 9.2 to 23.2 mmol kg^{-1} after exchange of the medium (Fig. 1A). The $\Omega_{Calcite}$ values increased from 2 to 65 on day 48, and from 23 after the medium exchange to 44 at the end of the experiment (Fig. 1B). The Mg^{2+} concentration decreased from 51.8 to 50.1 mmol l^{-1} prior to medium exchange and varied between 49.5 and 49.9 mmol l^{-1} afterwards (Fig. 1C). The Ca^{2+} concentration decreased from 10.0 to 9.3 mmol l^{-1} on day 48 and further decreased to 9.2 mmol l^{-1} at the end of the experiment (Fig. 1D). Initial medium Sr^{2+} concentrations of 78.3 µmol l^{-1} decreased to 70.7 µmol l^{-1} on day 48 and increased to 73.0 µmol l^{-1} at

the end of the experiment (Fig. 1E). The Mg/Ca ratio increased from 5.2 to 5.5 on day 48 and from 5.3 to 5.4 after the medium exchange (Fig. 1F). The Mg/Sr ratio increased from 0.66 to 0.72, and after day 48 from 0.67 to 0.68, while values of the Sr/Ca ratio were between 7.8 and 7.9, with a drop to 7.6 after the medium exchange (Fig.G, H). In the cell-free control, the pH slightly decreased during the experiment from 7.6 to 7.4 and TA alternated at values between 2.3 and 2.8 mmol kg^{-1} (Fig. 1A). The $\Omega_{Calcite}$ value varied between 1 and 2 (Fig. 1B). The Mg^{2+} concentrations in the cell-free control were decreasing from 52.5 to 49.8 mmol l^{-1} (Fig. 1C), Ca^{2+} concentrations decreased from 10.3 to 10.2 mmol l^{-1} (Fig. 1D), and Sr^{2+} concentrations were alternating between a minimum of 80.6 μmol l^{-1} and a maximum of 84.3 μmol l^{-1} (Fig. 1E). The Mg/Ca ratio was constant at around 5.1 (Fig. 1F), and the Mg/Sr ratio at around 0.63 (Fig. 1G). The Sr/Ca ratio went from an initial 8.04 to 8.13 at the end of the experiment (Fig. 1H).
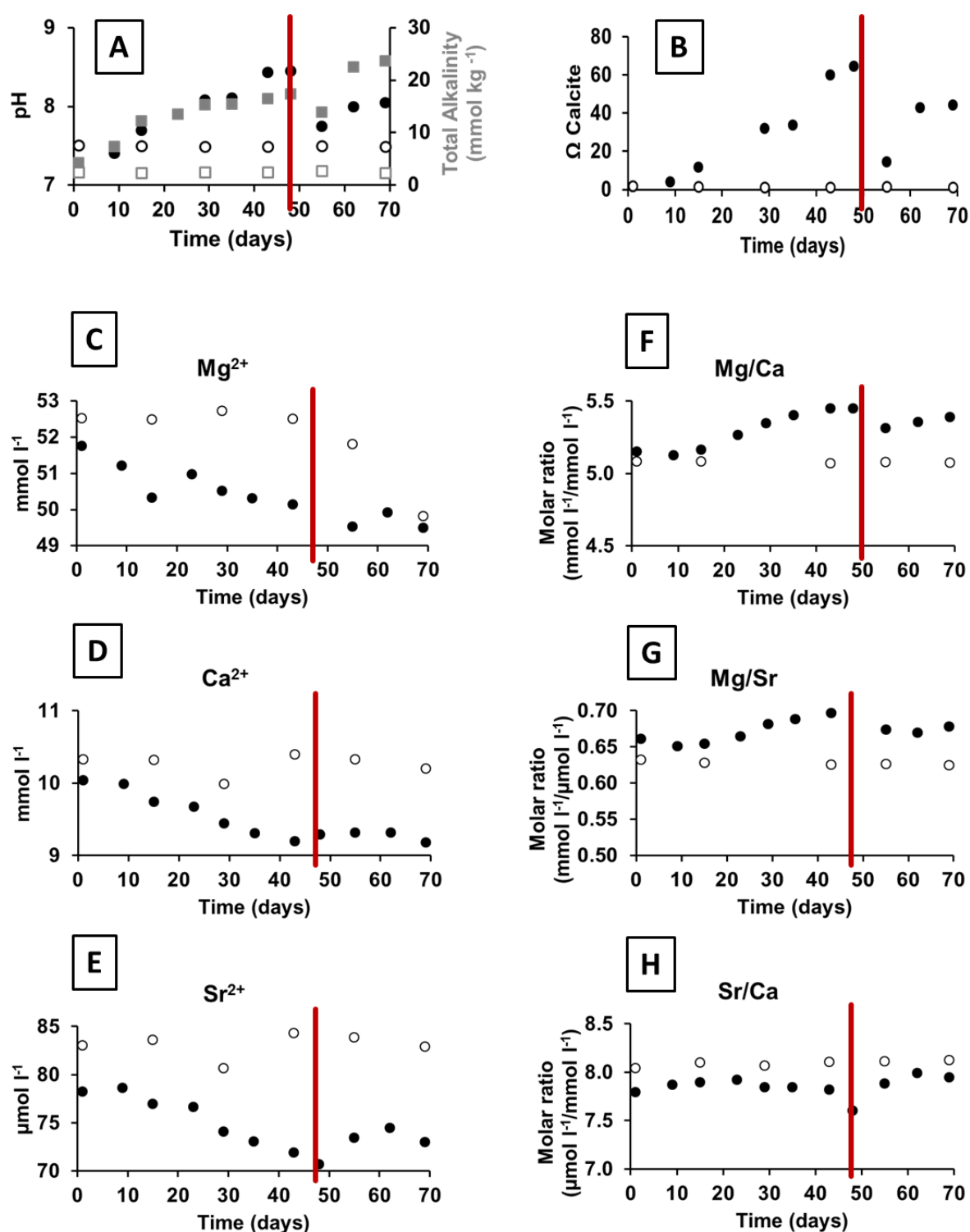
Figure 1. Medium chemistry of the *A. borkumensis* incubation: Temporal development of (A) pH (circles) and Total Alkalinity (TA) (squares), (B) $\Omega_{Calcite}$, (C-E) divalent-cation concentrations, and (F-H) divalent-cation ratios. Solid symbols show bulk-medium values, open symbols show control values. Red lines indicate the medium exchange on day 48.

Anoxic bacterial culture medium

During the experiment, no change in the added resazurin indicator from colorless (anoxic conditions) to pink (partial or fully oxic conditions) was observed. The pH in the *S. sediminis* medium alternated between 6.8 and 7.0, TA values increased from 2.2 to 4.8 and 4.4 mmol kg^{-1} at the end of the experiment (Fig. 2A). The medium was undersaturated with respect to Calcite, with a $\Omega_{Calcite}$ of 0.4 at the experimental start and increased to 1 and 0.7 at the end of the experiment (Fig. 2B). The Mg^{2+} concentrations were around 50.0 mmol l^{-1} until day 43, where they decreased to 49.0 mmol l^{-1} (Fig. 2C). The Ca^{2+} concentrations increased from 9.8 to 10.2 mmol l^{-1} and decreased to values of 9.9 mmol l^{-1} at day 43, and 9.8 mmol l^{-1} at the end of the experiment (Fig. 2D). The Sr^{2+} concentration increased from initial 77.1 to 85 μmol l^{-1} on day 35 and decreased to 82.9 and 82.4 μmol l^{-1} at the end of the experiment (Fig. E). The pH in the cell-free control had values between 7.1 and 7.2, and TA values were between 2.3 and 2.6 mmol kg^{-1} with a peak of 2.9 on day 48 but without a visible trend (Fig. 2A). The $\Omega_{Calcite}$ reflected undersaturation in the medium with values between 0.4 and 0.6 throughout the experiment (Fig. 2B). Initial Mg^{2+} concentrations in the control fluctuated between 51.9 mmol l^{-1}, 52.5 mmol l^{-1} and 50.7 mmol l^{-1} towards the end of the experiment (Fig. 2C). The Ca^{2+} concentrations were between 10.0 and 10.3 mmol l^{-1} (Fig. 2D), and the Sr^{2+} concentrations decreased from 83.9 to 80.2 μmol l^{-1} (Fig. 2E). The Mg/Ca and Mg/Sr ratios were constant throughout the experiment with values of 5.1 and 0.6, respectively, (Fig. 2F, G) the Sr/Ca ratio slightly decreased from 8.1 to 8.0 (Fig. 2H).
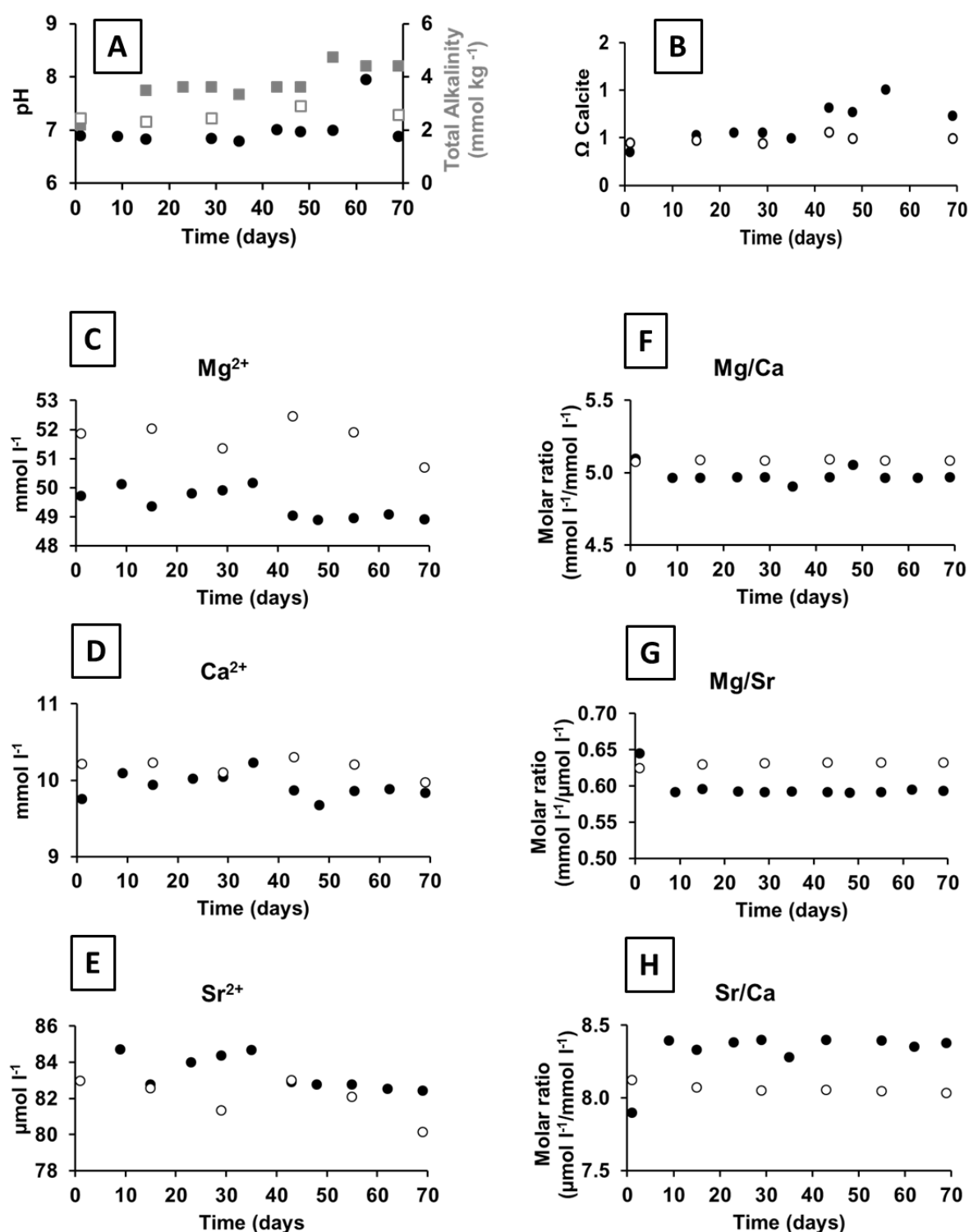
Figure 2. Medium chemistry of the *S. sediminis* incubation: Temporal development of (A) pH (circles) and Total Alkalinity (TA) (squares), (B) $\Omega_{Calcite}$, (C-E) divalent-cation concentrations, and (F-H) divalent-cation ratios. Solid symbols show bulk-medium values, open symbols show control values.

Anoxic sediment

During the experiment, no change in the added resazurin indicator from colorless (anoxic conditions) to pink (partial or fully oxic conditions) was observed. The pH in the anoxic-sediment incubation decreased from initial 8.1 to 7.8 and re-established at 8.1, TA increased from 2.5 to 4.7 mmol kg^{-1} (Fig. 3A). $\Omega_{Calcite}$ increased from 3 to 6 on day 62, and decreased to 4 on day 69 (Fig. 3B). The initial Mg^{2+} concentration of 18.4 mmol l^{-1} decreased to 17.4 mmol l^{-1} (Fig. 3C). The Ca^{2+} concentrations were between 3.7 and 3.8 mmol l^{-1} throughout the experiment (Fig. 3D), and the Sr^{2+} concentrations decreased from initial 29.5 µmol l^{-1} to 28.9 µmol l^{-1} at the end of the experiment (Fig. 3E). The Mg/Ca ratio decreased from 4.9 to 4.6 (Fig. 3F), the Mg/Sr ratio remained stable at 0.6 (Fig. 3G), and the Sr/Ca ratio decreased from 7.9 to 7.7 at the end of the experiment (Fig. 3H). In the anoxic-sediment control, the pH was between 8.0 and 8.1 throughout the experimental duration, and TA increased from 2.1 to 4.7 mmol kg^{-1}(Fig. 3A). The $\Omega_{Calcite}$ increased from 2 to 5 (Fig. 3B). The Mg^{2+} concentrations decreased from 18.3 to 17.4 mmol l^{-1} (Fig. 3C), the Ca^{2+} concentrations had values between 3.7 and 3.8 mmol l^{-1} (Fig. 3D), and the Sr^{2+} concentrations slightly decreased from 29.4 to 28.9 µmol l^{-1} at the end of the experiment (Fig. 3E). The resulting Mg/Ca ratio decreased from 5.0 to 4.6 (Fig. 3F), the Sr/Ca ratio remained at 0.6 (Fig. 3G) and the Sr/Ca ratio decreased from 8.0 to 7.7 (Fig. 3H).
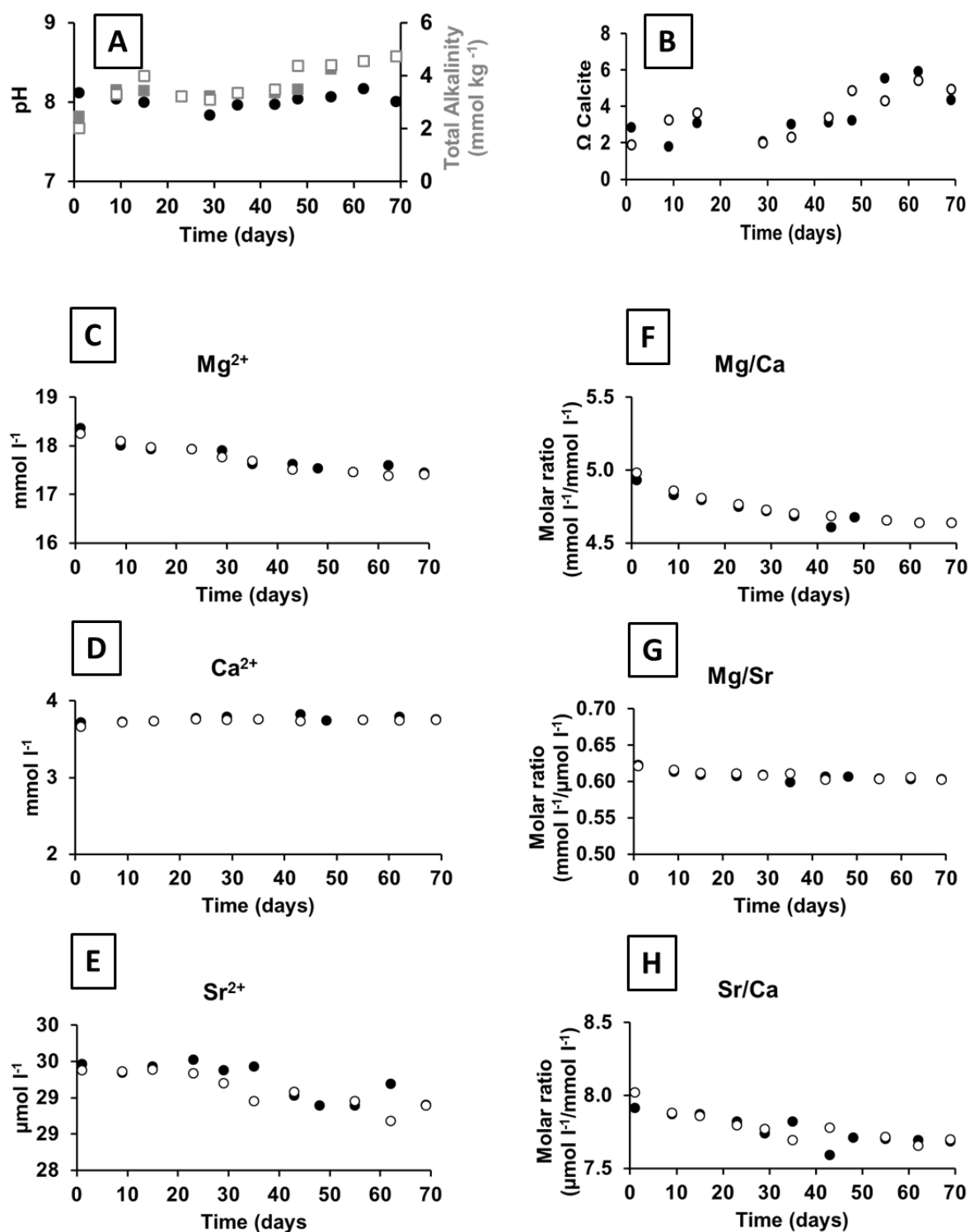
Figure 3. Medium chemistry of the anoxic-sediment incubation: Temporal development of (A) pH (circles) and Total Alkalinity (TA) (squares), (B) $\Omega_{Calcite}$, (C-E) divalent-cation concentrations, and (F-H) divalent-cation ratios. Solid symbols show bulk-medium values, open symbols show control values.

Test surface structure and elemental composition

Foraminiferal tests incubated in the *A. borkumensis* culture medium were extensively covered with carbonate-like structures (SEM micrographs, Fig. 4A). SEM micrographs of the samples incubated in the *S. sediminis* culture (Fig. 5A) or the anoxic sediment (Fig. 6A) showed no signs of surficial alteration relative to the respective controls (Figs. 5B, 6B). Electron Microprobe mapping of the incubated tests displayed an increase of Mg and, foremost, Ca in tests from the *A. borkumensis* culture medium relative to mapped values of the samples from the cell-free control (Fig. 7A, B). No deviation in element concentration was detected via EMP mapping of samples from the *S. sediminis* culture, relative to the respective control (Fig. 8A, B). Mapped element concentrations of samples incubated in the anoxic sediment displayed an increase in Mg concentrations along the inner organic lining of one sample, relative to the unaltered reference (Fig. 9A, B).
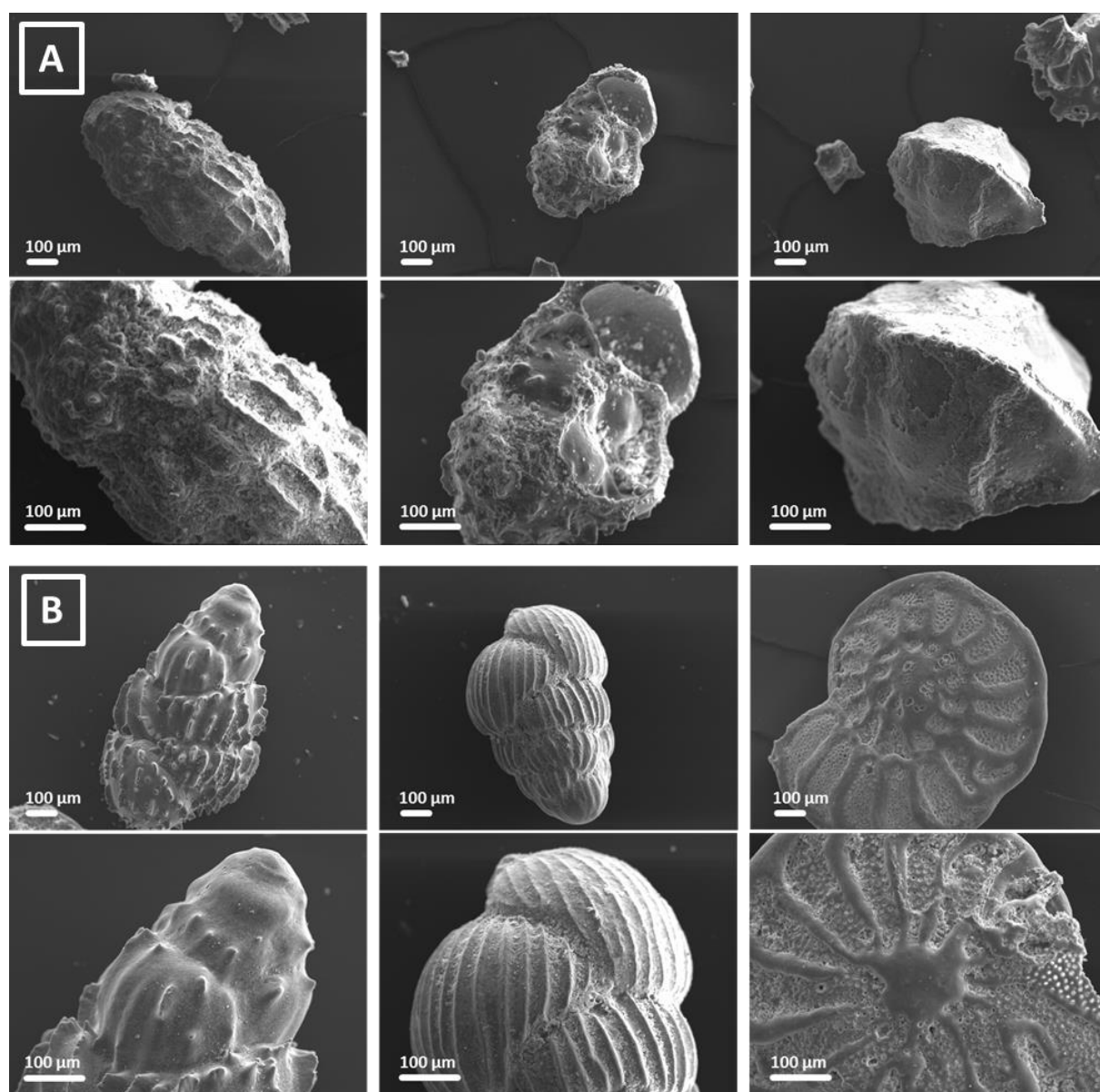
Figure 4. Scanning Electron Microscopy (SEM) micrographs of foraminiferal tests incubated in (A) the *A. borkumensis* culture, and (B) the cell-free control.
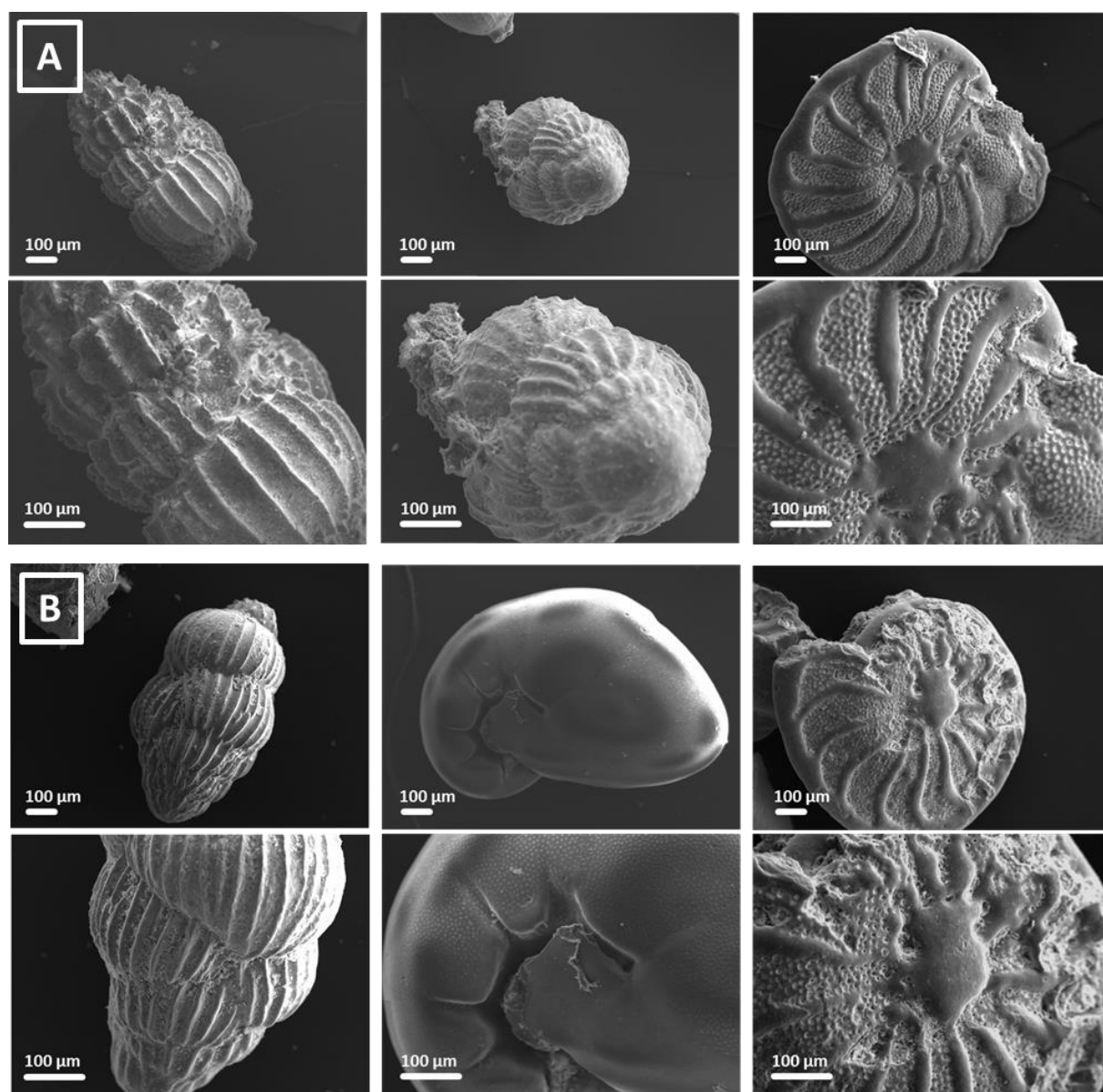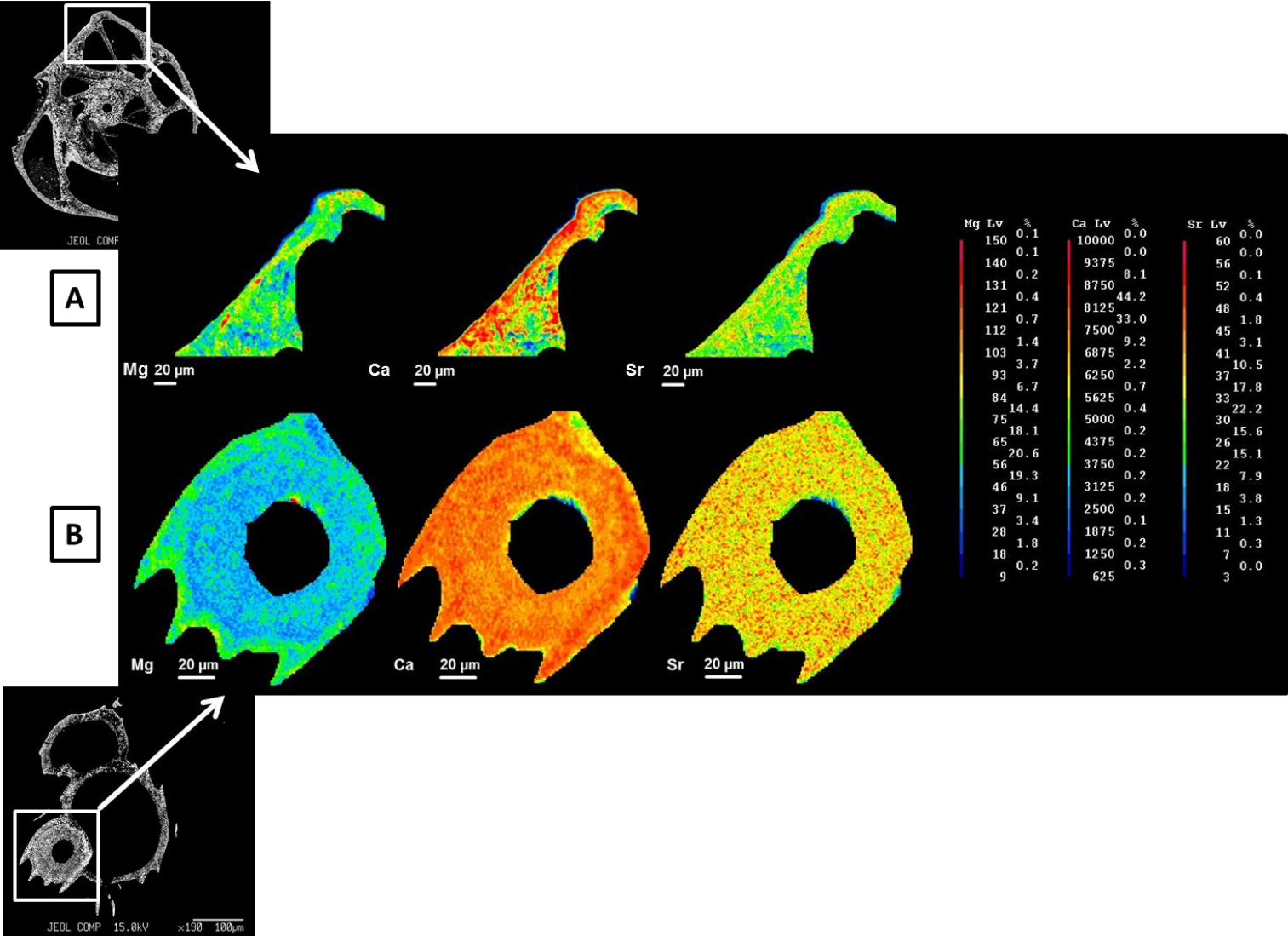
Figure 5. Scanning Electron Microscopy (SEM) micrographs of foraminiferal tests incubated in (A) the *S. sediminis* culture, and (B) the cell-free control.
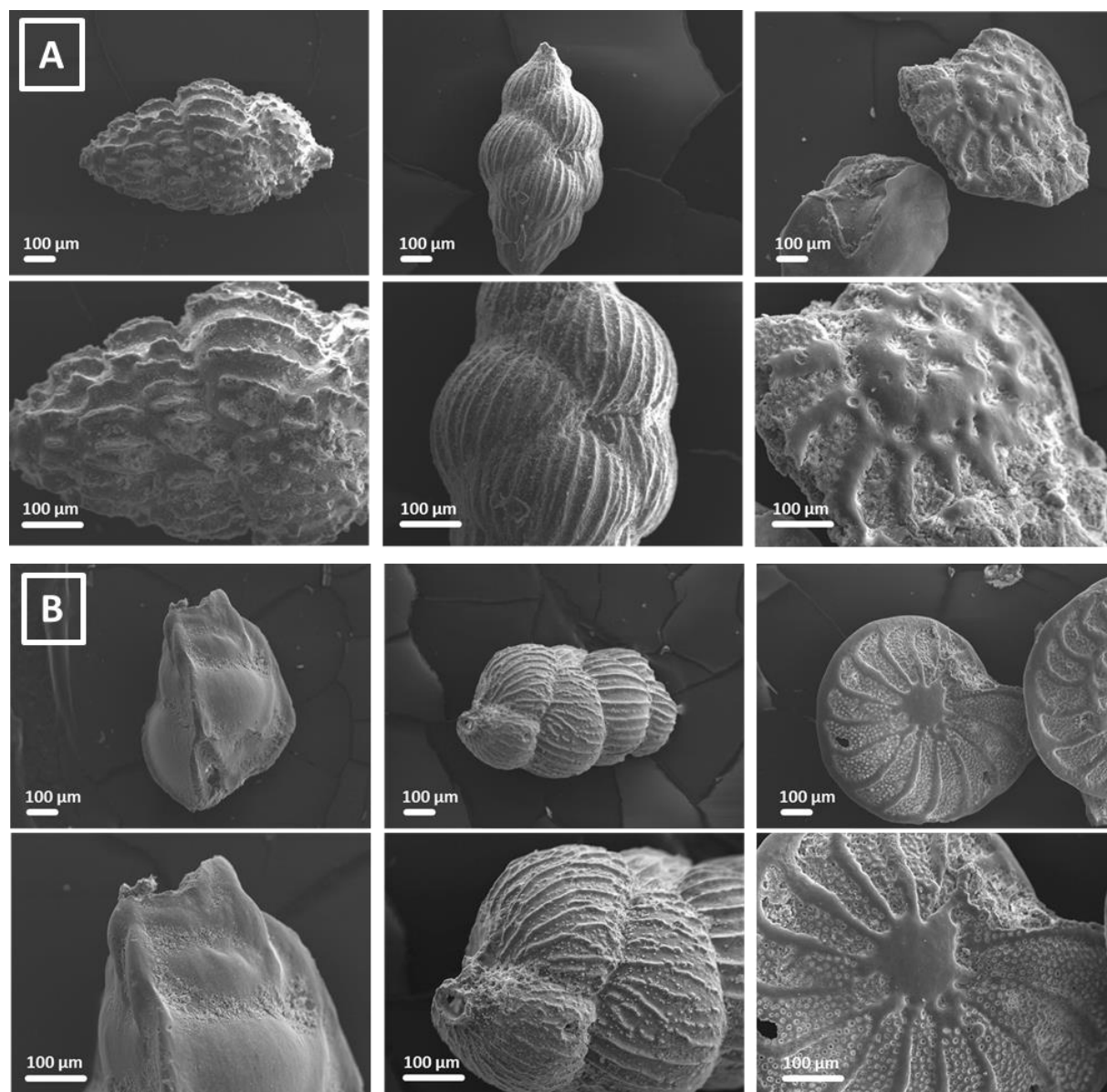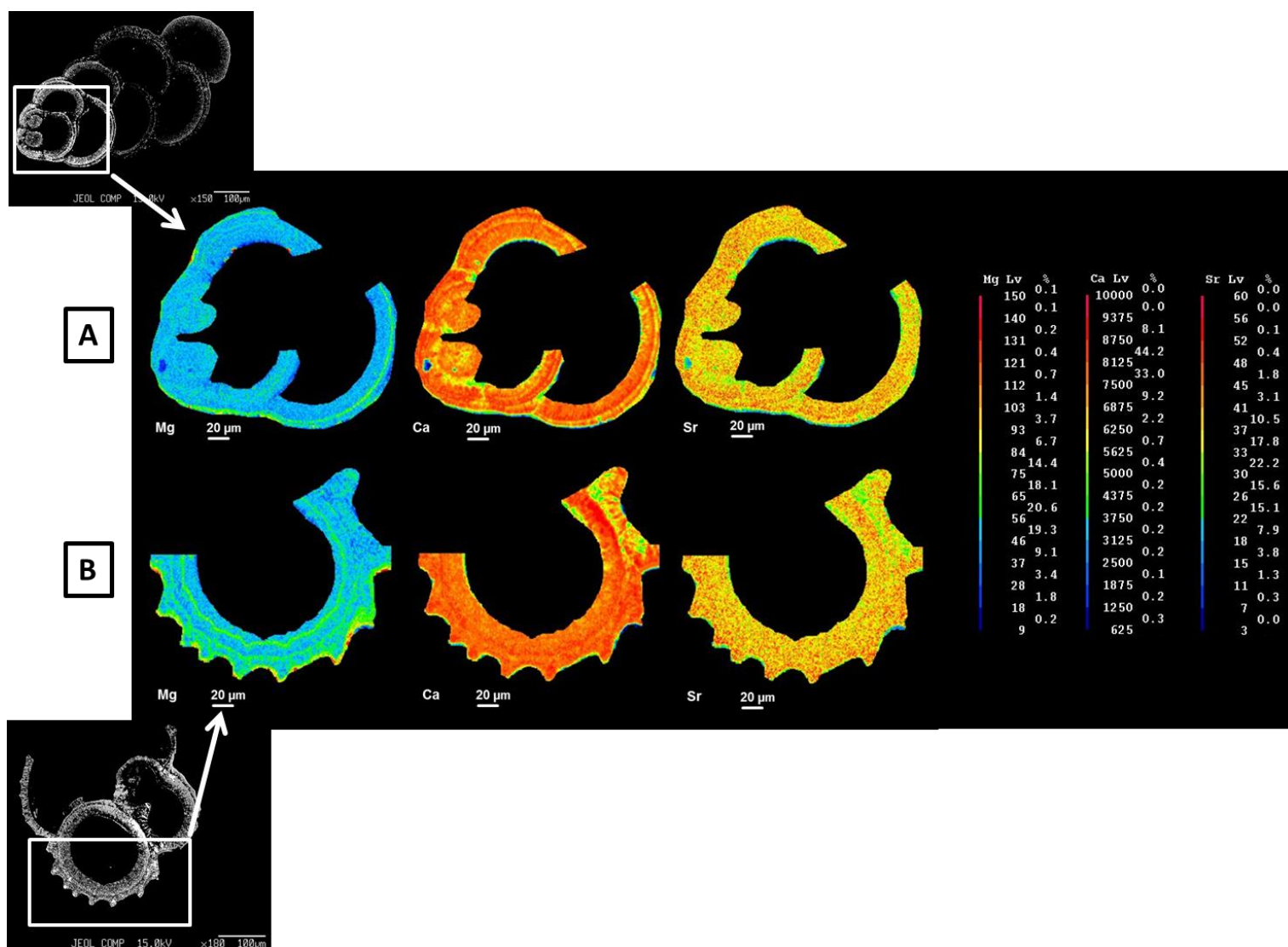
Figure 6. Scanning Electron Microscopy (SEM) micrographs of foraminiferal tests. (A) Tests incubated in the anoxic sediment, and (B) unaltered reference samples.
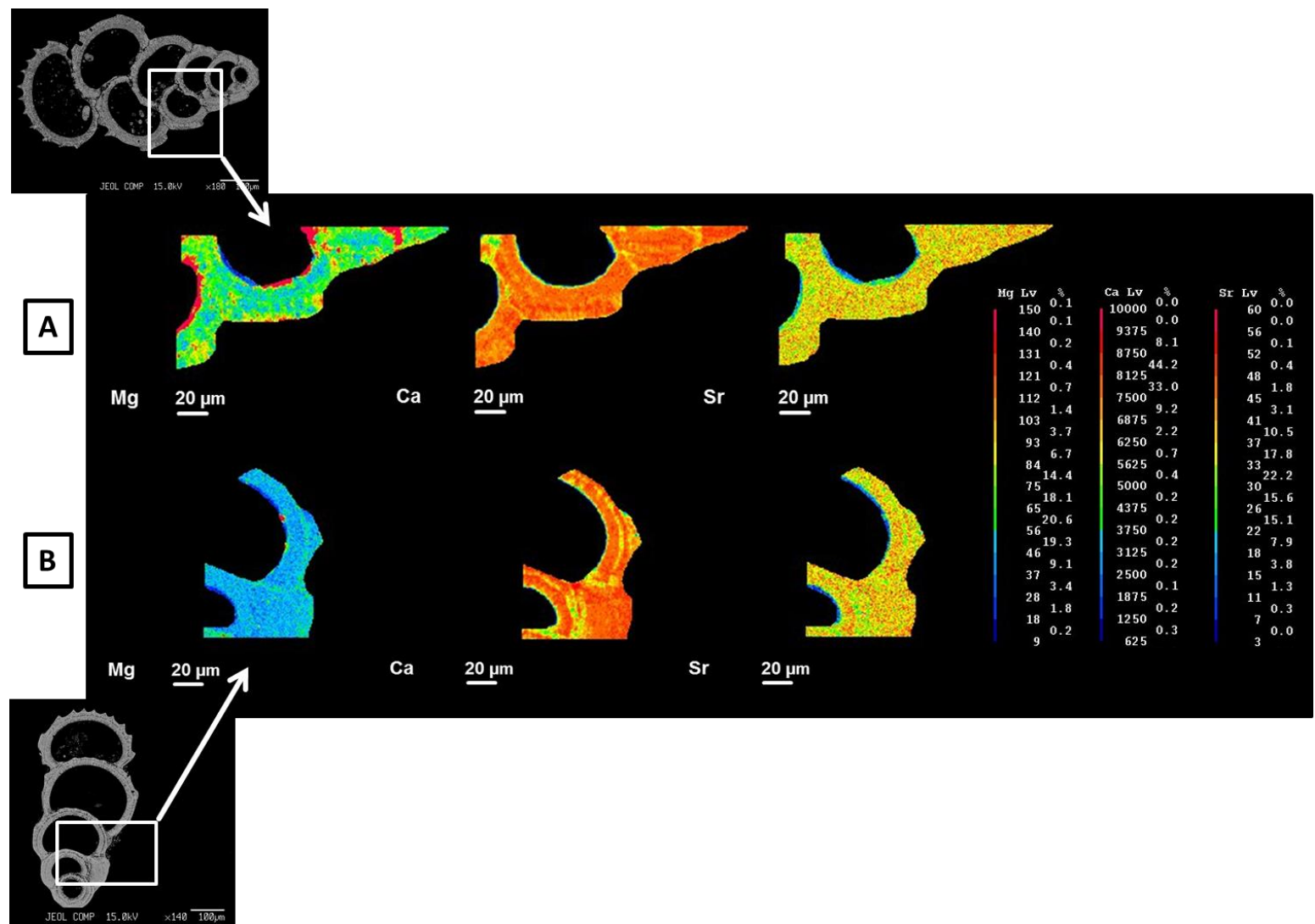
Figure 7. Electron Microprobe maps of Mg, Ca and Sr in foraminiferal tests incubated in (A) the *A. borkumensis* culture, and (B) the cell-free control. Maps show intensity in counts per second.

Figure 8. Electron Microprobe maps of Mg, Ca and Sr in foraminiferal tests incubated in (A) the *S. sediminis* culture, and (B) the cell-free control. Maps show intensity in counts per second.

Figure 9. Electron Microprobe maps of Mg, Ca and Sr in foraminiferal tests incubated in (A) the anoxic sediment, and (B) unaltered reference sample. Maps show intensity in counts per second.

Discussion

Alteration of foraminiferal tests by *A. borkumensis*

The results obtained within the present study display the capability of *A. borkumensis* to distinctly alter foraminiferal calcitic tests through $CaCO_3$ precipitation within a time frame of only two months. Medium carbonate chemistry from the *A. borkumensis* culture incubation displayed drastically increasing TA and $\Omega_{Aragonite}$ values over time and simultaneous withdrawal of Mg^{2+}, Ca^{2+}, and Sr^{2+} from the medium. Moreover, the samples were nearly fully covered with precipitates.

The majority of aerobic bacterial metabolisms in marine sediments involves the generation of acidic (micro-) zones through generation of metabolic CO_2 (Jørgensen, 2006) that potentially facilitate carbonate dissolution. *Alcanivorax borkumensis*, in contrast, employs a hydrocarbonoclastic metabolism with biosurfactants (i.e. glucose lipids) as the metabolic end product (Yakimov et al., 1998; Schneiker et al., 2006). It is therefore unlikely, that the observed secondary carbonate precipitation is directly linked to *A. borkumensis* metabolites, unless a further metabolic pathway exists for this bacterium, including the generation of alkaline metabolic products. Microbial carbonic-anhydrase activity has been reported to induce secondary carbonate-, specifically calcite precipitation (Douglas and Beveridge, 1998; Zavarzin, 2002). This process is often combined with urease activity where urea is hydrolyzed to ammonia (NH_3) and bicarbonate (HCO_3^-), thereby generating a highly alkaline environment that is favoring the formation of CO_3^{2-} and, in the presence of Ca^{2+}, leads to $CaCO_3$ precipitation (Achal and Pan, 2011). Recently, Krause et al. (2014) provided evidence for carbonic-anhydrase induced high-Mg calcite precipitation by *A. borkumensis*. The continuous TA increase and a $\Omega_{Calcite}$ of up to 65 during this study correspond with these findings. However, ammonium levels measured within the present experiment were below the detection limit of 0.15 µmol l^{-1}, despite the fast cell growth in the culture (data not shown). Consequently, *A. borkumensis* urease-activity during the experiment is unlikely. It can therefore be hypothesized that solely carbonic-anhydrase activity and subsequent generation of HCO_3^- must have led to the observed increase in TA during the present study. The highly alkaline medium apparently favored the generation of CO_3^{2-} which could form $CaCO_3$ with the abundant Ca^{2+} ions in the medium. The latter is further reflected by the Ca^{2+} withdrawal from the medium. Decreasing Mg^{2+} concentrations in the medium furthermore indicate precipitation of high-Mg calcite. Due to its comparably low hydration enthalpy (Burgess, 1978), Sr^{2+} is prone to cation scavenging by either EPS or cell-wall functional groups. These moieties become deprotonated at high pH and their resulting negative charge allows for binding of abundant cations (Liu and Fang, 2002). The withdrawal of Sr^{2+} from the *A. borkumensis* culture medium could therefore reflect binding of the ions to functional groups.

Alteration of foraminiferal tests by *S. sediminis*

Within a former experiment, *S. sediminis* metabolic activity induced dissolution of bivalve aragonite and changes in shell-elemental composition, thereby altering carbonate Mg/Ca and Sr/Ca ratios. The dissolution was suggested to be induced by hydrolysis of the aragonite inter- and intracrystalline chitin-organic matrix by means of a *S. sediminis* chitinase. The organic-carbon fraction of foraminiferal test from different species consists of protein-containing macromolecules and either glycosaminoglycan (Weiner and Erez, 1984), or chitin (Fhlaithearta, 2013). Hence, different degrees of *Shewanella*-induced dissolution, according to the respective substrate, were possible. Furthermore, a comparably weak degree of dissolution was expected, as the calcitic test of foraminifera is less soluble than the aragonitic bivalve shell ($K_{sp, calcite} \approx 3.35 \times 10^{-9}$, $K_{sp, Aragonite} \approx 5 \times 10^{-9}$; Mucci, 1983; Pilson, 1998). However, no parameters reflecting carbonate dissolution were detected in the *S. sediminis* culture medium or on the respective incubated tests. In the bacterial culture medium, a moderate increase in TA was observed, and the medium was, despite a slightly increasing $\Omega_{Calcite}$, undersaturated with respect to calcite during most of the experiment. All divalent-cation concentrations in the medium slightly increased until day 35 and then decreased towards the end of the experiment. Furthermore, SEM micrographs showed no signs of dissolution on any of the tests, and no change in elemental composition of the foraminiferal tests was detected by EMP mapping. In the incubations, no dense cell aggregations were observed with the naked eye as compared to the *A. borkumensis* incubation, and it is therefore probable, that the culture had a low cell growth with most of the cells not reaching the log phase

Alteration of foraminiferal tests by benthic microbial communities

Element concentrations in the sediment slurries were comparably low as seawater was diluted to achieve the salinity (11.5) of the sampling site in the Baltic Sea. TA increased in both, the anoxic sediment and the anoxic-sediment control, thereby reflecting natural anaerobic bacterial activity with the related production of alkaline metabolites. However, the TA values were low (4.7 mmol l^{-1}) when compared to previous experiments (up to 12.0 mmol l^{-1}). The sediment sampling was conducted in spring at a depth of 101 m and the share of labile organic carbon in the sediments presumably was exhausted over winter. Hence, the limitation in organic substrate probably resulted in a weak metabolic turnover. The initial dilution of the seawater and the resulting low ion concentrations probably added to the condition in the sediment. However, at present no analyses of the sediment´s C_{org} content are at hand. The oversaturation with respect to calcite in the anoxic sediment control was moderately increased compared to the $\Omega_{Calcite}$ in the anoxic sediment (5.0 and 4.4, respectively), while the Ca^{2+} concentrations in the both incubation set ups were stable

throughout the experiment. The Mg^{2+} concentrations decreased about 1 mmol l^{-1}, and the same trend was observed in the sediment control. The uptake of specifically Mg^{2+} was reported for gram-negative bacteria during their exponential growth phase (Webb, 1968) and could have accounted for the decreasing values in the medium, but the values observed in total alkalinity were contradicting this assumption. No precipitates or weathering characteristics on the foraminiferal tests from the anoxic sediment incubation were detected via SEM. Interestingly, EMP maps displayed an increase of Mg in one incubated specimen that suggested secondary carbonate precipitation, presumably through bacterially generated alkaline conditions in the sediment, or bacterially induced precipitation. Yet, the increased Mg was located at the tests organic lining, and high-Mg calcite phases are predominantly associated with organic layers of foraminiferal tests (Erez, 2003). In general, the Mg content of foraminiferal tests of different taxa ranges from 0.1 mole% to 20 mole% of $MgCO_3$ (Blackmon and Todd, 1959) and the observed Mg increase may therefore be attributed to taxon-specific variations.

Conclusions

The results obtained in the frame of this study display distinct structural and geochemical alteration of foraminiferal tests by *A. borkumensis* through carbonate precipitation. The exact Mg/Ca ratio has yet to be determined and no values for stable-isotope composition of the samples are at hand. However, the signature of bacterially-induced carbonate differs considerably from that of control samples: As bulk foraminiferal test were used for the incubations, it cannot be ruled out that the control samples were not pristine but already diagenetically altered in their geochemical properties. However, the distinct changes in Mg concentration were solely observed in the tests exposed to the bacterial culture. Given, that carbonic anhydrase activity is widespread in bacteria, the alteration potential of the respective strains on biogenic carbonate structures should be considered in studies applying these proxies. No signs for carbonate alteration were observed in the *S. sediminis*-culture medium or the respective incubated tests. In an increasingly growing culture, primarily during the exponential growth phase, the metabolic requirement for organic carbon could have facilitated bacterially-mediated decomposition of test C_{org} constituents. However, due to weak cell growth, apparently no organic-carbon source other than that present in the medium was required by the bacteria. The anoxic-sediment medium chemistry only moderately reflected benthic anaerobic bacterial activity, and no signs for bacterially-induced alteration were observed in the tests´ structure or geochemistry. It is likely, that sediment sampling before the phytoplankton spring bloom and related supply of labile organic carbon for bacterial metabolism, as well as the seawater dilution prior to the experiment were the underlying factors.

Acknowledgements

References

Abu-Zied, R.H., Rohling, E.J., Jorissen, F.J., Fontanier, C., Casford, J.S.L. and Cooke, S. (2007) Benthic foraminiferal response to changes in bottom water oxygenation and organic carbon flux in the eastern Mediterranean during LGM to Recent times. *Marine Micropaleontology*, **67**, 1-2, 46-68.

Achal, V., and Pan, X. (2011) Characterization of Urease and Carbonic Anhydrase Producing Bacteria and Their Role in Calcite Precipitation. *Current Microbiology*, **62**, 894-902.

Altenbach, A.V., Pflaumann, U., Schiebel, R., Thies, A., Timm, S., and Tratuth, M. (1999) Scaling percentages and distributional patterns of benthic foraminifera with flux rates of organic carbon. *Journal of Foraminiferal Research*, **29**, 3, 173-185.

Belanger, P.E., Curry, W. B., and Matthews R.K. (1981) Core-top evaluation of benthic foraminiferal isotopic ratios for paleo-oceanographic interpretations. *Palaeogeography, Palaeoclimatology, Palaeoecology,* **33**, 205-220.

Blackmon, P.D. and Todd, R. (1959) Mineralogy of some foraminifera as related to their classification and ecology. *Journal of Paleontology*, **33**, 1, 1-15.

Burgess, J. (1978) Metal ions in solution. *Halsted Press*, New York, 481 pp.

Creech, J.B., Baker, J.A., Hollis, C.J., Morgans, H.E.G., and Smith, E.G.C. (2010) Eocene sea temperatures for the mid-latitude southwest Pacific from Mg/Ca ratios in planktonic and benthic foraminifera. *Earth and Planetary Science Letters*, **299**, 483-495.

Douglas, S., and Beveridge, T.J. (1998) Mineral formation by bacteria in natural microbial communities. *FEMS Microbiology Ecology*, **26**, 79-88.

Eggins, S., De Deckker, P., and Marshall, J. (2003) Mg/Ca variation in planktonic foraminifera tests: implications for reconstructing paleo-seawater temperature and habitat migration. *Earth and Planetary Science Letters*, **212**, 3-4, 291-306.

Erez, J. (2003) The Source of Ions for Biomineralization in Foraminifera and Their Implications for Paleoceanographic Proxies. *Reviews in Mineralogy and Geochemistry*, **54**, 1.

Fhlaithearta, S., Ernst, S.R., Nierop, K.G.J., de Lange, G.J., and Reichart, G.-J. (2013) Molecular and isotopic composition of foraminiferal organic linings. *Marine Micropaleontology*, **102**, 69-78.

Froelich, P.N., Klinkhammer, G.P., Bender, M.L., Luedtke, N.A., Heath, G.R., Cullen, D., Dauphin, P., Hammond, D. and Hartman, B. (1979) Early oxidation of organic matter in pelagic sediments of the eastern equatorial Atlantic : suboxic diagenesis*. Geochimica et Cosmochimica Acta* **43**, 1057-1090.

Graham D.W., Bender M.L., Williams, D.F., and Keigwin Jr., L.D. (1981) Strontium-calcium ratios in Cenozoic planktonic foraminifera. *Geochimica et Cosmochimica Acta*, **46**, 99, 1281-1292.

Golubic, S., Campbell, S.E., Drobne, K., Cameron, B., Balsam, W.L., Cimeran, F., and Dubois, L. (1984) Microbial endoliths: A benthic overprint in the sedimentary record, and a paleobathymetric cross-reference with foraminifera. *Journal of Paleontology*, **58**, 2, 351-361.

Gupta, B.K.S. (1999) Modern Foraminifera. *Springer*, Netherlands, 371 pp.

Hastings, D.W. (1998) Foraminiferal magnesium in *Globeriginoides sacculifer* as a paleotemperature proxy. *Paleoceanography*, **13**, 2, 161-169.

Jørgensen, B.B. (2006) Bacteria and marine Biogeochemistry. In: *Marine Geochemistry* (Eds H.D. Schulz and M. Zabel), pp. 173-207. *Springer*, Berlin, Heidelberg.

Kozdon, R., Kelly, D.C., Kitajima, K., Strickland, A., Fournelle, J.H., Valley, J.W. (2013) In situ δ^{18}O and Mg/Ca analyses of diagenetic and planktic foraminiferal calcite preserved in a deep-sea record of the Paleocene-Eocene thermal maximum. P*aleoceanography*, **28**, 517-528.

Lange, S.M., Krause, S., Ritter, A.-C., Fichtner, V., Immenhauser, A., Strauss, H., and Treude, T. (2017) Anaerobic microbial activity affects earliest diagenetic pathways of bivalve shells. In revision for *Sedimentology*.

Liu, H. and Fang, H.H.P. (2002) Characterization of electrostatic binding sites of extracellular polymers by linear programming analysis of titration data. *Biotechnology and Bioengineering*, **80**, 806-811.

Loubere, P., Gary, A., and Lagoe, M. (1992) Generation of the benthic foraminiferal assemblage: Theory and preliminary data. *Marine Micropaleontology*, **20**, 165-181.

Martin, P.A., Lea, D.W., Rosenthal, Y., Shakleton, N.J., Sarnthein, M., Papenfuss, T. (2002) Quaternary deep sea temperature histories derived from benthic foraminiferal Mg/Ca. *Earth and Planetary Science Letters*, **198**, 193-209.

Mitchell, S. F., Ball, J.D., Crowley, S.F., Marshall J.D., Paul, C.R.C., Veltkamp, C.J., and Samir, A. (1997) Isotope data from Cretaceous chalks and foraminifera: Environmental or diagenetic signals? *Geology*, **25**, 8, 691-694.

Murray, J. (2006) Ecology and Applications of Benthic Foraminifera. *Cambridge University Press.*

Nägler, T.F., Eisenhauer, A., Müller, A., Hemleben, C., and Kramers, J. (2000). The δ^{44}Ca-temperature calibration on fossil and cultured *Globigerinoides sacculifer*: New tool for reconstruction of past sea surface temperatures. *Geochemistry, Geophysics, Geosystems*, **1**.

Nürnberg, D., Buma, J., and Hemleben, C. (1995) Assessing the reliability of magnesium in foraminiferal calcite as a proxy for water mass temperatures. *Geochimica et Cosmochimica Acta*, **60**, 5, 803-814.

Orcutt, B.N., Sylvan, J.B., Knab, N.J. and Edwards, K.J. (2011) Microbial Ecology of the Dark Ocean above, at, and below the Seafloor. *Microbiology and Molecular Biology Reviews*, **75**, 361-422.

Peebles, M.W., and Lewis, R.D. (1988) Differential Infestation of Shallow-Water Benthic Foraminifera by Microboring Organisms: Possible Biases in Preservation Potential. *Palaios*, **3**, 345-351.

Rodionov, D.A., Yang, C., Li, X., Rodionova, I.A., Wang, Y., Obraztsova, A.Y., Zagnitko, O.P., Overbeek, R., Romine, M.F., Reed, S., Fredrickson, J.K., Nealson, K.H. and Osterman, A.L. (2010)

Genomic encyclopedia of sugar utilization pathways in the *Shewanella* genus. *BMC genomics*, **11**, 494-494.

Sadekov, A.Y., Eggins, S.M., and De Deckker, P. (2005) Characterization of Mg/Ca distributions in planktonic foraminifera species by electron microprobe mapping. *Geochemistry, Geophysics, Geosystems*, **6**, 12, Q12P06.

Savin, S. M. and Douglas R.G. (1973) Stable Isotope and Magnesium Geochemistry of Recent Planktonic Foraminifera from the South Pacific. *Geological Society of America Bulletin*, **84**, 2327-2342.

Schneiker, S., Martins dos Santos, V.A.P., Bartels, D., Bekel, T., Brecht, M., Buhrmester, J., Chernikova, T.N., Denaro, R., Ferrer, M., Gertler, C., Goesmann, A., Golyshina, O.V., Kaminski, F., Khachane, A.N., Lang, S., Linke, B., McHardy, A.,C., Meyer, F., Nechitaylo, T., Pühler, A., Regenhardt, D., Rupp, O., Sabrpva. J.S., Selbitschka, W., Yakimov, M.M., Timmis, K.N., Vorhölter, F.-J., Weidner, S., and Glyshin, P.N. (2000) Genome sequence of the ubiquitous hydrocarbon-degrading marine bacterium Alcanivorax borkumensis. *Nature Biotechnology*, **24**, 8, 997-1004.

Towe, K.M., and Hemleben, C. (1976) Diagenesis of magnesian calcite: Evidence from miliolacean foraminifera. *Geology*, **4**, 337-339.

Webb, M. (1968) The Influence of Certain Trace Metals on Bacterial Growth and Magnesium Utilization. *Journal of General Microbiology*, **51**, 325-335.

Weiner, S. and Erez, J. (1984) Organic matrix of the shell of the foraminifer *Heterostegina depressa*. *Journal of Foraminiferal Research*, **14**, 3, 206-212.

Yakimov, M.M., Golyshin, P.N., Lang, S., Moore, E.R.B., Abraham, W.R., Lünsdorf, H., and Timmis, K.N. (1998) Alcanivorax borkumensis gen. nov. , sp. nov., a new, hydrocarbon-degrading and surfactant-producing marine bacterium. *International Journal of Systematic Bacteriology*, **48**, 339-348.

Yang, C., Rodionov, D.A., Li, X., Laikova, O.N., Gelfand, M.S., Zagnitko, O.P., Romine, M.F., Obraztsova, A.Y., Nealson, K.H. and Osterman, A.L. (2006) Comparative genomics and experimental characterization of N-acetylglucosamine utilization pathway of *Shewanella oneidensis*. *Journal of Biological Chemistry*, **281**, 29872-29885.

Zavarzin, G.A. (2002) Microbial Geochemical Calcium Cycle. *Microbiology*, **71**, 1, 1-17.

Chapter 5

Summary and final discussion

Preface

Within this thesis, the alteration potential of benthic bacterial cultures and microbial communities on different biogenic carbonate structures and polymorphs was investigated:

- The alteration potential of a benthic anaerobic bacterial culture and benthic anaerobic microbial communities on aragonitic bivalve shells

- The alteration potential of a benthic aerobic bacterial culture in two different temperature regimes, a benthic anaerobic bacterial culture, and benthic anaerobic microbial communities on aragonitic coral skeleton hard parts

- The alteration potential of a benthic aerobic bacterial culture, a benthic anaerobic bacterial culture, and benthic anaerobic microbial communities on calcitic foraminiferal tests

Section 1 is a summary of the results obtained in the three different studies. In section 2, the respective results are discussed and in section 3 the final conclusion is obtained. A future research outlook is given in section 4. A critical method evaluation is provided in section 5.

Preface

1   Summary

The results presented in this thesis display an overall high potential of benthic aerobic and anaerobic bacterial cultures and microbial communities to alter biogenic carbonate structure and geochemistry during early diagenesis. Different intensities and characteristics of microbially-induced carbonate alteration were observed.

Chapter 2 displayed the susceptibility of aragonitic shells from the bivalve *Arctica islandica* to benthic anaerobic microbial activity within a time frame of only three months. The surface structure of samples incubated in a *Shewanella sediminis* culture medium showed weathering features, and loss in shell Ca concentrations was observed in sample areas exposed to the culture medium, relative to pristine inner shell areas. Furthermore, a moderate increase in Sr concentrations was detected at the exposed sample areas, presumably caused by attachment of Sr^{2+} adsorbing cells and/or EPS to the sample. The medium reflected carbonate dissolution with increasing TA and $\Omega_{Aragonite}$ values and increasing Ca^{2+} and Sr^{2+} concentrations. The dissolution supposedly was induced by *S. sediminis*-chitinase activity, namely through hydrolysis of the shell organic matrix constituent chitin to N-acetylglucosamine monomers and subsequent fermentation of the latter. Shell samples incubated in an anoxic slurry of natural sediment, containing the respective anaerobic heterotrophic microbial communities, displayed similar alteration characteristics. Surface dissolution features and a decrease in Ca concentration in the sediment-exposed shell area were observed. In the medium, TA and $\Omega_{Aragonite}$ values, along with increasing Ca^{2+} and Sr^{2+} concentrations were observed over time. As the sediment was sampled before the onset of spring bloom, it probably was exhausted in labile organic carbon, and the shell organic constituents therefore were used as metabolic substrates by the microbial communities. The stable isotopic composition of samples from both incubation set-ups did not display any distinct microbially induced alteration patterns, thus, apparently no recrystallization took place.

In **Chapter 3**, argonitic skeleton hard parts from the scleractinian coral *Porites* sp. were incubated in (i) two oxic media with *A. borkumensis* cultures growing at either 10°C or 12°C for 25 days, (ii) an oxic *S. sediminis* culture medium or (ii) an anoxic-sediment slurry with incubations of 3 months each. While the incubation media chemistry indicated carbonate precipitation in the oxic incubations and carbonate dissolution in the anoxic incubation set-ups, alteration of coral structure or geochemistry was not detected. Furthermore, the stable isotopic composition of the coral samples exposed to bacterial cultures or anoxic sediment was not significantly different to that of the control samples. The main underlying factor for missing alteration characteristics in the coral samples apparently was

the comparably low organic share in the coral samples (ca. 0.04 wt%). Thus, a relatively low susceptibility of coral aragonite to heterotrophic microbially-induced alteration was hypothesized.

In **Chapter 4**, we investigated the influence of benthic aerobic and anaerobic bacterial cultures and communities on calcitic foraminiferal tests. Bulk tests were incubated in (i) an oxic seawater medium containing the aerobic microbial strain *Alcanivorax borkumensis* SK^T, (ii) an anoxic seawater medium containing the anaerobic microbial strain *Shewanella sediminis* HAW EB3, and (iii) a natural anoxic sediment-slurry. Neither the tests incubated in the anoxic incubations, nor the respective media chemistry reflected potential carbonate precipitation or dissolution, which was presumably owed to weak microbial activity in both incubation set-ups. However, tests incubated in the oxic *A. borkumensis* incubation were overgrown with precipitates, and the respective medium chemistry displayed a strong increase in TA and $\Omega_{Calcite}$, and a concomitant withdrawal of Mg^{2+}, Ca^{2+} and Sr^{2+} from the medium. The suggested underlying process included an increase in system alkalinity through *A. borkumensis* carbonic-anhydrase activity, favoring the formation of $CaCO_3$. Carbonate precipitation was subsequently facilitated by the available Ca^{2+} in the medium. While the withdrawal of Sr^{2+} supposedly is owed to cation binding by cell-wall functional groups, the simultaneous decrease in Mg^{2+} could indicate calcite precipitation.

2   Discussion

The outcome of the present thesis displays a considerable involvement of microbial activity in early diagenetic carbonate alteration, and five main factors apparently determine the impact of microbial activity on biogenic carbonates: The primary factor is the experimental duration (i.e. time), the second factor is the accessible organic-carbon share in the respective carbonate, the third factor are the proximate environmental conditions for microbial activity, foremost substrate availability in the sediments and (growth-)temperature, the fourth factor are cell-wall and EPS functional groups interacting with the respective carbonate. Additionally, microbial enzymatic activity might play an important role in the degree of microbially-induced carbonate alteration.

2.1 Factors determining the impact of microbial carbonate alteration

2.1.1 Time

The herein observed microbially-induced alteration features displayed rather subtle changes in the affected carbonates compared to alteration characteristics observed in diagenetic research (for a detailed description see Berner, 1980). However, it is important to note the short experimental duration of the conducted studies, ranging from weeks to months. Carbonate alteration through diagenetic processes in natural settings spans over geological time scales (Bathurst, 1972; Tucker and Bathurst, 1990). Given, that the effects observed within this thesis would increase with time, specifically in natural, open systems with seasonal renewal of constituents for microbial growth, the impact of microbial carbonate alteration over longer time-scales can be assumed to be substantial.

2.1.2 The organic-carbon constituents in the carbonate

The incubated bivalve shell samples (chapter 2) had a mean organic carbon content of 0.4 wt% (bulk aragonite) and 3 wt% (aragonite with periostracum), and samples with varying periostracal thickness were chosen for the incubations. Thus, the shell organic carbonate was a metabolic substrate easy to access, and the resulting degradation process was enhancing the shell-reactive surface. Subsequent exchange with pore-water and direct contact with microbial cells apparently led to the observed alteration in shell-carbonate geochemistry. In contrast, neither structural nor geochemical alteration characteristics were observed in incubated coral samples (chapter 3). The coral aragonite had an organic-carbon share of only 0.04 wt% and incubated subsamples were free of surface organic remains. Although the sample pore-space increased the surface to volume ratio, thus facilitated microbial settling, the low fraction of organic carbon presumably prevented direct microbe-mineral interaction. Foraminiferal tests incubated in the *A. borkumensis* culture (chapter 4) were prone to

secondary carbonate precipitation and changes in Mg concentrations, while the tests incubated in the anoxic incubations remained unaltered. Foraminiferal tests have an organic carbon content of about 1 wt% (Schroeder, 1975) and the tests are thin (20 - 50 µm, Billubs and Spero, 1995), compared to bivalve shells or coral skeleton hard parts. Consequently, it was expected that the susceptibility of both organic constituents and test surfaces to microbial activity would be relatively high. Furthermore, based on the results obtained in chapter 2, moderate dissolution of the test carbonate was expected, due to the low solubility of calcite, compared to that of aragonite (Mucci, 1983). However, anoxic media chemistry implicated weak microbial activity in the *S. sediminis* culture and the anoxic sediment incubation, compared to the other conducted experiments (chapter 2, 3). In incubations with a high metabolic turnover, alteration of foraminiferal tests might be facilitated. This could furthermore hold for natural sediment environments, specifically in the presence of newly deposited biogenic carbonates including the organisms´organic tissue, where the formation of CO_2 and organic acids through microbial organic-matter degradation in near proximity to the inorganic carbonate fraction would lead to enhanced dissolution of the latter.

2.1.3 Environmental factors in microbial carbonate alteration

In marine sediments, primary production (i.e. phytoplankton blooms) and coastal upwelling largely determine the C_{org} input in marine sediments (Müller and Suess, 1979; Wollast et al., 1991, Field et al., 1998). Besides the availability of electron acceptors, the fraction of labile organic carbon in the sediment is substantial for heterotrophic microbial metabolism and growth (Alongi, 1990; White, et al., 1991; Eiler et al., 2003). Hence, in organic-rich sediments a high metabolic turnover and related production of metabolites is facilitated through sufficient substrate availability. Under these conditions, microbial metabolic products (here, generation of mainly CO_2, organic acids/HCO_3^-, HS^-) might play the dominant role in carbonate alteration, while in times of C_{org} exhaust the direct use of carbonate C_{org} constituents might predominantly supply the microorganisms with metabolic substrate in deprivation of sources easier to obtain (as suggested for chapter 2). The related attachment of microbial cells and EPS to the carbonate surface could foster dissolution (Donlan, 2002) and subsequent cation exchange with the respective crystal lattices, or secondary carbonate precipitation (Aloisi et al., 2006). Westrich and Berner (1984) reported that sulfate-reducing bacteria preferred "fresh" organic carbon to that partly degraded through microbial aerobic respiration. This preference resulted in alternating rates of organic-matter decomposition and related sulfate reduction. It should therefore be considered, that even during sufficient C_{org} supply organic-matter reactivity can vary with the grade of decomposition. Thus, in organic-rich sediments with high rates of microbial respiration in the top most sediment column, sulfate reduction and related release of alkaline metabolites might as well be hampered to some degree. The adsorption of benthic organic

carbon to mineral surfaces was hypothesized to prevent mineralization by microbial communities as the sites of adsorption were pores small enough to exclude bacterial cells and hydrolytic enzymes (Mayer, 1993), albeit mineral-desorbed organic carbon was rapidly remineralized by both aerobic and anaerobic microbial communities (Kell, 1994). The loss in shell Ca concentrations observed in chapter 2 affected areas that were free of periostracum. Therefore, microbial organic matter degradation presumably affected inter- and intracrystalline organic constituents difficult to access, additionally to the periostracum. It is therefore feasible, that organic carbon sorbed to mineral surfaces is prone to microbial activity, thus further enhancing microbe-mineral interaction in marine sediments. The results obtained in chapter 3 displayed the influence of temperature on microbial carbonate-alteration potential. The optimum growth temperature for *A. borkumensis* is between 20°C and 30°C (Yakimov et al., 1998), and all changes in medium carbonate chemistry, were enhanced in the 20°C incubation, relative to the 10°C incubation. Hence, the potential of *A. borkumensis* to alter biogenic carbonates apparently is a function of temperature, and in temperate zones, biogenic carbonates might be more susceptible to *A. borkumensis* induced alteration than in cold zones. The temperature-dependent intensity of carbonate-alteration potential is presumably transferrable to the majority of benthic heterotrophic bacteria with different temperature adaptations and related growth optima. It is therefore suggested, that carbonate-alteration characteristics might be linked to seasonal patterns (i.e. input of organic matter and temperature variations) in the respective environment. This might be of further importance when considering possible microbial carbonate alteration over geological timescales of different temperature regimes during glacial/interglacial variations (as e.g. reviewed by Zachos et al., 2001) that could have promoted an alternating dominance of different benthic microbial communities with different carbonate-alteration potential.

2.1.4 Cell-wall and EPS functional groups

The trace-elemental composition of biogenic carbonates used for the present studies was distinctly altered by microbial activity during the experiments conducted in the frame of chapter 2 and 3. In chapter 2, surface dissolution features and loss in Ca concentrations relative to cell-free control samples were observed in the exposed areas of shells incubated in both the *S. sediminis*-culture medium, and the anoxic sediment. The increasing TA, $\Omega_{Aragonite}$, and Ca^{2+} and Sr^{2+} concentrations in the medium reflected carbonate (i.e. aragonite) dissolution, but decreased again towards the end of the experiment. As dense biofilm fragments were isolated from the incubated samples, the observed development presumably displayed the cation-adsorption capability by functional groups in cell-walls and extracellular polymeric substances (EPS) (McCalla, 1939; Beveridge, 1980), with the EPS binding affinity being cation-species specific (Guibaud et al., 2008). The increase of Sr concentrations in

exposed areas of another shell sample supported this assumption and furthermore indicated direct microbe-mineral interaction in these areas, specifically as the cell wall of *Shewanella* sp. has a high affinity for Sr^{2+} adsorption under the given experimental conditions (Small et al, 1999). Furthermore, the enrichment in Sr, together with the decrease in Ca concentrations in exposed sample parts hints at replacement of Ca by Sr in the mineral. In the specimen incubated in the anoxic sediment, the obtained data displayed alteration characteristics similar to that of the bacterial culture incubation, with the area of decreased Ca concentration in the shell protruding further towards non-exposed, pristine areas (< 200µm). This was mirrored by the respective medium chemistry with an increase in foremost $\Omega_{Aragonite}$, and Ca^{2+} and Sr^{2+} concentrations that led to a distinct decrease in the respective medium divalent-cation ratios, relative to the sediment control and reflected slowly ongoing carbonate dissolution. The concomitant increase in pH and TA, and the availability of dissolved Ca^{2+} in the medium expectedly would lead to subsequent carbonate precipitation. However, cell-wall and EPS functional groups undergo deprotonation in a high pH, highly alkaline environment, leading to a net negative charge of the moieties (Coughlin et al., 1983; Sutherland, 2001). This in turn could have facilitated Ca^{2+} binding, thus preventing secondary precipitation. The results indicate that cell-wall and EPS interaction with the respective carbonate could lead to cation exchange, resulting in a change in element concentrations, and subsequent alteration of the respective divalent cation ratios in the mineral. These changes could add to the natural variability in trace-elemental composition of biogenic carbonates, thereby compromising archive interpretation.

2.1.5 Microbial enzymatic activity

The results from chapter 2 and 4 indicate that enzymes might play an important role in microbially-induced carbonate alteration. Heterotrophic microorganisms gain energy for catabolic processes by carbohydrate degradation through extracellular hydrolytic enzymes (Hoppe, 1993). Furthermore, in deprivation of external electron acceptors microbial cells generate adenosine triphosphate (ATP) through glycolysis and/or fermentation processes (Fuchs, et al., 2007; Hoelzle et al., 2014), i.e. the step-wise breakdown of monosaccharides. In chapter 2, we suggested *S. sediminis* chitinase to have induced degradation of shell organic-matrix chitin constituents, thereby facilitating subsequent carbonate dissolution through N-acetylglucosamine fermentation and the respective products. Chitinases are highly abundant enzymes in marine microorganisms (Svitil et al., 1997; Yamano et al., 2000). In addition, a chitin deacetylase was reported for marine (Kadokura et al., 2007) and freshwater microbes (Zhou et al., 2010). The enzyme converts chitin to chitosan by N-acetylglucosamin deacetylation and the resulting acetate reacts with water to acetic acid (Sutherland, 1977), thus leading to acidification of the proximate environment. Chitin is an integral constituent of the bivalve shell inter- and intracrystalline organic matrix (Marin et al., 1996) and

bivalve shells are frequently applied carbonate archives (Andreasson and Schmitz, 1998; Schöne et al., 2004; Chauvaud et al., 2005). Chitin was furthermore detected in skeleton organic carbon constituents of some coral species (Wainwright, 1963; Leland et al., 1980), albeit for other species the occurrence of glycosaminoglycan in coral-skeleton organic matrices was alternatively reported (Constantz and Weiner, 1988; Fricain et al., 2000). Glycosaminoglycan furthermore is a constituent of the insoluble fraction in the foraminiferal organic matrix (Weiner and Erez, 1984). The microbial ability to enzymatically breakdown polysaccharides could therefore add to the metabolically-induced alteration processes of carbonate archives.

Carbonic anhydrase is a highly efficient acid-base catalyst that regulates the cellular carbonate system in catalyzing the reversive formation from CO_2 to HCO_3^- (Eigen and Hammes, 1963). Carbonic-anhydrase activity in marine microorganisms was foremost reported for cyanobacteria (Miller and Colman, 1980) and gammaproteobacteria (Appanna et al., 1994; Smith, et al., 1999). The enzyme was held responsible for dissolution of foraminiferal tests through generation of acidified test-associated microbial EPS (Freiwald, 1998), and for secondary carbonate precipitation through conversion of CO_2 to HCO_3^- (Douglas and Beveridge, 1998; Zavarzin, 2002). This process was reported to be coupled to urease activity that additionaly generates HCO_3^- through hydrolysation of urea (Achal and Pan, 2011). The related conversion of urea to ammonia (NH_3) further adds to system alkalinity, thereby facilitating $CaCO_3$ precipitation. Recently, carbonic-anhydrase activity in *A. borkumensis* was demonstrated to induce precipitation of high-Mg calcite (Krause et al., 2014). Foraminiferal tests (chapter 4) incubated in the *A. borkumensis* culture medium were covered with precipitates to a great extent. While ammonium levels measured during the experiment (not shown) were below detection level and rule out the presence of active urease, secondary carbonate precipitation through *A. borkumensis* carbonic-anhydrase activity is feasible. As the precipitates have yet to be analyzed for their exact composition, a description of the precipitated polymorph cannot be given in the frame of this thesis. Carbonates precipitated through microbial carbonic-anhydrase activity range from the high-Mg calcite reported by Krause et al. (2014) to strontium carbonate (Anderson and Appanna, 1994). Precipitation of polymorphs other than that of the pristine carbonate could lead to a different elemental composition of the whole bulk mineral structure, possibly similar to abiotically-induced neomorphism observed in diagenetically altered minerals.

2.2 Alteration effects on stable-isotopic composition

In the frame of chapter 2 and 3, potential microbially-induced alteration effects on stable isotopic composition of the incubated carbonates were investigated. The obtained results will be discussed in the following.

In the experiments conducted in the frame of chapter 2, the δ^{13}C and δ^{18}O values in bivalve samples from the anoxic incubations were scattered, relative to values obtained during measurements on pristine samples from the same bulk shell material, conducted by Ritter et al. (2017). The most ^{18}O enriched sample, however, had been incubated in the cell free control. In the experiments conducted for chapter 3, coral samples exposed to the *A. borkumensis*-culture medium were slightly enriched in ^{13}C on the outermost, exposed surface, relative to inner regions and non-incubated samples. However, the observed variations were not statistically significant (p > 0.5). Furthermore, metabolically-induced carbon isotope fractionation includes the release of metabolic light carbon (i.e. DIC) into the environment (Londry and Des Marais, 2009), and the comparably heavy isotopic composition in the coral-sample surface was contradictory. Both bivalve and hermatypic coral carbonate in general display a natural variability in δ^{13}C isotopic composition due to isotope fractionation foremost caused by metabolic processes (Klein et al., 1996; Heikoop et al., 2000). Furthermore, in hermatypic corals the rates of symbiont photosynthesis to respiration determine the availability and subsequent use of ^{13}C for the calcification process (McConnaughey, 1989; McConnaughey et al., 1997). The observed scatter in carbon isotopic composition within the experimental time frames may be attributed to these observations. Variability in bivalve and coral oxygen isotopic composition mainly derives from abiotic influences, such as varying seawater δ^{18}O, salinity and temperature (Epstein et al., 1953; Rollion-Bard et al., 2003, Dunca et al., 2008). The microbial influence on oxygen isotopic composition has predominantly studied in aerobic metabolic pathways and their effects on the δ^{18}O of dissolved oxygen (Balci et al., 2007; Casciotti et al, 2010), and no information of the influence of anaerobic microbial activity on oxygen isotopic composition is at hand. All values for bivalve and coral carbon- and oxygen-isotopic composition obtained in the frame of this thesis were within the previously reported ranges (See chapter 2 and 3). However, over longer timescales microbial influence, specifically on carbon isotopic composition, cannot be fully ruled out.

Overall, the present results display that microbial activity can play a considerable role in the post-mortem fate of biogenic carbonates. The combined biotic and abiotic effects during early diagenesis could lead to a inertwined cascade in carbonate alteration processes. These include the deposition in the uppermost sediment layers were boring organisms and acidic conditions in the proximate environment, the latter caused by microbial oxic respiration, can induce partial weathering of carbonate surface structures. The latter would lead to an increase in reactive surface and related cation exchange between pore-water and carbonate crystal lattice, thereby changing the carbonate´s geochemical signature. Furthermore, the accessibility of carbonate organic constituents as a metabolic substrate for microbial communities would be facilitated, inducing increased surface dissolution. Further shallow burial in the sediments, i.e. in an alkaline environment generated through anaerobic microbial metabolic activity in the anoxic zone, would expose the carbonate structures to secondary carbonate precipitation of different polymorphs, adding to abiotically-induced neomorphism. Enzymatic degradation of organic intra- and intercrystalline organic constituents would further induce carbonate dissolution at all burial stages, thereby further increasing the reactive carbonate surface for biotic and abiotic processes. Cation scavenging through cell-wall or EPS functional groups could change carbonate geochemical signature, and further induce surface dissolution by decreasing the saturation state of carbonate in the very proximate cell-environment. Additionally, the attachment of microbial biofilms to carbonate structures might induce carbonate weathering or precipitation, depending on the pH and the elemental composition in the respective EPS microzone.

3   Conclusion

Microbial alteration of biogenic carbonate archives should be considered a significant component of the early diagenetic system. During two of the present studies, articulate structural and geochemical alteration of aragonitic shell and calcitic test carbonate was observed. The alterations apparently were induced by microbial metabolic redox processes, cell-wall and EPS physico-chemical properties, and microbial enzymatic activity. While no clear results in stable isotopic composition were obtained during either of the conducted studies, specifically the change in carbonate trace-elemental composition and the resulting change in carbonate divalent-cation ratios could lead to misinterpretation of the respective signals in these frequently applied paleo-archives, thereby compromising their stability.

5 Method evaluation

Experimental duration and conduction

The experimental duration for all three studies was determined via conduction of a pre-experiment and the therein observed indications for microbial carbonate-alteration potential. However, the time spans were short (25 days to three months). To allow for more articulate alteration effects, future experiments should be extended to at least 1 year.

pH measurements

The pH measurements were conducted with a standard pH electrode. The measured anoxic medium samples were therefore exposed to ambient conditions prior to- and during the measurements, and subsequently equilibrated with the surrounding atmospheric CO_2. To allow for accuracy of measurements, specifically with regard to using pH values for calculations of medium pCO_2, pH microsensors should be applied in future measurements, to avoid contamination with ambient CO_2.

Reproducibility of results

Due to limited amounts of medium and/or samples (i.e. foremost shell samples), only one medium sample was taken per sampling point for all chemical analyses, and only two shell samples per incubation were available for structural and geochemical analyses. A higher medium volume and sample amount should be provided for in future experiments. Furthermore a triple determination of medium chemistry should be obligatory.

Sample preparation

Post-incubation sawing or cutting of coral samples with attached biofilms biased the outcome of stereomicroscopic analyses through jolting of the conglomerates (not shown). For analyses of biofilm attachment to carbonate samples by means of e.g. stereomicroscopy and SEM, thin subsamples of bulk shell- or skeleton hard parts should be prepared prior to the incubation to allow for careful preservation of samples with attached biofilms after the experiment.

The choice of bulk foraminiferal tests for the experiment and related analyses did not allow for comparisons of either surface structure or element composition between two samples of the same species. The high species-specificity with regard to both characteristics should be considered in future experiments. Consequently tests used in the experiments should be sorted according to species prior to the incubation.

Furthermore, to allow for mass-balance analyses, all incubated samples should be weighed prior to and after the respective experiment.

5 Research outlook

The presented thesis displayed that microbe-carbonate mineral interaction comprises a manifold of complex, intertwined factors. The observations during the conducted experiments raised questions that should be addressed more detailed in future studies.

- **Evaluating the natural carbonate trace-elemental/isotopic variability in biogenic carbonates used for the experiments**

  Future studies should include the rearing of (e.g.) bivalves for experimental use under controlled environmental conditions. The respective specimen should be sampled regularly during the rearing period, and shells should be analyzed for their structural, elemental and stable-isotopic composition. The methods should include high-resolution/synchrotron based analyses and isotope dilution.

- **Determining the role of EPS as mineral-nucleation matrices and/or agents of mineral dissolution**

  Biofilms should be regularly analyzed for micro-environmental parameters (pH, TA, DIC) and trace-element concentrations. For the latter, radioisotopes should be applied.

- **Investigating the role of enzymes in microbial carbonate-mineral alteration**

  Bacterial cultures for future experiments should be regularly screened for enzyme activity through conventional photometry and molecular tests for gene-expression. Furthermore, inhibition of enzymes in additional controls should be conducted.

References

Achal, V.and Pan, X. (2011) Characterization of Urease and Carbonic Anhydrase Producing Bacteria and Their Role in Calcite Precipitation. *Current Microbiology*, **62**, 894-902

Alongi, D.M. (1995) Bacterial growth rates, production and estimates of detrital carbon utilization in deep-sea sediments of the Solomon and Coral seas. *Deep Sea Research Part A. Oceanographic Research Papers*, **37**, 5, 731-746.

Aloisi, G., Gloter, A., Krüger, M., Wallmann, K., Guyot, F. and Zuddas, P. (2006) Nucleation of calcium carbonate on bacterial nanoglobules. *Geology*, **34**, 2017-2020.

Anderson, S. and Appanna, V.D. (1994) Microbial formation of crystalline strontium carbonate. *FEMS Microbiology Letters*, **116**, 1, 43-48.

Andreasson, F.P. and Schmitz, B. (1998) Tropical Atlantic seasonal dynamics in the early middle Eocene from stable oxygen and carbon isotope profiles of mollusk shells. *Paleoceanography*, **13**, 2, 183-192.

Balci, N., Shanks, W.C., Mayer, B. and Mandernack, K.W. (2007) Oxygen and sulfur isotope systematics of sulfate produced by bacterial and abiotic oxidation of pyrite. *Geochimica et Cosmochimica Acta*, **71**, 3796-3811

Bathurst, R.G.C (1975) Carbonate Sediments and Their Diagenesis**.** *Developments in Sedimentology*, Elsevier Science, Oxford, 640 pp.

Berner, R.A. (1980) Early Diagenesis: A Theoretical Approach. Princeton University Press, New Jersey, 256 pp.

Beveridge, T.J. and Murray, R.G.E. (1980) Sites of Metal Deposition in the Cell Wall of Bacillus subtilis. *Journal of Bacteriology*, **141,2**, 876-887.

Billups, K. and Spero, H.J. (1995) Relationship between shell size, thickness and stable isotopes in individual planktonic foraminifera from two equatorial Atlantic cores*. Oceanographic Literature Review*, **42**, 10, 854.

Casciotti, K. L., McIlvin, M., and Buchwald, C. (2010) Oxygen isotopic exchange and fractionation during bacterial ammonia oxidation. Limnology and Oceanography, **55**, 2, 753-762

Chauvaud, L., Lorrain, A., Dunbar, R.B., Paulet, Y.-M., Thouzearu, G., Jean, F., Guraini, J.-M., and Mucciarone, D. (2005) Shell of the Great Scallop *Pecten maximus* as a high-frequency archive of paleoenvironmental changes. *Geochemistry, Geophysics, Geosystems*, **6**, 8, Q08001.

Constantz, B. and Weiner, S., (1988). Acidic Macromolecules Associated With the Mineral Phase of Scleractinian Coral Skeletons. *The Journal of Experimental Zoology*, **248**, 253-258.

Coughlin, R.T., Tonsager, S., and McGroarty, E.J. (1983) Quantitation of Metal Cations Bound to Membranes and Extracted Lipopolysaccharide of Escherichia coli. *Biochemistry*, **22**, 2002-2007.

Donlan, R.M. (2002) Biofilms: Microbial Life on Surfaces. *Emerging Infectious Diseases*, **8**, 881-890

Douglas, S., and Beveridge, T.J. (1998) Mineral formation by bacteria in natural microbial communities. *FEMS Microbiology Ecology*, **26**, 79-88.

Dunca, E., Mutvei, H., Göransson, P., Mörth, C.-M., Schöne, B.R., Whitehouse M.J., Elfman, M. and Baden, S. (2008) Ocean quahog (Arctica islandica) shells to reconstruct paleoenvironment in Öresund, Kattegat and Skagerrak, Sweden. *International Journal of Earth Sciences*, **98**, 3-17.

Eigen, M. and Hammes, G.G. (1963) Elementary steps in enzyme reactions. *Advances in Enzymology*, **25**, 1-38.

Eiler, A., Langenheder, S., Bertilsson, S., and Tranvik, L.J. (2003) Heterotrophic Bacterial Growth Efficiency and Community Structure at Different Natural Organic Carbon Concentrations. *Applied and Environmental Microbiology*, **83**, 14, 3701-3709.

Fenchel, T.M. and Jørgensen, B.B. (1977) Detritus Food Chains of Aquatic Ecosystems: The Role of Bacteria. In: *Advances in Microbial Ecology*, **1**, 1-58 (Ed Alexander, M.). Springer International Publishing.

Freiwald, A. (1995) Bacteria-Induced Carbonate Degradation: A Taphonomic Case Study of *Cibicides lobatulus* from a High-Boreal Carbonate Setting. *PALAIOS*, **10**, 4, 337-346.

Fricain, J.C., Alouf, J., Bareille, R., Rouais, F., and Rouvillain, J.L. (2002). Cytocompatibility study of organic matrix extracted from carribean coral *Porites astroides*. *Biomaterials*, **23**, 673-679.

Fuchs, S., Pané-Farré, J. Kohler, C., Hecker, M., and Engelmann, S. (2007) Anaerobic Gene Expression in *Staphylococcus aureus*. *Journal of Bacteriology*, **189**, 11, 4275-4289.

Guibaud, G., Bordas, F., Saaid, A., D'Abzac, P. and Van Hullebusch, E. (2008) Effect of pH on cadmium and lead binding by extracellular polymeric substances (EPS) extracted from environmental bacterial strains. *Colloids and Surfaces B: Biointerfaces*, **63**, 48-54.

Heikoop, J.M., Dunn, J.J., Risk, M.J., Schwarcz, H.P., McConnaughey, T.A., and Sandeman, I.M. (2000) Seperation of kinetic and metabolic isotope effects in carbon-13 records preserved in reef coral skeletons. *Geochimica et Cosmochimica Acta*, **64**, 6, 975-987.

Hoelzle, R.D., Virdis, B., and Batstone, D.J. (2014) Regulation mechanisms in mixed and pure culture microbial fermentation. *Biotechnology and Bioengineering*, **111**, 11, 2139-2154.

Hoppe, H.G. (1993) Microbial Extracellular Enzyme Activity: A New Key Parameter in Aquatic Ecology. In: *Microbial Enzymes in Aquatic Environments*. Springer Series in Contemporary Bioscience (Ed Chróst, R.), 60-83.

Kadokura, K., Rokutani, A., Yamamoto, M., Ikegami, T., Sugita, H., Itoi, S., Hakamata, W., Oku, T., and Nishio, T. (2007) Purification and characterization of *Vibrio parahaemolyticus* extracellular chitinase and chitin oligosaccharide deacetylase involved in the production of heterodisaccharide from chitin. *Applied Microbiology and Biotechnology*, **75**; 357.

Klein, R.T., Lohmann, K.C., and Thayer, C.W. (1996) SrCa and $^{13}C^{12}C$ ratios in skeletal calcite of *Mytilus trossulus*: Covariation with metabolic rate, salinity, and carbon isotopic composition of seawater. *Geochimica et Cosmochimica Acta*, **60**, 21, 4207-4221.

Krause, S., Liebetrau, V., Eisenhauer, A., and Treude, T. (2014) Carbonic anhydrase - a geological relevant enzyme? Goldschmidt Conference abstract.

Leland, C., Ellis Jr., R., Chandross, J., and Bear, R.S. (1980) X-ray diffraction evidence of chitin in the axial skeletons of antipatharian corals. *Comparative Biochemistry and Physiology Part B: Comparative Biochemistry*, **66**, 1, 163-165.

Londry, K.L. and Des Marais, D.J. (2003) Stable carbon isotope fractionation by sulfate-reducing bacteria. *Applied and Environmental Microbiology*, **69**, 2942-9.

Marin, F., Smith, M., Isa, Y., Muyzer, G., Westbroek, P., Isat, Y., Muyzert, G. and Westbroek, P. (1996) Skeletal matrices, muci, and the origin of invertebrate calcification. *Proceedings of the National Academy of Sciences of the United States of America*, **93**, 1554-9.

McCalla, T.M. (1939) Cation adsorption by bacteria. *Journal of Bacteriology*, **40 (1)**, 23-32.

McConnaughey, T.A. (1989) ^{13}C and ^{18}O isotopic disequilibrium in biological carbonates: I Patterns. *Geochimica et Cosmochimica Acta*, **53**, 151-162.

McConnaughey, T.A., Burdett, J., Whelan, J.F., and Paull, C.K. (1997) Carbon isotopes in biological carbonates: Respiration and photosynthesis. *Geochimica et Cosmochimica Acta*, **61**, 611-622.

Miller, G. and Colman, B. (1980) Evidence for HCO_3^- Transport by the Blue-Green-Alga (Cyanobacterium) *Coccochloris peniocystis*. *Plant Physiology*, **65**, 2, 65.2.397.

Mucci, A. (1983) The solubility of calcite and aragonite in seawater at various salinities, temperatures, and one atmosphere total pressure. *American Journal of Science*, **283**, 7, 780-799.

Müller, P.J. and Suess, E. (1979) Productivity, sedimentation rate, and sedimentary organic matter in the Oceans – I. Organic carbon preservation. *Deep-Sea Research*, **26A**, 1347-1362.

Ritter, A.-C., Mavromatis, V., Dietzel, M., Kwiecien, O., Wiethoff, F. , Griesshaber, E., Casella, L.A. Schmahl, W.W., Koelen, J., Neuser, R., Leis, A., Buhl, D., Niedermayr, A., Breitenbach, S.F.M., Bernasconi, S.M. and Immenhauser, A. (2017) Exploring the impact of diagenesis on (isotope) geochemical and microstructural alteration features in biogenic aragonite. Accepted article, doi: 10.1111/sed.12356.

Rollion-Bard, C., Blamart, D., Cuif, J.-P. and Juillet-Leclerc, A. (2003) Microanalysis of C and O isotopes of azooxanthellate and zooxanthellate corals by ion microprobe. *Coral reefs*, **22**, 4, 405-415.

Schöne, B.R., Castro, A., Fiebig, J. and Houk, S.D. (2004) Sea surface water temperatures over the period 1884 – 1983 reconstructed from oxygen isotope ratios of a bivalve mollusk. *Palaeogeography, Palaeoclimatology, Palaeoecology*, **212**, 215-232.

Schroeder, R.A. (1975). Absence of ß-alanine and γ-aminobutyric acid in cleaned foraminiferal shells: Implications for use as a chemical criterion to indicate removal of non-indigenous amino acid contaminants. *Earth and Planetary Science Letters*, **25**, 3, 274-278.

Small, T.D., Warren, L.A. and Roden, E.E. (1999) Sorption of Strontium by Bacteria, Fe (III) Oxide, and Bacteria - Fe (III) Oxide Composites. *Environmental Science and Technology*, **33**, 4465-4470.

Smith, K.S., Jakubzick, C., Whittam, T.S., and Ferry, J.G. (1999) Carbonic anhydrase is an ancient enzyme widespread in prokaryotes. *Proceedings of the National Academy of Sciences of the United States of America,* **96**, 26, 15184-15189.

Sutherland, I.W. (1977) Enzymes acting on bacterial surface carbohydrates. In: *Surface Carbohydrates of the Prokaryotic Cell*. Academic Press, London.

Svitil, A.L., Ní Chadhain, S.M., Moore, J.A., and Kirchman, D.L. (1997) Chitin Degradation Proteins Produced by the Marine Bacterium *Vibrio harveyi* Growing on Different Forms of Chitin. *Applied and Environmental Microbiology*, **63**, 2, 408-413.

Tucker, M.E. and Bathurst, R.G.C. (1990) Carbonate Diagenesis. Blackwell Scientific Publications, 320 pp.

Wainright, S.A. (1963) Skeletal organization in the coral, *Pocillopora damicornis*. *Journal of Cell Science*, **s3-104**: 169 – 183.

Weiner, S. and Erez, J. (1984) Organic Matrix of the Shell of the Foraminifer *Heterostegina depressa*. *Journal of Foraminiferal Research*, **14**, 3, 206-212.

Westrich, J.T. and Berner R.A. (1984) The role of sedimentary organic matter in bacterial sulfate reduction: The *G* model tested. *Limnology and Oceanography*, **23**, 2, 236-249.

White, P.A., Kalff, J., Rasmussen, J.B., and Gasol, J.M. (1991) The effect of temperature and algal biomass on bacterial production and specific growth rate in freshwater and marine habitats. *Microbial Ecology*, **21**, 1, 99-118.

Yakimov, M.M., Golyshin, P.N., Lange, S., Moore, E.R.B., Abraham, W.R., Lünsdorf, H., and Timmis, K.N. (1998) *Alcanivorax borkumensis* gen. nov., sp. nov., a new, hydrocarbon-degrading and surfactant-producing marine bacterium. *International Journal of Systematic Bacteriology*, **48**, 339-348.

Yamano, M., Higashida, N., Endo, C., Sakata, N., Fujishima, S., Akihiko, M., and Higashihara, T. (2000) Purification and Characterization of N-Acetylglucosamine-6-phosphate Deacetylase from a Psychotrophic Marine Bacterium, *Alteromonas* Species. *Marine Biotechnology*, **2**, 1, 57-64.

Zachos, J., Pagani, M., sloan, L., Thomas, E., Billups, K. (2001) Trends, Rhythms, and Aberrations in Global Climate 65 Ma to Present. *Science*, **292**, 5517, 686-693.

Zavarzin, G.A. (2002) Microbial Geochemical Calcium Cycle. *Microbiology*, **71**, 1, 1-17.

Zhou, G., Zhang, H., He, Y., and He, L. (2010) Identification of a chitin deacetylase producing bacteria isolated from soil and its fermentation optimization. *African Journal of Microbiology Research*, **4**, 23, 2597-2603.

Acknowledgements

Ich danke meinen Freunden, meiner Liebe, dafür, dass sie immer an meiner Seite waren - ganz gleich, in welche Richtung ich mit welcher Intensität gestürmt oder gekrochen bin.

Ich liebe Euch unverbrüchlich!

Meiner Mutter.
Ich wünschte, Du wärst hier und wohlauf.

You cannot rehearse the unknown.
Wayne Shorter